1.4 Presolar Grains

E Zinner, Washington University, St. Louis, MO, USA

1.4.1 Introduction

Traditionally, astronomers have studied the stars by using, with rare exception, electromagnetic radiation received by telescopes on and above the Earth. Since the mid-1980s, an additional observational window has been opened in the form of microscopic presolar grains found in primitive meteorites. These grains had apparently formed in stellar outflows of late-type stars and in the ejecta of stellar explosions and had survived the formation of the solar system. They can be located in and extracted from their parent meteorites and studied in detail in the laboratory. Their stellar origin is recognized by their isotopic compositions, which are completely different from those of the solar system and, for some elements, cover extremely wide ranges, leaving little doubt that the grains are ancient stardust.

By the 1950s, it had been conclusively established that the elements from carbon on up are produced by nuclear reactions in stars (See **Chapter 2.1**), and the classic papers by Burbidge et al. (1957) and Cameron (1957) provided a theoretical framework for stellar nucleosynthesis. According to these authors, nuclear processes produce elements with very different isotopic compositions, depending on the specific stellar source. The newly produced elements are injected into the interstellar medium (ISM) by stellar winds or as supernova (SN) ejecta, enriching the galaxy in 'metals' (all elements heavier than helium), and after a long galactic history, the solar system is believed to have formed from a mix of this material. In fact, the original work by Burbidge et al. and Cameron was stimulated by the observation of regularities in the abundance of the nuclides in the solar system as obtained by the study of meteorites (Suess and Urey, 1956). Although providing only a grand average of many stellar sources, the solar system abundances (See **Chapter 2.1**) of the elements and isotopes (Anders and Grevesse, 1989; Asplund et al., 2005; Grevesse et al., 1996; Lodders, 2003; Lodders et al., 2009; Palme and Jones, 2004) remained an important test for nucleosynthesis theory (e.g., Timmes et al., 1995).

In contrast, the study of stellar grains permits information to be obtained about individual stars, complementing astronomical observations of elemental and isotopic abundances in stars (e.g., Lambert, 1991), by extending measurements to elements that cannot be measured astronomically. In addition to nucleosynthesis and stellar evolution, presolar grains provide information about galactic chemical evolution, physical properties in stellar atmospheres, mixing of SN ejecta, destruction processes in the ISM, and conditions in the solar nebula and in the parent bodies of the meteorites in which the grains are found.

This new field of astronomy has grown to an extent that not all aspects of presolar grains can be treated in detail in this chapter. The interested reader is therefore referred to some recent reviews (Anders and Zinner, 1993; Bernatowicz et al., 2006; Clayton and Nittler, 2004; Davis, 2011; Hoppe, 2004, 2010; Hoppe and Zinner, 2000; Lodders and Amari, 2005; Lugaro, 2005; Meyer et al., 2008; Nittler, 2003; Ott, 1993;

Zinner, 1998a,b, 2008) and to the compilation of papers found in *Astrophysical Implications of the Laboratory Studies of Presolar Material* (Bernatowicz and Zinner, 1997). That book contains not only several detailed review papers on presolar dust grains but also a series of chapters on stellar nucleosynthesis. Further information on nucleosynthesis can be obtained from the textbooks by Clayton (1983b) and Arnett (1996) and from reviews by Käppeler et al. (1989), Meyer (1994), Wallerstein et al. (1997), and Meyer and Zinner (2006).

1.4.2 Historical Background

Although the work by Burbidge et al. (1957) and Cameron (1957) and subsequent work by nuclear astrophysicists made it clear that many different stellar sources must have contributed to the material that formed the solar system and although astronomical observations indicate that some of this material was in the form of interstellar (IS) grains (e.g., Mathis, 1990), it was generally believed that it had been thoroughly homogenized in a hot solar nebula (Cameron, 1962). The uniform isotopic composition of all available solar system material seemed to confirm this opinion.

The first evidence for isotopic heterogeneity of the solar nebula and a hint of the survival of presolar grains came from hydrogen (Boato, 1954) and the noble gases xenon (Reynolds and Turner, 1964) and neon (Black, 1972; Black and Pepin, 1969). However, it was only after the discovery of anomalies in oxygen, a rock-forming element (Clayton et al., 1973), that the concept of survival of presolar material in primitive meteorites was widely accepted. The finding of ^{16}O excesses was followed by the detection of isotopic anomalies in other elements, such as magnesium, calcium, titanium, chromium, and barium in refractory inclusions (CAIs for Ca,Al-rich inclusions, See **Chapter 1.3**) (Clayton et al., 1988; Lee, 1988; Wasserburg, 1987). Also large anomalies in carbon (Halbout et al., 1986) and nitrogen (Lewis et al., 1983) indicated the presence of presolar grains. However, it was the pursuit of the carriers of the 'exotic' (i.e., isotopically anomalous) noble gas components of neon and xenon (**Figure 1**) by Edward Anders and his colleagues at the University of Chicago that led to their ultimate isolation (see Anders and Zinner, 1993). The approach taken by these scientists, 'burning down the haystack to find the needle,' consisted of tracking the noble gas carriers through a series of increasingly harsher chemical dissolution and physical separation steps (Amari et al., 1994; Tang and Anders, 1988b). Their effort culminated in the isolation and identification of diamond, the carrier of Xe–HL (Lewis et al., 1987), silicon carbide, the carrier of Ne–E(H) and Xe–S (Bernatowicz et al., 1987; Tang and Anders, 1988b), and graphite, the carrier of Ne–E(L) (Amari et al., 1990).

Once isolated, SiC and graphite (for diamond, see succeeding text) were found to be anomalous in all measured isotopic ratios, and it is this feature that identifies them as presolar grains. This distinguishes them from other materials in meteorites, such as CAIs, which also carry isotopic anomalies in some elements but, in contrast to bona fide stardust, formed in the solar system. They apparently inherited their anomalies from incompletely homogenized presolar material. Another distinguishing feature is that anomalies in presolar grains are up to several orders of magnitude larger than those in CAIs and match those expected for stellar atmospheres (Zinner, 1997).

1.4.3 Types of Presolar Grains

Table 1 shows the types of presolar grains identified so far. It also lists the sizes, approximate abundances, and stellar sources. In addition to the three carbonaceous phases that were discovered because they carry exotic noble gas components (**Figure 1**) and which can be isolated from meteorites in almost pure form by chemical and physical processing, presolar oxide, silicon nitride (Si_3N_4), and silicates were identified by isotopic measurements in the ion microprobe, and the number of such grains available for study is much smaller than that of carbonaceous phases. Most oxide grains are spinel ($MgAl_2O_4$) and corundum (Al_2O_3), but hibonite ($CaAl_{12}O_{19}$), chromite ($FeCr_2O_4$), chromium spinel ($Mg(Al,Cr)_2O_4$), titanium oxide, and iron oxide have also been found (Choi et al., 1998; Floss et al., 2008; Hutcheon et al., 1994; Nittler and Alexander, 1999; Nittler et al., 1994, 2005b, 2008; Zinner et al., 2003b). While all

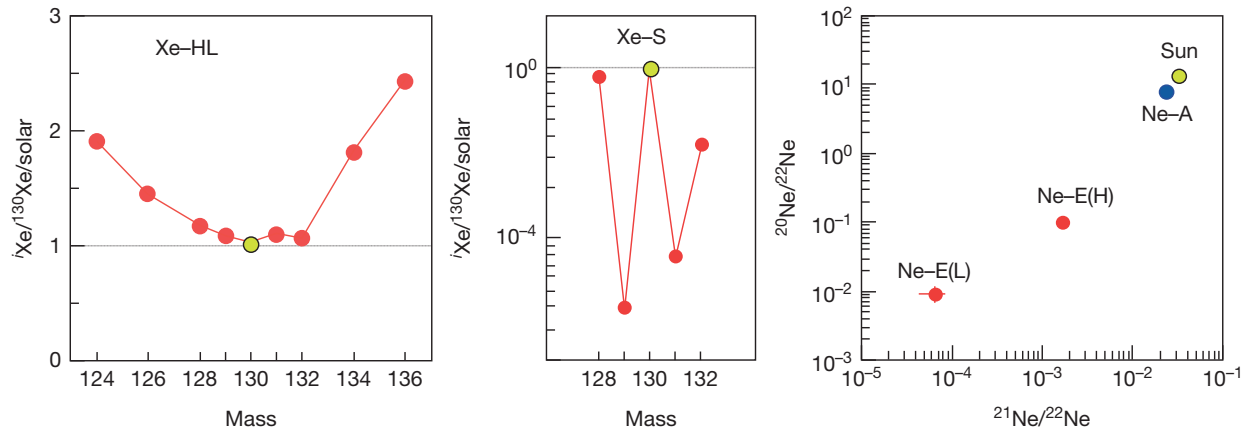

Figure 1 Exotic noble gas components present in presolar carbonaceous grains. Diamond is the carrier of Xe–HL, SiC the carrier of Xe–S and Ne–E(H), and graphite the carrier of Ne–E(L). Reproduced from Anders E and Zinner E (1993) Interstellar grains in primitive meteorites: Diamond, silicon carbide, and graphite. *Meteoritics* 28, 490–514.

Table 1 Types of presolar grains in primitive meteorites and IDPs

Grain type	*Noble gas components*	*Size*	*Abundance*[a,b]	*Stellar sources*
Diamond	Xe–HL	2 nm	1400 ppm	Supernovae?
Silicon carbide	Ne–E(H), Xe–S	0.1–20 μm	150 ppm	AGB, SNe, J stars, novae, born-again AGB
Graphite	Ne–E(L)	1–20 μm	1–2 ppm	SNe, AGB, born-again AGB
Silicates in IDPs		0.2–1 μm	>1.5%	RG, AGB, SNe
Silicates in meteorites		0.2–0.9 μm	>220 ppm	RG, AGB, SNe
Oxides		0.15–3 μm	>80 ppm	RG, AGB, SNe, novae
Silicon nitride		0.3–1 μm	~3 ppb	SNe
Ti, Fe, Zr, Mo carbides		10–200 nm		AGB, SNe
Kamacite, iron		~10–20 nm		SNe

[a]Abundances vary with meteorite type. Shown here are maximum values.
[b]Because detection efficiency for ion imaging identification are not included, given abundances are lower limits (see Nguyen et al., 2007).

these grains, with the exception of iron oxide, as well as presolar Si_3N_4 (Nittler et al., 1995), were located by single grain analysis of acid residues, presolar silicates were discovered by isotopic imaging of chemically untreated interplanetary dust particles (IDPs (See **Chapter 1.8**)) (Messenger et al., 2003), meteoritic grain-size separates and polished sections (Nagashima et al., 2004; Nguyen and Zinner, 2004), and Antarctic meteorite samples (Yada et al., 2008).

Finally, titanium-, zirconium-, and molybdenum-rich carbides, cohenite ($(Fe,Ni)_3C$), kamacite (Fe–Ni), rutile (TiO_2), oldhamite (CaS), elemental-iron and ruthenium-iron metal, and iron and nickel silicide (Fe_2Si, Ni_2Si) were found as tiny subgrains inside of SiC grains and graphite spheres (Bernatowicz et al., 1991, 1996; Croat et al., 2003, 2008, 2011a,b, 2012; Hynes et al., 2010, 2011). While TiC inside of a SiC grain (Bernatowicz et al., 1992) could have formed by exsolution, there can be little doubt that interior grains in graphite must have formed prior to the condensation of the spherules.

1.4.4 Analysis Techniques

Although the abundance of carbonaceous presolar grains in meteorites is low, once they are identified, almost pure samples can be prepared and studied in detail. Enough material of these phases can be obtained for 'bulk' analysis, that is, the analysis of collections of large numbers of grains either by gas mass spectrometry (GMS) of carbon, nitrogen, and the noble gases (Lewis et al., 1994; Russell et al., 1996, 1997; Verchovsky et al., 2006), by thermal ionization mass spectrometry (TIMS) of strontium, barium, neodymium, samarium, and dysprosium (Ott and Begemann, 1990; Podosek et al., 2004; Prombo et al., 1993; Richter et al., 1993, 1994), or by secondary ion mass spectrometry (SIMS) (Amari et al., 2000; Zinner et al., 1991). Isotopic ratios of barium, neodymium, samarium, europium, gadolinium, dysprosium, erbium, yttrium, and hafnium on SiC-rich bulk samples have recently been obtained by inductively coupled plasma mass spectrometry (ICP-MS) (Yin et al., 2006). While only averages over many grains are obtained by bulk analysis, it allows the measurement of trace elements, such as the noble gases, and heavy elements that cannot be analyzed otherwise.

However, because presolar grains come from different stellar sources, information on individual stars is obtained by the study of single grains. This challenge has been successfully taken up by the application of a series of microanalytical techniques. For isotopic analysis, the ion microprobe has become the instrument of choice. While most SIMS measurements have been made on grains 1 μm in size or larger, a new type of ion probe, the NanoSIMS, allows measurements of grains an order of magnitude smaller (e.g., Zinner et al., 2003b). Ion probe analysis has led to the discovery of new types of presolar grains, such as corundum (Hutcheon et al., 1994; Nittler et al., 1994) and silicon nitride (Nittler et al., 1995). It also has led to the identification of rare subpopulations of presolar dust, such as SiC grains of type X (Amari et al., 1992) and type Y (Hoppe et al., 1994). Searches for presolar oxide grains and rare subpopulations of SiC profited from the application of isotopic imaging in the ion probe, which allows the rapid analysis of a large number of grains (Gröner and Hoppe, 2006; Gyngard et al., 2010c; Nittler and Alexander, 2003; Nittler et al., 1997). Whereas earlier analyses have been made on well-separated grains, isotopic imaging of tightly packed grains, of polished sections of meteorites, and of samples pressed into a metal foil allows the automatic analysis of many thousands of grains (Nguyen et al., 2003) and has been essential in the discovery of presolar silicate grains (Messenger et al., 2003; Nagashima et al., 2004; Nguyen and Zinner, 2004).

Laser ablation and resonant ionization mass spectrometry (RIMS) (Savina et al., 2003b) have been successfully applied to isotopic analysis of the heavy elements strontium, zirconium, molybdenum, ruthenium, barium, and chromium in individual SiC and graphite grains (Levine et al., 2009; Nicolussi et al., 1997, 1998a,c; Savina et al., 2003a, 2004, 2007, 2010). A RIMS instrument under development that uses a finely focused gallium beam for atom sputtering promises isotopic analysis on the 10 nm scale (Stephan et al., 2010, 2011). Single grain measurements of helium and neon have been made by laser heating and GMS (Heck et al., 2005, 2006, 2007, 2009b; Meier et al., 2012; Nichols et al., 1995).

The surface morphology of grains has been studied by secondary electron microscopy (SEM) (Hoppe et al., 1995). Such studies have been especially useful for pristine SiC grains that have not been subjected to any chemical treatment (Bernatowicz et al., 2003; Tizard et al., 2005). Finally, the transmission electron microscope (TEM) has played an important role in the discovery of presolar SiC (Bernatowicz et al., 1987) and internal TiC and other subgrains in graphite

(Bernatowicz et al., 1991). Electron diffraction analysis in the TEM allows the determination of the crystal structure of grains (Bernatowicz et al., 1987; Stroud et al., 2004a). The TEM also has been successfully applied to the study of diamonds (Daulton et al., 1996; Stroud et al., 2011) and of polytypes of SiC (Daulton et al., 2002, 2003). The focused-ion-beam (FIB) microscope had become increasingly important for preparing grain samples for TEM analysis (Holzapfel et al., 2009; Zega et al., 2007). Another instrument that gives information about the degree of crystallinity in presolar grains is the Raman microprobe (Wopenka et al., 2010, 2011b).

The Auger Nanoprobe has been used for obtaining chemical and mineralogical information of submicrometer grains identified as stardust in the NanoSIMS (Stadermann et al., 2009). Synchrotron x-ray fluorescence (XRF) analysis makes the analysis of heavy elements in single presolar SiC grains possible (Kashiv et al., 2002, 2010). A technique that promises to be able to measure carbon isotopic ratios in individual nanodiamonds is atom probe tomography, which allows determination of the mass and position of single atoms (Heck et al., 2011; Stadermann et al., 2011).

A survey of recent advances in analytical techniques for the analysis of extraterrestrial samples is given by Zinner et al. (2011).

1.4.5 Astrophysical Implications of the Study of Presolar Grains

There are many stages in the long history of presolar grains from their stellar birth to their incorporation into primitive meteorites, and in principle, the study of the grains can provide information on all of them.

The isotopic composition of a given circumstellar grain reflects that of the stellar atmosphere from which the grain condensed. The atmosphere's composition, in turn, is determined by several factors: (i) by the galactic history of the material from which the star itself formed, (ii) by nucleosynthetic processes in the star's interior, and (iii) by mixing episodes in which newly synthesized material is dredged from the interior into the star's envelope. In supernovae, mixing of different layers with different nucleosynthetic histories accompanies the explosion and the ejection of material. The isotopic compositions of grains provide information on these processes.

Grain formation occurs when temperatures in the expanding envelope of red giants (RGs) or in SN ejecta are low enough for the condensation of minerals. Many late-type stars are observed to be surrounded by dust shells of grains whose mineral compositions reflect the major chemistry of the gas (e.g., Little-Marenin, 1986). The study of morphological features of pristine grains, of internal grains, and of trace element abundances can give information on the physical and chemical properties of stellar atmospheres (Amari et al., 1995a; Bernatowicz et al., 1996, 2005; Croat et al., 2003, 2008, 2012; Kashiv et al., 2001, 2002, 2010; Lodders and Fegley, 1998).

After their formation as circumstellar grains or as SN condensates, grains enter a long journey through the ISM. They should be distinguished from true IS grains that form in the ISM, for example, in dense molecular clouds. Grains of stellar origin are most likely to be covered by mantles of IS cloud material. During their IS history, grains are subjected to a variety of destructive processes, such as evaporation in SN shocks and sputtering by shocks and stellar winds. They are also exposed to galactic cosmic rays that leave a record in the form of cosmogenic nuclides (Gyngard et al., 2009a,c; Heck et al., 2009c; Ott and Begemann, 2000; Ott et al., 2005, 2009; Tang and Anders, 1988a).

Grains might go in and out of IS clouds before some were finally incorporated into the dense molecular cloud from which our solar system formed. The final step in the complex history of stellar grains is the formation of planetesimals and of the parent bodies of the meteorites in which we find these presolar fossils. By far, the largest fraction of the solids, even in primitive meteorites, formed in the solar system and the fraction of surviving presolar grains is small (see **Table 1**). Primitive meteorites experienced varying degrees of metamorphism (See **Chapter 1.7**) on their parent bodies, and these metamorphic processes affected different types of presolar grains in different ways. The abundance of different grain types can thus give information about conditions in the solar nebula and about parent-body processes (Floss and Stadermann, 2009a, 2012; Huss and Lewis, 1995; Leitner et al., 2012b; Mendybaev et al., 2002).

1.4.6 Silicon Carbide

Silicon carbide is the best-studied presolar grain type. It has been found in carbonaceous, unequilibrated, ordinary, and enstatite chondrites with concentrations ranging up to ~150 ppm (Huss and Lewis, 1995; Leitner et al., 2012b; Zhao et al., 2011b). Most SiC grains are less than 0.5 μm in diameter. Murchison is an exception in that grain sizes are, on average, much larger than those in other meteorites (Amari et al., 1994; Huss et al., 1997; Russell et al., 1997). This difference is still not understood but it, and the fact that plenty of Murchison is available, is the reason that, by far, most measurements have been made on Murchison SiC (see presolar grain database; Hynes and Gyngard, 2009). Many SiC grains show euhedral crystal features (**Figure 2**), but there are large variations. Morphological studies by high-resolution SEM (Bernatowicz et al., 2003; Stroud and Bernatowicz, 2005) reveal detailed crystallographic features that give information about growth conditions. Such information is also obtained from TEM studies (Hynes et al., 2010; Stroud and Bernatowicz, 2005; Stroud et al., 2003, 2004b). Electron diffraction measurements in the TEM show that only the cubic (3C) (~80%) and hexagonal (2H) polytypes are present, indicating low pressures and condensation temperatures in stellar outflows (Bernatowicz et al., 1987; Daulton et al., 2002, 2003). A preponderance of cubic SiC has been observed astronomically in carbon stars (Speck et al., 1999).

The availability of >1 μm SiC grains and relatively high concentrations of trace elements (Amari et al., 1995a; Kashiv et al., 2002, 2010) allow the isotopic analysis of the major and of many trace elements in individual grains. In addition to the major elements carbon and silicon, isotopic data are available for the diagnostic (in terms of nucleosynthesis and stellar origin) elements nitrogen, magnesium, calcium, titanium, iron, nickel, the noble gases, and the heavy elements strontium, zirconium, molybdenum, ruthenium, barium, neodymium, samarium,

dysprosium, europium, tungsten, and lead. Refractory elements, such as aluminum, titanium, vanadium, and zirconium, are believed to have condensed into SiC (Lodders and Fegley, 1995, 1997, 1999). However, Verchovsky and coworkers (Verchovsky et al., 2004; Verchovsky and Wright, 2004) argued on the basis of the grain-size dependence of elemental concentrations that implantation played a major role not only for noble gases but also for relatively refractory elements, such as strontium and barium. These authors identified two components with different implantation energies: the low-energy component is implanted from the stellar wind and has the composition of the AGB envelope; the high-energy component is implanted during the planetary nebula phase from the hot remaining white dwarf star and has the composition of helium-shell material. The $^{134}Xe/^{130}Xe$ ratio found in the grains confirms their conclusion that most *s*-process xenon in SiC originated in the envelope (Pignatari et al., 2004a).

Carbon, nitrogen, and silicon isotopic, as well as inferred $^{26}Al/^{27}Al$ ratios in a large number of individual grains (**Figures 3–5**), have led to the classification into different populations (Hoppe and Ott, 1997): mainstream grains (~93% of the total), minor subtypes AB, C, X, Y, Z, and nova grains. Most of presolar SiC is believed to have originated from carbon stars, late-type stars of low mass (1–3 $M_\odot$) in the thermally pulsing (TP) asymptotic giant branch (AGB) phase of evolution (Iben and Renzini, 1983). Dust from such stars has been proposed already one decade prior to identification of SiC to be a minor constituent of primitive meteorites (Clayton, 1983a; Clayton and Ward, 1978; Srinivasan and Anders, 1978). Several pieces of evidence point to such an origin. Mainstream grains have $^{12}C/^{13}C$ ratios similar to those found in carbon stars (**Figure 6**), which are considered to be the most prolific injectors of carbonaceous dust grains into the ISM (Ferrarotti and Gail, 2006; Gail et al., 2009; Tielens, 1990). Many carbon stars show the 11.3 μm emission feature typical of SiC (Speck et al., 1997; Treffers and Cohen, 1974). Finally, AGB stars are believed to be the main source of the *s*-process (slow neutron-capture nucleosynthesis)

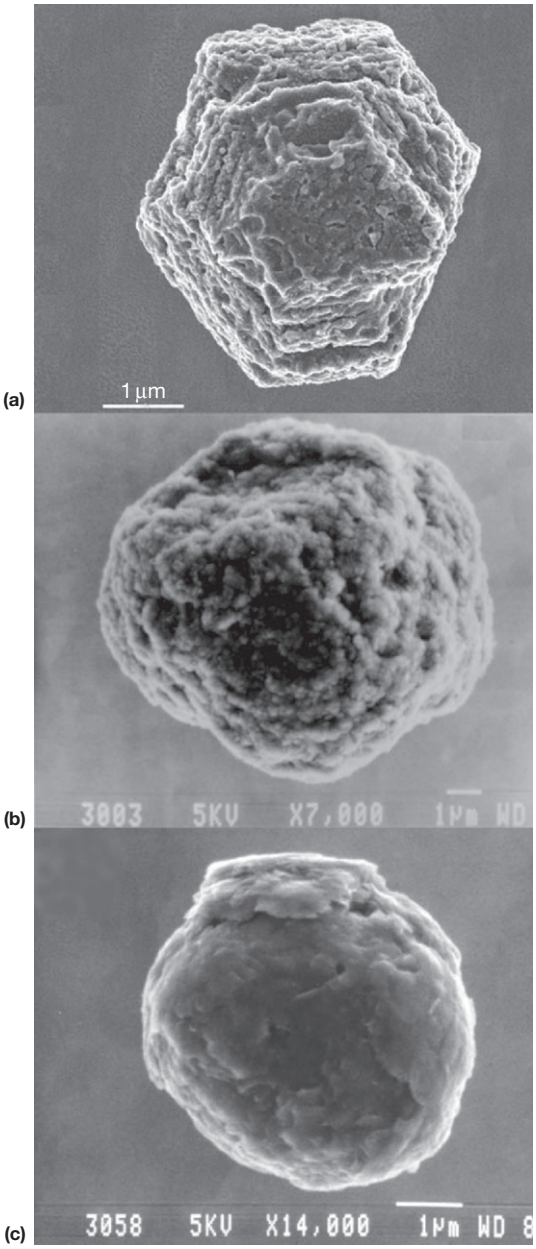

Figure 2 Secondary electron micrographs of (a) presolar SiC, (b) presolar graphite (cauliflower type), and (c) presolar graphite (onion type). Photographs courtesy of Sachiko Amari and Scott Messenger.

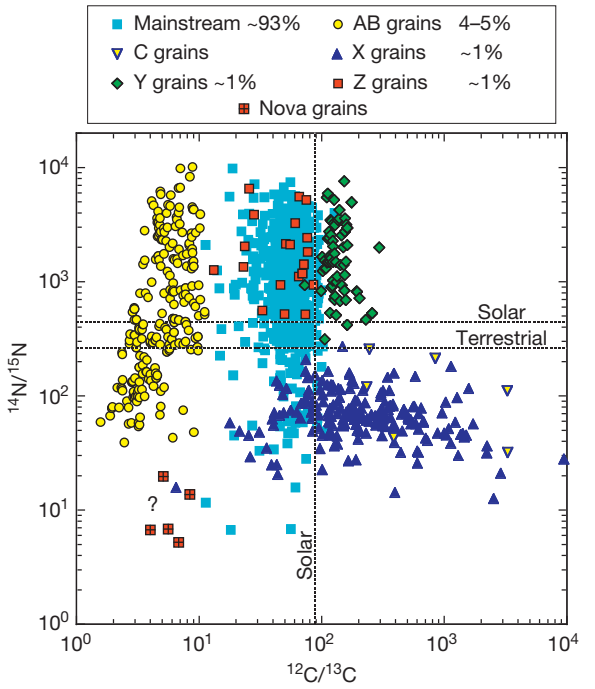

Figure 3 Nitrogen and carbon isotopic ratios of individual presolar SiC grains. Because rare grain types were located by automatic ion imaging, the numbers of grains of different types in the plot do not correspond to their abundances in the meteorites; these abundances are given in the legend. The grain plotted as a question mark in this figure and in **Figures 4** and **5** has both nova and SN signatures (Nittler and Hoppe, 2005). The analysis of solar wind implanted into Genesis samples showed that the Sun's nitrogen isotopic ratio is different from the terrestrial ratio (Marty et al., 2011). Both are indicated in the figure. Source: Presolar database (Hynes and Gyngard, 2009).

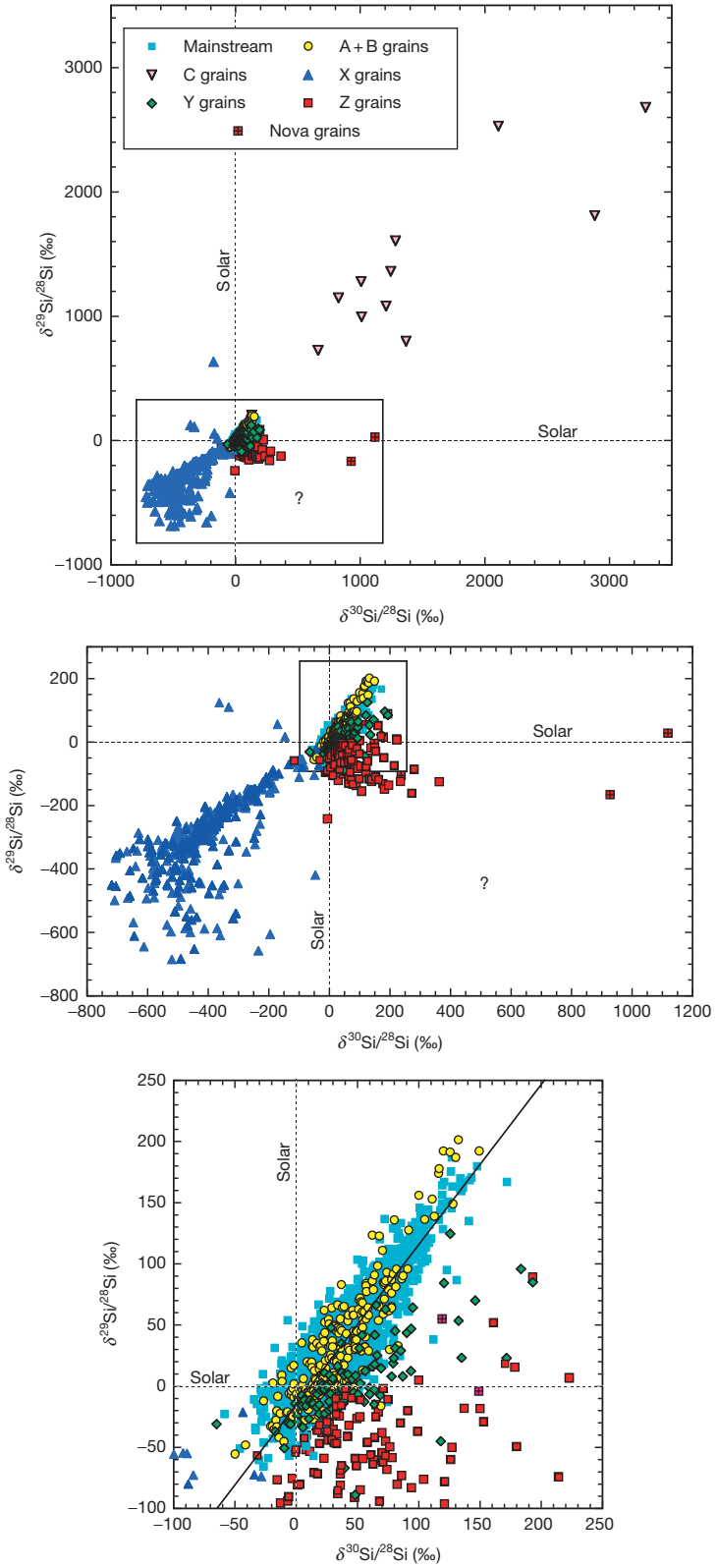

Figure 4 Silicon isotopic ratios of different types of presolar SiC grains plotted as δ-values, deviations in per mill (‰) from the solar ratios: $\delta^{i}Si/^{28}Si = \{(^{i}Si/^{28}Si)_{meas}/(^{i}Si/^{28}Si)_{\odot} - 1\} \times 1000$. Mainstream grains plot along a line of slope 1.4 (solid line). Symbols are the same as those in **Figure 3**. Source: Presolar database (Hynes and Gyngard, 2009).

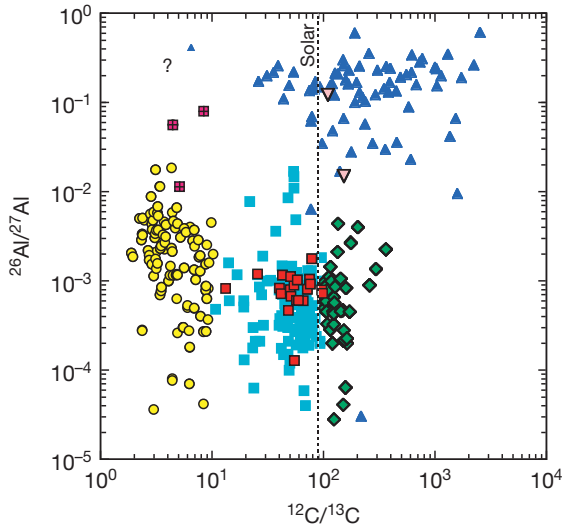

Figure 5 Aluminum and carbon isotopic ratios of individual presolar SiC grains. Symbols for the data are the same as those for **Figures 3** and **4**. Source: Presolar database (Hynes and Gyngard, 2009).

elements (e.g., Busso et al., 2001), and the *s*-process isotopic patterns of the heavy elements exhibited by mainstream SiC provide the most convincing argument for their origin in carbon stars (see succeeding text).

1.4.6.1 Mainstream Grains

Mainstream grains have $^{12}C/^{13}C$ ratios between 10 and 100 (**Figure 3**). They have carbon and nitrogen isotopic compositions that are roughly in agreement with an AGB origin. There exist too many carbon and nitrogen isotopic analyses of mainstream grains to list them individually. I thus refer to the presolar grain database (Hynes and Gyngard, 2009). Carbon-13 and ^{15}N excesses relative to solar are the signature of hydrogen burning via the CNO cycle that occurred during the main sequence phase of the stars. Material having undergone the CNO cycle is brought to the star's surface by the first (and second) dredge-up. The carbon isotopic ratios are also affected by shell helium burning and the third dredge-up during the TP-AGB phase (Busso et al., 1999; Herwig, 2005). This process adds ^{12}C to the envelope, increases the $^{12}C/^{13}C$ ratio from the low values resulting from the first dredge-up, and by making $C > O$, causes the star to become a carbon star.

Envelope $^{12}C/^{13}C$ ratios predicted by canonical stellar evolution models range from ~20 after first dredge-up in the RG phase to ~300 in the late TP-AGB phases of solar-metallicity stars (Amari et al., 2001b; El Eid, 1994; Gallino et al., 1994) and to several thousand in low-metallicity stars (Nittler et al., 2005c; Zinner et al., 2006d). Predicted $^{14}N/^{15}N$ ratios range from 600 to 1600 (Becker and Iben, 1979; El Eid, 1994), falling short of the range observed in the grains. However, the assumption of deep mixing ('cool-bottom processing') of envelope material to deep hot regions close to the H-burning shell in $M < 2.5\ M_\odot$ stars during their RG and AGB phases (Charbonnel, 1995; Langer et al., 1999; Nollett et al., 2003; Palmerini et al., 2011; Wasserburg et al., 1995) results in partial hydrogen burning, with higher $^{14}N/^{15}N$ and lower

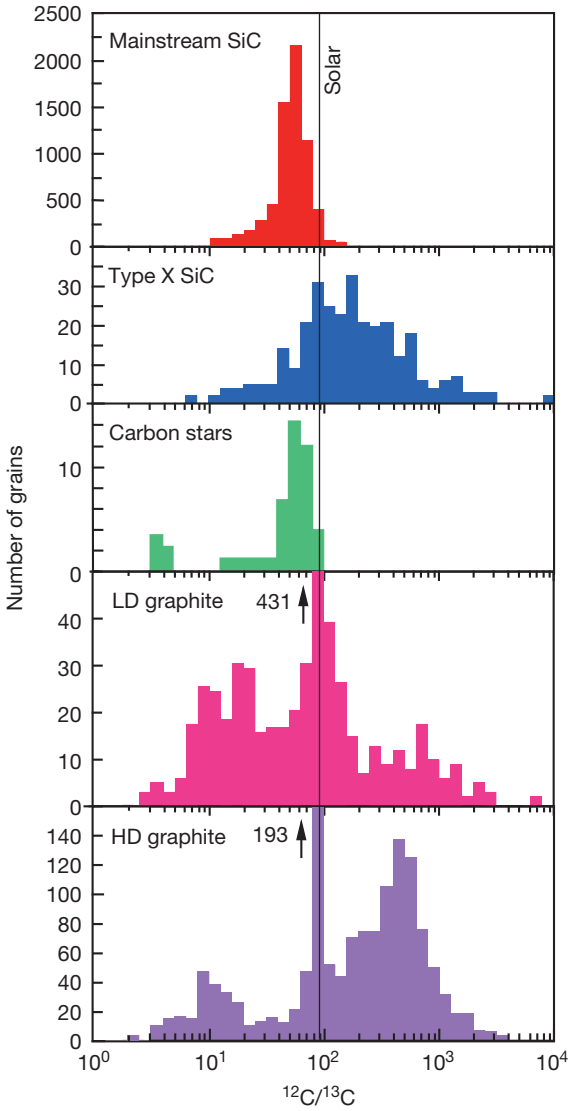

Figure 6 The distributions of carbon isotopic ratios measured in presolar SiC and graphite grains are compared to astronomical measurements of the atmospheres of carbon stars (Lambert et al., 1986). Source of grain data: presolar database (Hynes and Gyngard, 2009).

$^{12}C/^{13}C$ ratios in the envelope than in canonical models (see also Huss et al., 1997). However, the low $^{14}N/^{15}N$ ratios observed in a fraction of mainstream grains (**Figure 3**) remain unexplained (Palmerini et al., 2011).

Two other isotopes that are a signature for AGB stars are ^{26}Al and ^{22}Ne. **Figure 5** shows inferred $^{26}Al/^{27}Al$ ratios in different types of SiC grains. The existence of the short-lived radioisotope ^{26}Al ($T_{1/2} = 7.3 \times 10^5$ years) is inferred from large ^{26}Mg excesses. Aluminum-26 is produced in the hydrogen-burning shell by proton capture on ^{25}Mg and mixed to the surface by the third dredge-up (Forestini et al., 1991; Karakas and Lattanzio, 2003; Mowlavi and Meynet, 2000). It can also be produced during 'hot-bottom burning' (Lattanzio et al., 1997), but this process is believed to prevent carbon-star formation (Frost and Lattanzio, 1996). Neon-22, the main

component in Ne–E, is produced in the helium shell by $^{14}N + 2\alpha$. The neon isotopic ratios measured in SiC bulk samples (Lewis et al., 1990, 1994) are very close to those expected for helium-shell material (Gallino et al., 1990). In contrast to krypton and xenon and heavy refractory elements, neon and helium and argon show very little dilution of helium-shell material with envelope material, indicating a special implantation mechanism by an ionized wind (Verchovsky and Wright, 2004; Verchovsky et al., 2004). Another piece of evidence that the Ne–E(H) component originated from the helium shell of AGB stars and not from the decay of ^{22}Na (Clayton, 1975) is the fact that in individual grains, of which only ~5% carry ^{22}Ne, it is always accompanied by ^{4}He (Heck et al., 2006, 2007; Nichols et al., 1995).

Excesses in ^{21}Ne in SiC relative to the predicted helium-shell composition have been interpreted as being due to spallation by galactic cosmic rays (Lewis et al., 1990, 1994; Tang and Anders, 1988a), which allows the determination of grain lifetimes in the IS medium. Inferred exposure ages depend on grain size and range from 10 to 130 Ma (Lewis et al., 1994). However, this interpretation has been challenged (Ott and Begemann, 2000) because recoil loss of neon from SiC grains is higher than assumed. Ott et al. (2005) recently determined recoil losses of xenon isotopes and concluded that most of spallation xenon (from barium) is retained in 1 μm large SiC grains. Based on the amount of ^{126}Xe present in >1 μm grains, they conclude that exposure ages of such grains are smaller than 40 Ma and are smaller than ~175 Ma for submicrometer grains, much shorter than theoretically expected lifetimes of IS grains (Jones et al., 1997). Recently, Gyngard et al. (2009a,b,c) found ^{6}Li excesses in large SiC grains ranging up to 50 μm in size. They interpreted these excesses as being produced by spallation from galactic cosmic rays and derived exposure ages ranging from 30 to 1000 Ma. Heck et al. (2009c) measured helium and neon isotopes in large SiC grains from the same size fraction (although not the same grains analyzed by Gyngard et al.) and obtained exposure ages ranging from 10 to 1000 Ma. Although recoil corrections appear to be well understood (Ott et al., 2009), the ages derived from the noble gases tend to be on average smaller than those derived from lithium.

The silicon isotopic compositions of most mainstream grains are characterized by enrichments in the heavy silicon isotopes of up to 200‰ relative to their solar abundances (**Figure 4**). In a silicon three-isotope plot, the data fall along a line with slope 1.35, which is shifted slightly to the right of the solar system composition. In contrast to the light elements carbon, nitrogen, neon, and aluminum and the heavy elements (see succeeding text), the silicon isotopic ratios of mainstream grains cannot be explained by nuclear processes taking place within their parent stars. In AGB stars, the silicon isotopes are affected by neutron capture in the helium shell leading to excesses in ^{29}Si and ^{30}Si along a slope 0.2–0.5 line in a δ-value silicon three-isotope plot (Amari et al., 2001b; Brown and Clayton, 1992; Gallino et al., 1990, 1994; Lugaro et al., 1999; Nittler and Alexander, 2003; Zinner et al., 2006d). Predicted excesses are only on the order of 20‰ in low-mass AGB stars of close to solar metallicity (metallicity is the abundance of all elements heavier than He). This led to the proposal that many stars with varying initial silicon isotopic compositions contributed SiC grains to the solar system (Alexander, 1993; Clayton et al., 1991) and that neutron-capture nucleosynthesis in these stars only plays a secondary role in modifying these compositions. Several explanations have been given for the initial silicon ratios in the parent stars, which in their late stages of evolution became the carbon stars that produced the SiC. One is the evolution of the silicon isotopic ratios through galactic history as different generations of supernovae produced silicon with increasing ratios of the secondary isotopes ^{29}Si and ^{30}Si to the primary ^{28}Si (Clayton and Timmes, 1997a,b; Gallino et al., 1994; Timmes and Clayton, 1996). Clayton (1997) addressed the problem that most SiC grains have higher than solar ^{29}Si/^{28}Si and ^{30}Si/^{28}Si ratios by considering the possibility that the mainstream grains originated from stars that were born in central, more metal-rich regions of the galaxy and moved to the molecular cloud from which our Sun formed. Alexander and Nittler (1999), alternatively, suggested that the Sun has an atypical silicon isotopic composition. Lugaro et al. (1999) explained the spread in the isotopic compositions of the parent stars by local heterogeneities in the galaxy caused by the stochastic nature of the admixture of the ejecta from supernovae of varying type and mass. Finally, Clayton (2003) invoked merger of our galaxy, assumed to have high metallicity, with a satellite galaxy of low metallicity some time before solar system formation to account for the silicon isotopic ratios of mainstream grains. A detailed discussion of the role of galactic chemical evolution for the silicon isotopic ratios in SiC grains from AGB stars is found in Nittler and Dauphas (2006).

Titanium isotopic ratios in single grains (Alexander and Nittler, 1999; Hoppe et al., 1994; Huss and Smith, 2007; Ireland et al., 1991; Zinner et al., 2007) and in bulk samples (Amari et al., 2000) show excesses in all isotopes relative to ^{48}Ti, a result expected of neutron capture in AGB stars. However, as for silicon, theoretical models (Lugaro et al., 1999) cannot explain the range of ratios observed in single grains. Furthermore, titanium ratios are correlated with those of silicon, also indicating that the titanium isotopic compositions are dominated by galactic evolution effects (Alexander and Nittler, 1999; Huss and Smith, 2007; Zinner et al., 2007). However, local heterogeneity cannot explain the correlations between titanium isotopic ratios, and the correlations between titanium and silicon isotopic ratios imply that at most 40% of the range of isotopic ratios in the grains can be accounted for by heterogeneous mixing of SN ejecta (Nittler, 2005). Excesses of ^{42}Ca and ^{43}Ca relative to ^{40}Ca observed in bulk samples (Amari et al., 2000) agree with predictions for neutron capture. Large ^{44}Ca excesses are apparently due to the presence of type X grains (see succeeding text).

All heavy elements measured so far for their isotopic ratios show the signature of the *s*-process (**Figure 7**, see also **Figure 10**). They include not only the noble gases krypton and xenon (Lewis et al., 1990, 1994) but also the heavy elements strontium (Podosek et al., 2004), silver (Ott et al., 2006), barium (Ott and Begemann, 1990; Prombo et al., 1993; Yin et al., 2006; Zinner et al., 1991), neodymium and samarium (Richter et al., 1993; Yin et al., 2006; Zinner et al., 1991), dysprosium (Richter et al., 1994; Yin et al., 2006), and erbium (Yin et al., 2006). Although most measurements were made on bulk samples, it is clear that mainstream grains dominate. Of interest are measurements by ICP-MS where the mass spectrometer can be rapidly

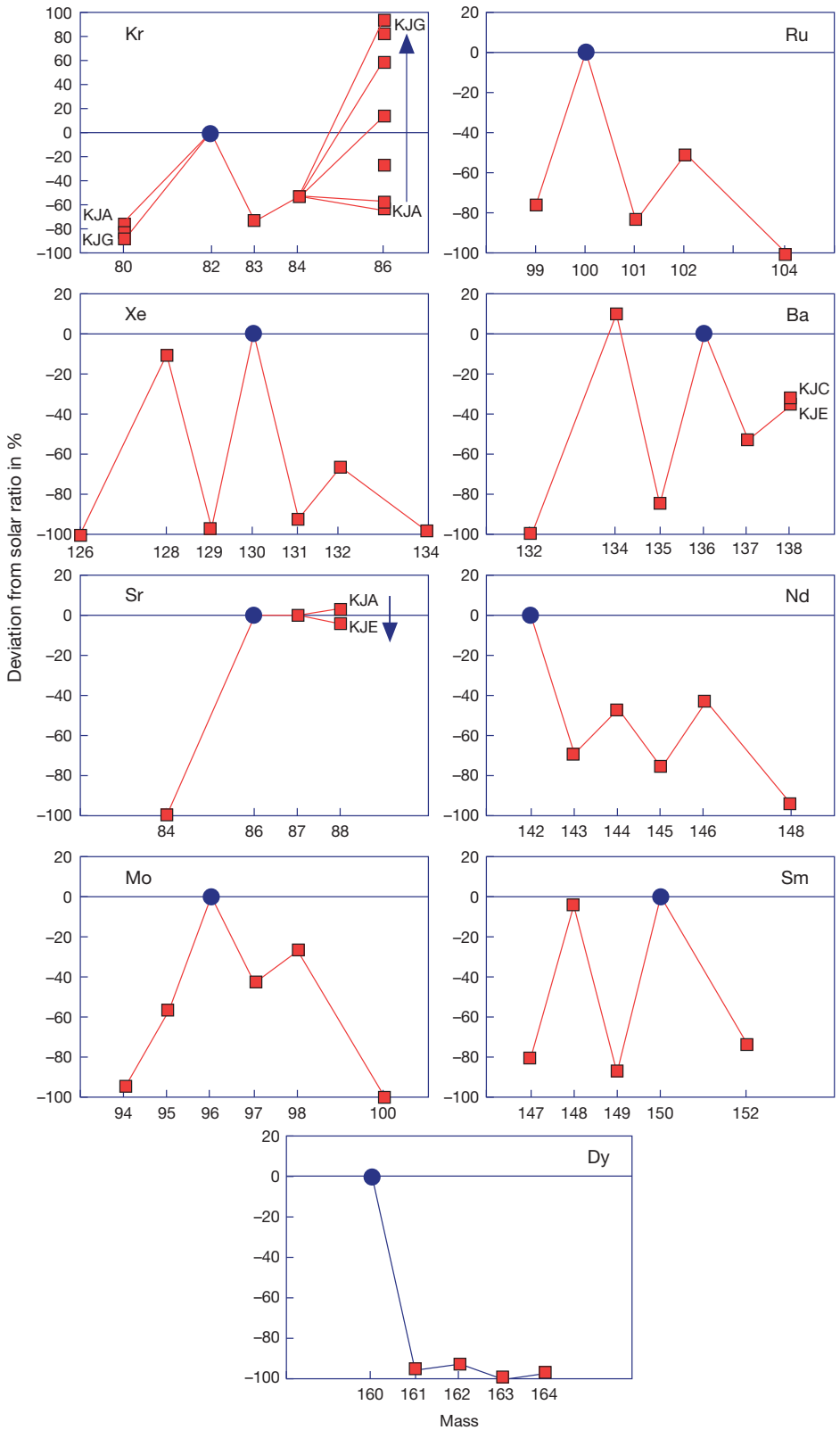

Figure 7 Isotopic patterns measured in bulk samples and individual grains of SiC extracted from the Murchison meteorite. Isotopic ratios are relative to the reference isotope plotted as a solid circle and are normalized to the solar isotopic ratios. Plotted are the pure *s*-process ratios, also called the G-component, that exist in the helium shell of AGB stars. The ratios measured in SiC are a mix of the G- and the N-components; the N-component is similar to, but not exactly the same as, the solar isotopic composition of a given element. For details see Hoppe and Ott (1997). Data are from Lewis et al. (1994) (Kr and Xe), Podosek et al. (2004) (Sr), Prombo et al. (1993) (Ba), Richter et al. (1993) (Nd and Sm), Richter et al. (1994) (Dy), Lugaro et al. (2003) (Mo), and Savina et al. (2004) (Ru).

scanned over a large mass range (Ott et al., 2006; Yin et al., 2006). In spite of limitations (the sample used was a nanodiamond residue and contained SiC only as contamination, and isobaric interferences could not be resolved), a mass scan from barium to hafnium shows *s*-process signatures not only in certain isotopic ratios but also in elemental abundances. In addition to barium and neodymium, where isotopic ratios are in agreement with previous TIMS results, the first results for erbium show also good agreement with theoretical predictions (Arlandini et al., 1999). Dysprosium isotopic ratios also agree with theoretical calculations but are in marked contrast to TIMS results (Richter et al., 1994), casting doubt on the latter. There is a hint of the initial presence of short-lived ^{107}Pd ($T_{1/2} = 6.5 \times 10^6$ years) from ^{107}Ag excesses (Ott et al., 2006).

Single grain measurements of chromium (Levine et al., 2009; Savina et al., 2010), strontium (Nicolussi et al., 1998b), zirconium (Barzyk et al., 2007; Nicolussi et al., 1997), molybdenum (Barzyk et al., 2007; Nicolussi et al., 1998a), ruthenium (Savina et al., 2004), and barium (Barzyk et al., 2007; Savina et al., 2003a) have been made with RIMS and of barium (Avila et al., in press; Marhas et al., 2007), tungsten and hafnium (Avila et al., 2012b), and lead (Avila et al., 2012a) with SIMS. By selecting grains free of contamination by multielement RIMS analysis, Barzyk et al. (2007) could, from measured molybdenum (and barium) isotopic ratios, restrict the range of the so-called ^{13}C pocket to close to the standard case that best explains the main component of *s*-element in the solar system. The ^{13}C $(\alpha,n)^{16}$O reaction is the main neutron source in AGB stars. From systematic excesses in ^{99}Ru in single SiC grains, Savina et al. (2004) concluded that the grains contained short-lived ^{99}Tc ($T_{1/2} = 2.1 \times 10^5$ years) when they condensed. Large enrichments of certain heavy elements, such as yttrium, zirconium, barium, and cerium in single mainstream grains, also indicate large overabundances of *s*-process elements in the parent stars (Amari et al., 1995a; Kashiv, 2004; Kashiv et al., 2002). Kashiv et al. (2010) interpreted large Nb/Zr ratios compared to those expected from the condensation of these elements into SiC grains in the envelope of AGB stars as evidence for the initial presence of short-lived ^{93}Zr ($T_{1/2} = 1.5 \times 10^6$ years). For all the isotopic compositions of the elements listed earlier, there is good agreement with theoretical models of the *s*-process in low-mass AGB stars (Arlandini et al., 1999; Cristallo et al., 2009; Fazio et al., 2003; Gallino et al., 1993, 1997; Karakas, 2010; Karakas et al., 2010; Lugaro et al., 2003, 2004; Pignatari et al., 2003, 2004b). Discrepancies with earlier model calculations were caused by incorrect nuclear cross sections and could be resolved by improved experimental determinations (e.g., Guber et al., 1997; Koehler et al., 1998; Wisshak et al., 1997).

The *s*-process isotopic patterns observed in grains allow the determination of different parameters affecting the *s*-process, such as neutron exposure, temperature, and neutron density (Hoppe and Ott, 1997). Since these parameters depend in turn on stellar mass and metallicity, as well as on the neutron source operating in AGB stars, they allow information to be obtained about the parent stars of the grains. For example, the barium isotopic ratios indicate a neutron exposure that is only half of that inferred for the solar system (Gallino et al., 1993; Ott and Begemann, 1990). Another example is provided by the abundance of ^{96}Zr in single grains, which is sensitive to neutron density because of the relatively short half-life of ^{95}Zr (~64 days). While the ^{13}C$(\alpha,n)^{16}$O source with its low neutron density destroys ^{96}Zr, activation of the ^{22}Ne$(\alpha,n)^{25}$Mg source during later thermal pulses in AGB stars restores some of this isotope, whose abundance thus varies with pulse number. Some grains have essentially no ^{96}Zr, indicating that the ^{22}Ne $(\alpha,n)^{25}$Mg source was weak in their parent stars, pointing to low-mass AGB stars as the source of mainstream grains (Lugaro et al., 2003).

1.4.6.2 Type Y and Z Grains

Type Y grains have ^{12}C/^{13}C > 100 and silicon isotopic compositions that lie to the right of the mainstream correlation line (**Figures 3** and **4c**) (Amari et al., 2001b; Hoppe et al., 1994; Nittler and Alexander, 2003). Type Z grains have even larger ^{30}Si excesses relative to ^{29}Si and, on average, lower δ^{29}Si values than Y grains. However, they are distinguished from Y grains by having ^{12}C/^{13}C < 100 (Alexander, 1993; Hoppe et al., 1997; Nittler and Alexander, 2003). Comparison of the carbon, silicon, and titanium isotopic ratios of Y grains with models of nucleosynthesis indicates an origin in low- to intermediate-mass AGB stars with approximately half the solar metallicity (Amari et al., 2001b). Such stars dredge up more ^{12}C, and silicon and titanium that experienced neutron capture, from the helium shell (see also Lugaro et al., 1999). According to their silicon isotopic ratios, Z grains came from low-mass stars of even lower (approximately one-third solar) metallicity (Hoppe et al., 1997). This interpretation is in agreement with the large depletions in ^{46}Ti, ^{47}Ti, and ^{49}Ti relative to ^{48}Ti, which are correlated with depletions in ^{29}Si (Amari et al., 2005a; Zinner et al., 2007). The relative excesses in ^{30}Si and ^{50}Ti are explained by the effects of neutron capture, which are more pronounced in low-metallicity AGB stars (Zinner et al., 2006d, 2007). Additional support for an origin of Y and Z grains in low-metallicity AGB stars comes from zirconium and barium abundances, which are higher than those in mainstream grains (Hoppe et al., 2009b). Barium concentrations are correlated with silicon isotopic shifts attributed to neutron capture, in agreement with model predictions for 2–3 $M_\odot$ AGB stars of a third to a half solar metallicity.

In order to achieve the relatively low ^{12}C/^{13}C ratios of Z grains, the parent stars must have experienced cool-bottom processing (Karakas et al., 2010; Nollett et al., 2003; Wasserburg et al., 1995) during their RG and AGB phase (Nittler et al., 2005c; Zinner et al., 2006d). However, inferred ^{26}Al/^{27}Al ratios in Z grains (Hoppe et al., 2004; Zinner et al., 2007) are not higher than those in mainstream SiC grains (**Figure 5**), much lower than those in many presolar oxide grains, for which cool-bottom processing has been invoked (see **Section 1.4.9** and **Figure 15**). The parametric model for cool-bottom processing by Nollett et al. (2003) assumes two independent parameters: the circulation rate of material from the (cool) bottom of the convective envelope to deep hot regions and the temperature reached by this material. The former affects mostly the production of ^{13}C and destruction of ^{18}O, the latter mostly the production of ^{26}Al, which requires a much higher temperature. Accordingly, cool-bottom processing in the parent stars of Z grains must have occurred with a high circulation rate but of low temperature.

Nittler et al. (2005c) and Zinner et al. (2006d) compared the carbon and silicon isotopic compositions of mainstream, Y, and Z grains with new theoretical models of AGB nucleosynthesis. They concluded that cool-bottom burning on the AGB was necessary to explain the carbon ratios and that the recent silicon neutron capture cross sections by Guber et al. (2003) yield a better fit to the silicon isotopic ratios. From the theoretically inferred metallicities and average silicon isotopic ratios of mainstream, Y, and Z grains, Zinner et al. (2001, 2006d) and Nittler et al. (2005c) derived the galactic evolution of the silicon isotopic ratios as function of metallicity. This evolution differs from the results of galactic evolution models based on the yields of supernovae (Timmes and Clayton, 1996) and has important implications concerning the relative contributions from Type II and Type Ia supernovae during the history of our galaxy.

1.4.6.3 Type AB Grains

Grains of type AB have $^{12}C/^{13}C < 10$, but their silicon isotopic ratios plot along the mainstream line (**Figures 3** and **4**). In contrast to mainstream grains, many AB grains have lower than solar $^{14}N/^{15}N$ ratios (Amari et al., 2001c; Hoppe et al., 1995, 1996a; Huss et al., 1997; Nittler and Alexander, 2003). On average, they have higher $^{26}Al/^{27}Al$ ratios than mainstream, Y, and Z grains (**Figure 5**). While the isotopic ratios of the latter grains find an explanation in nucleosynthetic models of AGB stars, a satisfactory explanation of the data in terms of stellar nucleosynthesis is more elusive for the AB grains. The low $^{12}C/^{13}C$ ratios of these grains combined with the requirement for a carbon-rich environment during their formation indicate helium burning followed by limited hydrogen burning in their stellar sources. However, the astrophysical sites for this process are not well known. There might be two different kinds of AB grains with corresponding different stellar sources (Amari et al., 2001c). Grains with no *s*-process enhancements (Amari et al., 1995a; Pellin et al., 2000b; Savina et al., 2003c) probably come from J-type carbon stars that also have low $^{12}C/^{13}C$ ratios (Lambert et al., 1986). Unfortunately, J stars are not well understood and there are no astronomical observations of nitrogen isotopic ratios in such stars. Furthermore, the low $^{14}N/^{15}N$ ratios observed in some of the grains and the carbon-rich nature of their parent stars appear to be incompatible with the consequences of hydrogen burning in the CNO cycle, which seems to be responsible for the low $^{12}C/^{13}C$ ratios of J stars and the grains. AB grains with *s*-process enhancements might come from post-AGB stars that undergo a very late thermal pulse. An example of such a star is Sakurai's object (e.g., Asplund et al., 1999; Herwig, 2001b; Herwig et al., 2004, 2011). However, grains with low $^{14}N/^{15}N$ ratios pose a problem. Huss et al. (1997) proposed that the currently used $^{18}O(p,\alpha)^{15}N$ reaction rate (Caughlan and Fowler, 1988) is too low by a factor of 1000. This would result in low $^{12}C/^{13}C$ and $^{14}N/^{15}N$ ratios if an appropriate level of cool-bottom processing is considered. However, a recently determined $^{18}O(p,\alpha)^{15}N$ reaction rate (La Cognata et al., 2008, 2010) is very similar to the old Caughlan and Fowler value and has an uncertainty of less than a factor of two, eliminating this explanation for low $^{14}N/^{15}N$ ratios. One AB grain shows excesses in the *p*-process isotopes ^{92}Mo, ^{94}Mo, ^{96}Ru, and ^{98}Ru and in the *r*-process isotopes ^{100}Mo and ^{104}Ru (Savina et al., 2003c, 2007), and another grain shows a molybdenum isotopic pattern similar to those found in X grains (**Figure 10**), indicating a neutron burst. While these signatures indicate a SN origin, the carbon and silicon isotopic ratios of AB grains are difficult to reconcile with such an origin. The authors suggest material transfer in a binary star system. TEM studies identified subgrains of oldhamite (CaS) in an AB grain (Hynes et al., 2011). The oldhamite is epitaxially aligned with SiC. One of the CaS grains has a marginal ^{34}S excess.

1.4.6.4 Type X Grains

Although SiC grains of type X account for only 1% of presolar SiC, a fairly large number can be located by ion imaging (Besmehn and Hoppe, 2003; Hoppe et al., 1996b, 2000; Lin et al., 2002; Nittler et al., 1997) or automatic isotopic measurements (Gyngard et al., 2010a; Hoppe et al., 2009a, 2010, 2012; Nittler and Alexander, 2003; Zinner et al., 2010). X grains are characterized by mostly ^{12}C and ^{15}N excesses relative to solar (**Figures 3** and **6**), excesses in ^{28}Si (**Figure 4**), and very large $^{26}Al/^{27}Al$ ratios ranging up to 0.6 (**Figure 5**). About 10–20% of the grains show large ^{44}Ca excesses, which must come from the decay of short-lived ^{44}Ti ($T_{1/2} = 60$ a) (Amari et al., 1992; Besmehn and Hoppe, 2003; Hoppe et al., 1996b, 2000; Lin et al., 2010; Nittler et al., 1996). Inferred $^{44}Ti/^{48}Ti$ ratios range up to 0.6 (**Figure 8**). Although the data are limited, ion images (Besmehn and Hoppe, 2003) and variations in the titanium ion signal in-depth profiles during titanium isotopic measurements in the NanoSIMS (Lin et al., 2010) indicate the presence of titanium-rich subgrains, most likely TiC. A TiC subgrain was identified by TEM analysis in an X grain (Hynes et al., 2010). Because ^{44}Ti can only be produced in SN explosions (Timmes et al., 1996), grains with evidence for ^{44}Ti, and by implication all X grains, must have an SN origin. In Type II supernovae, ^{44}Ti is produced in the nickel- and silicon-rich inner zones (see **Figure 9**) (Timmes et al., 1996; Woosley and Weaver, 1995). Silicon in the Si/S zone consists of almost pure ^{28}Si. Also the other isotopic signatures of X grains are compatible with an origin in Type II supernovae: high $^{12}C/^{13}C$ and low $^{14}N/^{15}N$ ratios are the signature of helium burning (**Figure 9**), and high $^{26}Al/^{27}Al$ ratios can be reached in the He/N zone by hydrogen burning.

However, these isotopic signatures occur in massive stars in very different stellar zones, which experienced different stages of nuclear burning before the SN explosion (**Figure 9**) (e.g., Rauscher et al., 2002; Woosley and Weaver, 1995). The isotopic signatures of the X grains suggest deep and inhomogeneous mixing of matter from these different zones in the SN ejecta. While the titanium and silicon isotopic signature of the X grains require contributions from the Ni, O/Si, and Si/S zones that experienced silicon-, neon-, and oxygen-burning, significant contributions must also come from the He/N and He/C zones that experienced hydrogen and incomplete helium burning in order to achieve C > O, the condition for SiC condensation (Larimer and Bartholomay, 1979; Lodders and Fegley, 1997). Furthermore, addition of material from the intermediate oxygen-rich layers must be severely limited. Astronomical observations indicate extensive mixing of SN ejecta (e.g., Ebisuzaki and Shibazaki, 1988; Hughes et al., 2000; Kifonidis et al., 2003)

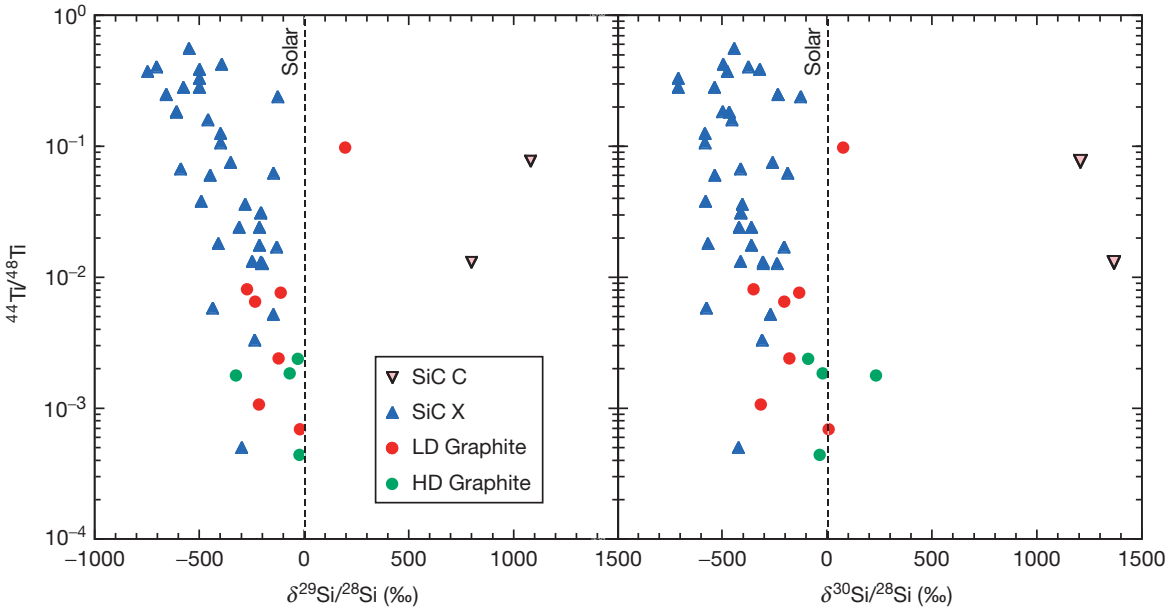

Figure 8 $^{44}Ti/^{48}Ti$ ratios are inferred from ^{44}Ca excesses in SiC grains of type X and C and, in graphite grains, are plotted against silicon isotopic ratios. Source: Presolar database (Hynes and Gyngard, 2009).

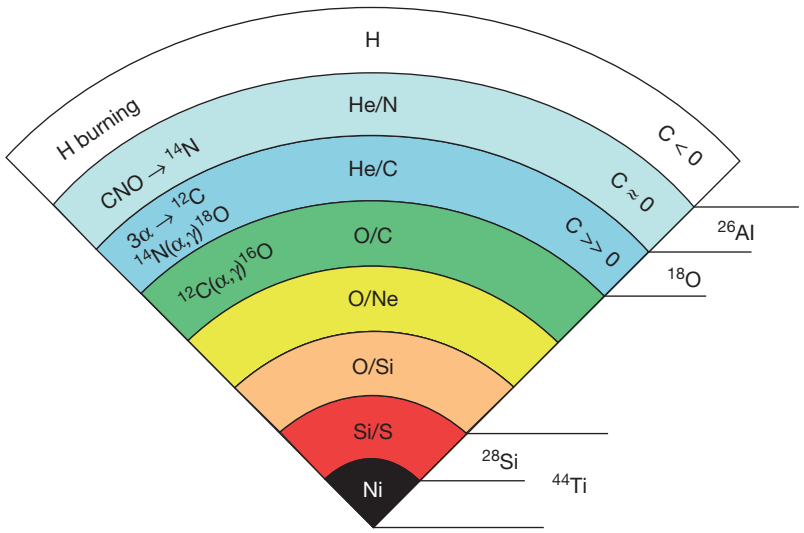

Figure 9 Schematic structure of a massive star before its explosion as a Type II supernova (source: Woosley and Weaver, 1995). Such a star consists of different layers, labeled according to their most abundant elements, that experienced different stages of nucleosynthesis. Indicated are dominant nuclear reactions in some layers and the layers in which isotopes abundant in grains of an inferred SN origin are produced.

and hydrodynamic models of SN explosions predict mixing in the ejecta initiated by the formation of Rayleigh–Taylor instabilities (e.g., Herant et al., 1994). However, it still has to be seen whether mixing can occur on a microscopic scale and whether these instabilities allow mixing of matter from non-neighboring zones while excluding large contributions from the intermediate oxygen-rich zones. Recent three-dimensional SN models show that material from inner zones penetrates outer layers (Hammer et al., 2010), thus mixing from inner zones with outer carbon-rich zones seems possible. Clayton et al. (1999) and Deneault et al. (2003, 2006) suggested condensation of carbonaceous phases in Type II SN ejecta even while C < O because of the destruction of CO in the high-radiation environment of the ejecta. It is doubtful whether SiC can condense from a gas with C < O (Ebel and Grossman, 2001) and the isotopic ratios in X grains do not agree with this scenario (Lin et al., 2010). Even for graphite, the presence of subgrains of elemental iron inside of graphite grains whose isotopic signatures indicate an SN origin argues against formation in an oxygen-rich environment (Croat et al., 2003). Furthermore, the isotopic compositions in low-density (LD) graphite grains do not support Clayton's model (Clayton, 2011). According to this, model grains must

condense in a narrow region at the inner O/Si zone in order to include the ^{28}Si and ^{44}Ti found in these grains. However, the isotopic ratios of the stable titanium isotopes measured in the grains (Jadhav et al., 2013; Travaglio et al., 1999) are completely different from predicted ratios from SN models (Rauscher et al., 2002). In order to account for ^{18}O excesses and high-inferred ^{26}Al/^{27}Al ratios, Clayton proposes that carbonaceous grains collect material from the He/C and He/N zones when they traverse material from these zones. However, the finding of correlated large ^{15}N and ^{18}O excesses in the interior of LD graphite grains (Groopman et al., 2012) shows that the Clayton model cannot be correct.

Although multizone mixing models can qualitatively reproduce the isotopic signatures of X grains (Yoshida, 2007; Yoshida and Hashimoto, 2004), several ratios, in particular the large ^{15}N excesses and excesses of ^{29}Si over ^{30}Si found in most grains, cannot be explained quantitatively and indicate deficiencies in the existing models (Lin et al., 2010). The latter is a long-standing problem: SN models cannot account for the solar ^{29}Si/^{30}Si ratio (Timmes and Clayton, 1996). Lin et al. (2010) distinguished between three types of X grains: a handful of X0 grains having ^{29}Si excesses and ^{30}Si deficits; X1 grains in the main trend, with δ^{29}Si/δ^{30}Si of ~0.65; and X2 grains plotting below the X1 grains on a three-isotope δ-value plot (see also Nittler and Alexander, 2003). Explaining the correlation line of the X1 grains requires a silicon isotopic component with ^{29}Si/^{28}Si ~ 0.024 (the solar ratio is 0.051) and essentially no ^{30}Si. Supernova models do not produce such a composition (Lin et al., 2010). Hoppe et al. (2009a) explained the silicon isotopic composition of an X0 grain (δ^{29}Si = 634‰, δ^{30}S = −177‰) by mixing material from the O/Si and Si/S zones and assuming that the ^{29}S in the O/Si zone is twice that of the 15 $M_\odot$ Rauscher et al. (2002) SN model.

Some SiC X grains also show large excesses in ^{49}Ti (Amari et al., 1992; Hoppe and Besmehn, 2002; Lin et al., 2010; Nittler et al., 1996). The correlation of these excesses with the V/Ti ratio (Hoppe and Besmehn, 2002) indicates that they come from the decay of short-lived ^{49}V ($T_{1/2}$ = 330 days) and that the grains must have formed within a few months of the explosion. Vanadium-49 is produced in the Si/S zone that contains almost pure ^{28}Si. However, Lin et al. (2010) showed that not all ^{49}Ti excesses in X grains can be attributed to ^{49}V decay, and material from the He/C zone, where ^{49}Ti excesses are the result of neutron capture, is needed to explain some grains. Marhas et al. (2008) reported the first iron and nickel isotopic measurements in X grains. They found substantial ^{57}Fe, ^{61}Ni, and ^{62}Ni excesses, as well as small ^{60}Ni excesses. These signatures indicate contribution from the He/C zone. What is puzzling is the lack of large ^{54}Fe excesses, predicted for material from the Si/S zone. The authors invoke elemental fractionation between iron and silicon from this zone, possible by the formation of FeS grains. Iron-57 deficits seen in some grains can be achieved by contribution of material from the Fe–Ni core, but the predicted effects in the nickel isotopes are not seen. It was also found in this study that nickel is uniformly distributed throughout the grain, whereas iron is concentrated in subgrains, some of which have larger ^{57}Fe excesses than the rest of the SiC grains. Iron- and nickel-rich subgrains were found in a TEM study of X grains and were identified as silicide grains with large variations in the Fe/Ni ratio (Hynes et al., 2010). After several unsuccessful attempts to analyze sulfur in X grains, ^{32}S excesses have recently been detected (Hoppe and Zinner, 2012; Hoppe et al., 2012). Sulfur-32 excesses are expected because the Si/S zone contains almost monoisotopic ^{28}Si and ^{32}S.

RIMS isotopic measurements of iron, strontium, zirconium, molybdenum, ruthenium, and barium have been made on X grains (Davis et al., 2002; Pellin et al., 1999, 2000a, 2006). The most complete and interesting are the molybdenum measurements, which reveal large excesses in ^{95}Mo and ^{97}Mo. **Figure 10** shows the molybdenum isotopic patterns of a mainstream and an X grain. The mainstream grain has a typical *s*-process pattern, in agreement with bulk measurements of other heavy elements, such as xenon, barium, and neodymium (**Figure 7**). The molybdenum pattern of the X grain, on the other hand, is completely different and indicates neutron capture at much higher neutron densities. While it does not agree with the pattern expected for the *r*-process, it is successfully explained by a neutron-burst model (Meyer et al., 2000). In the Type II SN models by Rauscher et al. (2002), an intense neutron burst is predicted to occur in the oxygen layer just below the He/C zone, accounting for the molybdenum isotopic patterns observed in X grains. The isotopic patterns in other elements, such as large excesses in ^{58}Fe, ^{88}Sr, ^{96}Zr, and ^{138}Ba, and depletions in ^{90}Zr and ^{100}Ru (Pellin et al., 2006) are consistent with a neutron-burst origin.

Type Ia supernovae offer an alternative explanation for the isotopic signature of X grains. In the model by Clayton et al.

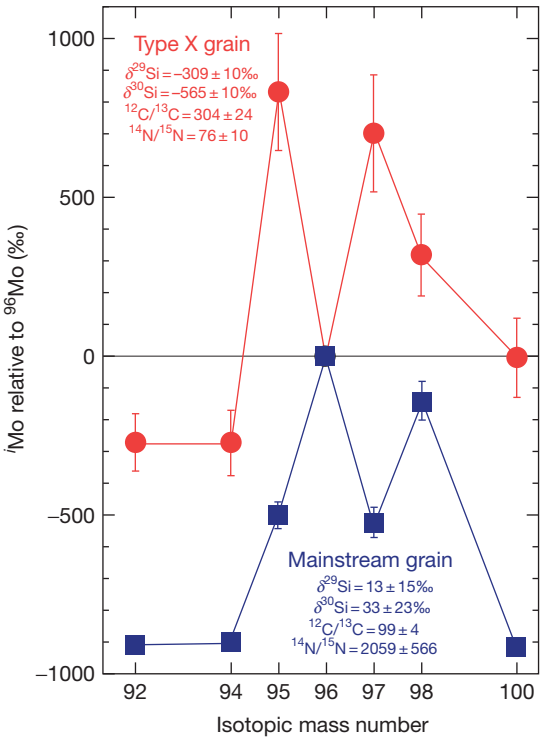

Figure 10 Molybdenum isotopic patterns measured by RIMS in a type X and a mainstream SiC grain. Reproduced from Pellin MJ, Davis AM, Lewis RS, Amari S, and Clayton RN (1999) Molybdenum isotopic composition of single silicon carbide grains from supernovae. *Lunar and Planetary Science* 30, 1969.

(1997), nucleosynthesis takes place by explosive helium burning of a helium cap on top of a white dwarf. This process produces most of the isotopic signatures of the SN grains. The isotopes ^{12}C, ^{15}N, ^{26}Al, ^{28}Si, and ^{44}Ti are all made by helium burning during the explosion, which makes the transport of ^{28}Si and ^{44}Ti through the massive oxygen-rich zone into the overlying carbon-rich zones of a Type II SN unnecessary. Mixing is limited to material from helium burning and to matter that experienced CNO processing. The best match with the X grain data, however, is achieved for mixing scenarios that yield O > C (Amari et al., 1998). Other problems include the questions whether high enough gas densities can be achieved in the ejecta for the condensation of micrometer-sized grains and whether Type Ia supernovae can generate a neutron burst necessary for the molybdenum isotopic pattern. More work is needed to decide whether a Type Ia SN origin for X grains is a realistic alternative.

TEM studies of X grains (Hynes et al., 2006, 2010; Stroud et al., 2004b) indicate a polycrystalline composition with crystallite sizes ranging from 10 to 200 nm. This is in marked contrast to the structure of most mainstream grains, which consist of single, twinned, or otherwise defect-laden crystals (Daulton et al., 2002, 2003; Stroud et al., 2004b) or, if polycrystalline, have much large domains than X grains (Hynes et al., 2010).

1.4.6.5 Nova Grains

A few grains have isotopic ratios that are best explained by a nova origin (Amari et al., 2001a; José and Hernanz, 2007). These grains have low $^{12}C/^{13}C$ and $^{14}N/^{15}N$ ratios (**Figure 3**), large ^{30}Si excesses (**Figure 4**), and high $^{26}Al/^{27}Al$ ratios (**Figure 5**). All these features are predicted to be produced by explosive hydrogen burning taking place in classical novae (e.g., José and Hernanz, 2007; José et al., 1999, 2003, 2004; Kovetz and Prialnik, 1997; Starrfield et al., 1998), but the predicted anomalies are much larger than those found in the grains, and the nova ejecta have to be mixed with material of close-to-solar isotopic compositions. A comparison of the data with the models implicates ONe novae with a white dwarf mass of at least 1.25 $M_\odot$ as the most likely sources (Amari et al., 2001a; José and Hernanz, 2007). Nittler and Hoppe (2005) identified a SiC grain with carbon and nitrogen isotopic ratios within the range spanned by nova candidate grains (**Figure 3**). However, this grain has a large ^{28}Si and ^{49}Ti excess and an $^{26}Al/^{27}Al$ ratio of 0.4 (**Figure 5**) and is almost certainly an SN grain. Another grain with small carbon and nitrogen isotopic ratios has a large ^{29}Si depletion and ^{30}Si excess, a ^{47}Ti excess, and a high $^{26}Al/^{27}Al$ ratio. It might be an SN grain as well, but in **Figures 3–5**, it is plotted as a question mark.

1.4.6.6 Type C Grains

A new type of SiC grains has been named type C grains (Croat et al., 2010). These grains have large excesses in ^{29}Si and ^{30}Si, larger than those in mainstream and AB grains (see **Figure 4**). The first such grain was identified by Amari et al. (1999). The grains found by Croat et al. (2010) were SiC subgrains within a high-density (HD) graphite grain from the Murchison density fraction KFC1. Additional type C grains were found during automatic grain searches in the NanoSIMS (Gyngard et al., 2010a; Hoppe et al., 2010, 2012; Zinner et al., 2010). These grains are very rare, constituting ~1‰ of all SiC grains. Most grains identified so far are small (<1 μm), but this might be the consequence of the fact that grain searches were made on small grains. Most type C grains have light carbon and heavy nitrogen, the signature of most X grains (**Figure 3**). Two grains were analyzed for ^{26}Al–^{26}Mg and have relatively high-inferred $^{26}Al/^{27}Al$ ratios (**Figure 5**). The same grains show evidence for the initial presence of ^{44}Ti (Hoppe et al., 2012). All these signatures indicate an SN origin of type C grains. What is puzzling, however, is that six grains analyzed for sulfur show an ^{32}S excess. The only SN zone with large ^{32}S excesses is the Si/S zone that has large ^{28}Si excesses as well. Hoppe et al. (2012) invoke element fractionation between sulfur and silicon by molecule chemistry in the SN ejecta to explain this result.

Two unusual grains have extremely small $^{12}C/^{13}C$ ratios: The first ($^{12}C/^{13}C = 1.04$, $^{14}N/^{15}N = 6.7$, $\delta^{29}Si = 138‰$, $\delta^{30}Si = 313‰$, and $^{26}Al/^{27}Al = 0.03$) might have a nova origin (Nittler et al., 2006); the second ($^{12}C/^{13}C = 1.3$, $\delta^{29}Si = 313‰$, and $\delta^{30}Si = 377‰$) has a marginal ^{32}S excess ($\delta^{33}S = -227 \pm 161‰$, $\delta^{34}S = -96 \pm 74‰$; 1σ), indicating a possible SN origin (Hoppe et al., 2012).

1.4.6.7 Abundances and Grain-Size Effect

As long as SiC abundances were determined from chemical separates from meteorites, maximum abundances were thought to be around 10 ppm (Amari et al., 1994; Huss and Lewis, 1995; Huss et al., 2003). This changed with the identification of presolar SiC grains in polished sections of meteorites by automatic raster imaging searches in the NanoSIMS (Bose et al., 2012; Davidson et al., 2009; Floss and Stadermann, 2009b; Haenecour and Floss, 2012; Leitner et al., 2012b; Nguyen et al., 2010c; Zhao et al., 2011b). Abundances determined in this way were found to be much higher than those derived from noble gas analysis on residues (Davidson et al., 2009; Floss and Stadermann, 2009b). Abundances are especially high in the CR and CO meteorites, 135 ppm in the CR2 GRV021710 (Zhao et al., 2011b), 160 ppm in the CR3 NWA852 (Leitner et al., 2012b), 109 ppm in the CO3 ALHA77307 (Bose et al., 2012), and 120 ppm in the CO3 LAP031117 (Haenecour and Floss, 2012). It should be emphasized that these values are lower limits since detection efficiencies are less than 100% but probably higher for SiC than for presolar silicates (Nguyen et al., 2007). Presolar SiC has also been found in IDPs (Busemann et al., 2009; Stadermann et al., 2006), and one SiC grain has been identified in cometary material returned by the stardust mission (Brownlee et al., 2009; Messenger et al., 2009).

Grain-size distributions of SiC have been determined for several meteorites, and while grain sizes vary from 0.1 to 50 μm, the distributions are different for different meteorites. Murchison appears to have, on average, the largest grains (Amari et al., 1994), while SiC from Indarch (Russell et al., 1997) and Orgueil (Huss et al., 1997) is much finer grained. Various isotopic and other properties vary with grain size. Both the ^{22}Ne–E(H)/^{130}Xe–S and the $^{86}Kr/^{82}Kr$ (**Figure 7**) ratios increase with grain size (Lewis et al., 1994), and the first ratio has been used as a measure for the average grain size in meteorites for which no detailed size distributions have been determined (Russell et al., 1997). The $^{86}Kr/^{82}Kr$ ratio is a function of

neutron exposure, and the data indicate that exposure decreases with increasing grain size. The $^{88}Sr/^{86}Sr$ and $^{138}Ba/^{136}Ba$ ratios also depend on grain size (Figure 7), but the dependence of neutron exposure on grain size inferred from these isotopic ratios is just the opposite of that inferred from the $^{86}Kr/^{82}Kr$ ratio. This puzzle has not been resolved. A possible explanation is a different trapping mechanism for noble gases and refractory elements, respectively (Zinner et al., 1991), or different populations of carrier grains if, as for neon (Heck et al., 2007; Nichols et al., 1995), only a small fraction of the grains carry krypton. Excesses in ^{21}Ne relative to the predicted helium-shell composition, interpreted as being due to spallation by galactic cosmic rays, increase with grain size (Lewis et al., 1990, 1994; Tang and Anders, 1988a). However, the correlation of the $^{21}Ne/^{22}Ne$ ratio with the *s*-process $^{86}Kr/^{82}Kr$ ratio (Hoppe and Ott, 1997) and the determination of spallation recoil ranges (Ott and Begemann, 2000) cast doubt on a chronological interpretation. Other grain-size effects are, on average, larger $^{14}N/^{15}N$ ratios for smaller grains (Hoppe et al., 1996a) and an increasing abundance of Z grains among smaller SiC grains (Hoppe et al., 1996a, 1997, 2010; Zinner et al., 2006c, 2007). There are also differences in the distribution of different grain types in SiC from different meteorites: whereas the abundance of X grains in SiC from Murchison and other carbonaceous chondrites is ~1%, it is only ~0.1% in SiC from the enstatite chondrites Indarch and Qingzhen (Besmehn and Hoppe, 2001; Lin et al., 2002).

1.4.7 Silicon Nitride

Presolar silicon nitride (Si_3N_4) grains are extremely rare (in Murchison, SiC-rich separates ~5% of SiC of type X), but automatic ion imaging has been successfully used to detect those with large ^{28}Si excesses (Besmehn and Hoppe, 2001; Lin et al., 2002; Nittler and Alexander, 2003; Nittler et al., 1998; Zinner et al., 2010). The carbon, nitrogen, aluminum, and silicon isotopic signatures of these grains are the same as those of SiC grains of type X, that is, large ^{15}N and ^{28}Si excesses and high $^{26}Al/^{27}Al$ ratios (Figure 12). Although, so far, no resolvable ^{44}Ca excesses have been detected (Besmehn and Hoppe, 2001), the similarity with X grains implies an SN origin for these grains. While Si_3N_4 grains in SiC-rich residues from Murchison are extremely rare and, if present, are of type X, enstatite chondrites contain much higher abundances of Si_3N_4 (Alexander et al., 1994; Amari et al., 2002; Besmehn and Hoppe, 2001). Most of them have normal isotopic compositions. Recent measurements of small (0.25–0.65 μm) grains from Indarch revealed several Si_3N_4 grains with carbon and nitrogen isotopic ratios similar to those of mainstream SiC grains, but contamination from attached SiC grains cannot be excluded (Amari et al., 2002; Zinner et al., 2003a, 2007).

1.4.8 Graphite

Graphite, the third type of carbonaceous presolar grains, was isolated because it is the carrier of Ne–E(L) (Amari et al., 1990, 1995b). Subsequent isotopic measurements of individual grains revealed anomalies in many different elements.

1.4.8.1 Physical Properties

Only grains ≥1 μm in diameter carry Ne–E(L), and only round grains that range up to 20 μm in size appear to be of presolar origin (Amari et al., 1990; Zinner et al., 1995). Presolar graphite has a range in density (1.6–2.2 g cm^{-3}). Essentially all studies of presolar graphite grains have been made on separates from Murchison and Orgueil. Four different density fractions, KE3 (1.6–2.05 g cm^{-3}), KFA1 (2.05–2.10 g cm^{-3}), KFB1 (2.10–2.15 g cm^{-3}), and KFC1 (2.15–2.20 g cm^{-3}), have been isolated from the Murchison meteorite (Amari et al., 1994) and eight from Orgueil (Jadhav et al., 2006), of which OR1d (1.75–1.92 g cm^{-3}), OR1f (2.02–2.04 g cm^{-3}), and OR1g 2.04–2.12 g cm^{-3}) have been studied in most detail (Jadhav et al., 2008, 2013). Although there exists no exact correspondence between the densities of Murchison and Orgueil grains, physical properties and isotopic compositions indicate the existence of two groups: LD grains (KE3, KFA1, and OR1d) and HD grains (KFB1, KFC1, OR1f, and OR1g). Average sizes of Murchison grains decrease with increasing density, and density fractions differ in the distribution of their carbon and noble gas isotopic compositions (Amari et al., 1995b; Hoppe et al., 1995). SEM studies revealed two basic morphologies (Hoppe et al., 1995): dense aggregates of small scales ('cauliflowers,' Figure 2(b)) and grains with smooth or shell-like platy surfaces ('onions,' Figure 2(c)). Graphite from Orgueil differs from Murchison graphite in that the average size increases with density and that cauliflower grains are very rare (Jadhav et al., 2006, 2013). TEM analysis of microtomed sections of graphite spherules (Bernatowicz et al., 1991, 1996) found the surface morphology reflected in the internal structure of the grains. Cauliflowers consist of concentrically packed scales of poorly crystallized carbon, whereas onions consist either of well-crystallized graphite throughout or of a core of tightly packed graphene sheets of only several atomic layers surrounded by a mantle of well-crystallized graphite. Croat et al. (2008) identified a morphology, called turbostratic, between more graphitic onions and less-ordered cauliflowers. Even when grains have similar surface morphologies, such as Orgueil HD and LD grains, differences in the internal structure are revealed by Raman analysis: while the spectra of HD grains from the OR1f fraction indicate fairly well-crystallized graphite (Wopenka et al., 2011b), those of LD grains from the OR1d fraction indicate a lesser degree of crystallinity and resemble spectra of what is known as 'glassy carbon' in the Raman literature (Wopenka et al., 2011a).

Graphite spherules of all external and internal morphologies contain small (20–500 nm) internal grains of mostly titanium carbide (TiC), which must have condensed before the graphite and were apparently captured and included by the growing spherules (Bernatowicz et al., 1991). Some onions show TiC grains at their center that apparently acted as condensation nuclei for the graphite (Figure 11). Sizes of internal grains and graphite spherules and their relationship and chemical compositions provide information about physical properties, such as pressure, temperature, and C/O ratio, in the gas from which the grains condensed (Bernatowicz et al., 1996, 2005; Croat et al., 2003, 2005b, 2008, 2013). Zirconium- and molybdenum-rich carbides have been found mostly in HD onions or grains with turbostratic structure (Bernatowicz et al., 1996; Croat et al.,

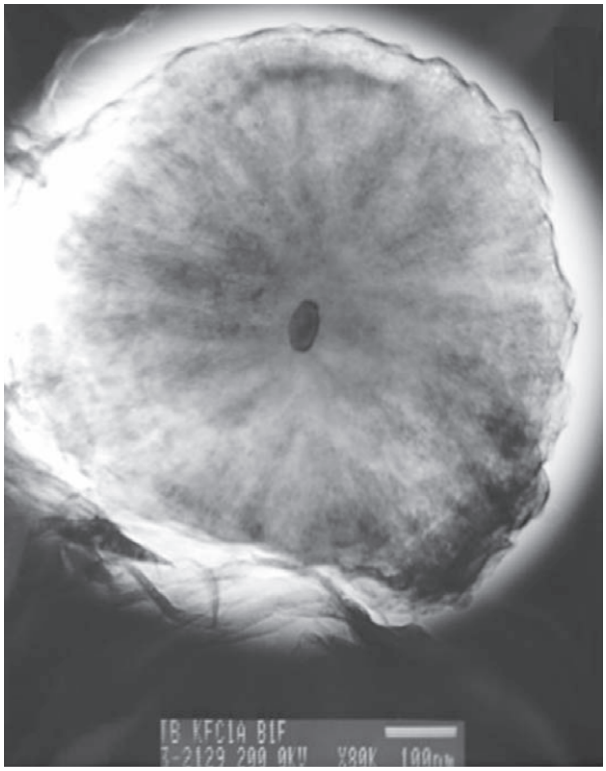

Figure 11 Transmission electron micrograph of a slice through a presolar graphite grain (onion). The grain in the center is TiC and apparently acted as condensation nucleus for the growth of the graphite spherule. Photo courtesy of Thomas Bernatowicz.

2005b, 2008). Studies of LD graphite spherules whose oxygen and silicon isotopic compositions indicated an SN origin (see succeeding text) did not detect zirconium- and molybdenum-rich carbides but revealed internal kamacite, cohenite, rutile, and iron grains in addition to TiC (Croat et al., 2003, 2011b, 2013). From the composition of refractory metal nuggets, Croat et al. (2013) concluded that HD graphite grains condensed at higher temperature than LD grains. Several HD graphite grains from Murchison KFC1 were found to contain SiC grains (one as many as 26) in addition to TiC and kamacite (Croat et al., 2010).

1.4.8.2 Isotopic Compositions

Noble gas measurements were made on bulk samples of the four density fractions from Murchison (Amari et al., 1995b) and in single grains (Heck et al., 2009a,b; Meier et al., 2012; Nichols et al., 1995). In contrast to SiC, a substantial fraction of Ne–E in graphite seems to come from the decay of short-lived ($T_{1/2}=2.6$ a) ^{22}Na (Clayton, 1975), most likely produced in supernovae (Amari, 2003, 2006, 2009). This is supported by the low ^{4}He/^{22}Ne ratios measured in individual grains (Nichols et al., 1995). Krypton in graphite has two *s*-process components with apparently different neutron exposures residing in different density fractions (Amari et al., 1995b, 2012). Krypton in LD graphite seems to have an SN origin, while that in HD graphite seems to have originated in low-metallicity AGB stars (Amari et al., 1995b, 2006, 2012). The analysis of single grains from Murchison KFB1 (Heck et al., 2009a,b) and KFC1 (Meier et al., 2012) indicates an AGB star origin for most of these HD grains, with ^{22}Ne coming from the He shell of such stars. However, several grains show SN isotopic signatures, in particular one KFB1 grain with monoisotopic ^{22}Ne, most like the product of ^{22}Na decay.

Ion microprobe analyses of single grains revealed the same range of ^{12}C/^{13}C ratios as in SiC grains but with clear differences between HD and LD grains (**Figure 6**). Most HD grains have ^{12}C excesses, similar to SiC X grains, with a peak at even higher ^{12}C/^{13}C ratios, whereas most LD grains have ^{12}C/^{13}C ratios smaller than solar. Both density fractions contain grains that have low ^{12}C/^{13}C ratios, such as SiC AB grains. There are also marked differences between HD and LD grains in other isotopic ratios. LD grains have ^{14}N and ^{18}O excesses (**Figure 12**), while HD grains have close-to-terrestrial nitrogen and solar oxygen isotopic ratios (Amari, unpublished; Hoppe et al., 1995; Jadhav et al., 2006, 2008, 2013; Stadermann et al., 2005; Zinner et al., 1995). In view of the enormous range in carbon isotopic ratios, these normal nitrogen and oxygen ratios cannot be intrinsic and most likely are the result of isotopic equilibration or contamination, either on the meteorite parent body or in the laboratory. Apparently, elements, such as nitrogen and oxygen, are much more mobile in graphite than in SiC. LD graphite grains have in general higher trace element concentrations than those with higher densities. They have high ^{26}Al/^{27}Al ratios that are as high as those of SiC X grains (**Figure 12**), whereas only a few HD grains have ^{26}Mg excesses. Many LD grains for which silicon isotopic ratios could be determined with sufficient precision show ^{28}Si excesses, although large ^{29}Si and ^{30}Si excesses, similar to those of SiC type C grains, are also seen (**Figure 13**). The similarities of the isotopic signatures with those of SiC type X grains point to an SN origin of LD graphite grains (Zinner et al., 2006a). The ^{18}O excesses are compatible with such an origin. Helium burning produces ^{18}O from ^{14}N, which dominates the CNO isotopes in material that had undergone hydrogen burning via the CNO cycle. As a consequence, the H/C zone in pre-SNII massive stars (see **Figure 9**), which experienced partial helium burning, has a high ^{18}O abundance (Rauscher et al., 2002; Woosley and Weaver, 1995). Wolf–Rayet stars during the WN–WC transitions are predicted to also show not only ^{12}C, ^{15}N, and ^{18}O excesses and high ^{26}Al/^{27}Al ratios (Arnould et al., 1997) but also large excesses in ^{29}Si and ^{30}Si and are therefore excluded as the source of LD graphite grains with ^{28}Si excesses.

There are additional features that indicate an SN origin of LD graphite grains. A few grains show evidence for ^{44}Ti (Jadhav et al., 2013; Nittler et al., 1996), others have large excesses of ^{41}K, which must be due to the decay of the radioisotope ^{41}Ca ($T_{1/2}=1.05\times10^{5}$ years) (Amari et al., 1996; Jadhav et al., 2013). Inferred ^{41}Ca/^{40}Ca ratios are much higher (0.001–0.01) than those predicted for the envelopes of AGB stars (Wasserburg et al., 1994; Zinner et al., 2006b) but are in the range expected for the carbon- and oxygen-rich

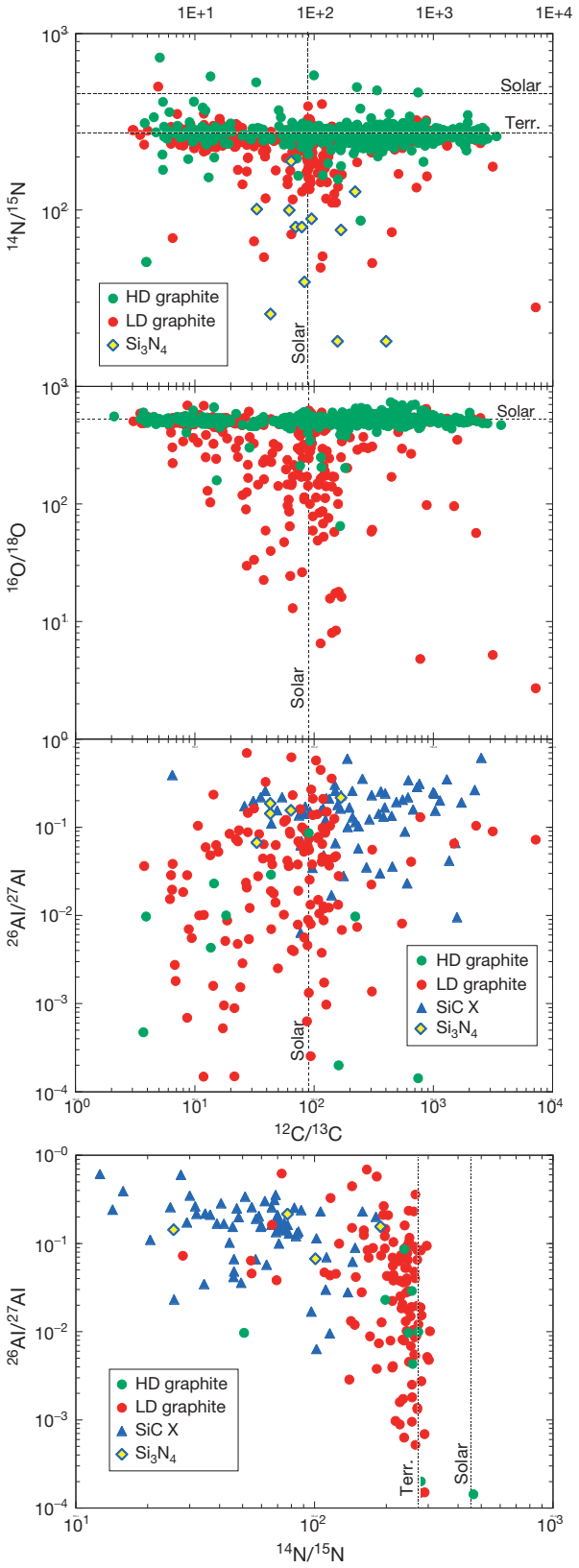

Figure 12 Nitrogen, oxygen, carbon, and aluminum isotopic ratios measured in individual LD and HD graphite grains. Also shown are data for presolar Si_3N_4 and SiC grains of type X. Source: Presolar database (Hynes and Gyngard, 2009).

zones of Type II supernovae, where neutron capture leads to the production of ^{41}Ca (Woosley and Weaver, 1995). Measurements of calcium isotopic ratios in grains without evidence for ^{44}Ti show excesses in ^{42}Ca, ^{43}Ca, and ^{44}Ca, with ^{43}Ca having the largest excess (Amari et al., 1996; Jadhav et al., 2013; Travaglio et al., 1999). This pattern is best explained by neutron capture in the He/C and O/C zones (**Figure 9**) of Type II supernovae. In cases where titanium isotopic ratios have been measured (Amari et al., 1996; Jadhav et al., 2013; Nittler et al., 1996; Stadermann et al., 2005; Travaglio et al., 1999), they show large excesses in ^{49}Ti and smaller ones in ^{50}Ti. This pattern also indicates neutron capture and is well matched by predictions for the He/C zone (Amari et al., 1996). However, large ^{49}Ti excesses in grains with relatively low (10–100) ^{12}C/^{13}C ratios can only be explained if contributions from the decay of ^{49}V are considered (Travaglio et al., 1999). Stadermann et al. (2005) measured oxygen isotopic ratios of individual TiC subgrains in microtome slices of a graphite spherule with SN signatures. These grains had variable ^{18}O excesses that are substantially larger than those in the graphite. Either they formed in a different region of the SN ejecta before accretion onto the growing graphite or they retained their original oxygen isotopic composition better than the graphite during partial equilibration with isotopically normal oxygen. Groopman et al. (2012) found regions with large correlated ^{15}N and ^{18}O excesses inside of microtome slices of LD grains from Orgueil. This material must come from the He/C zone, the only SN layer with ^{15}N and ^{18}O excesses, and was included into the grain growing from a gas that apparently had smaller excesses by having been mixed with material from outer zones (He/N and hydrogen-rich shell).

In order to obtain better constraints on theoretical models of SN nucleosynthesis, Travaglio et al. (1999) tried to match the isotopic compositions of LD graphite grains by performing mixing calculations of different Type II SN layers (Woosley and Weaver, 1995). While the results reproduce the principal isotopic signatures of the grains, there remain several problems. The models do not produce enough ^{15}N and yield too low ^{29}Si/^{30}Si ratios. The models also cannot explain the magnitude of ^{26}Al/^{27}Al, especially if SiC X grains are also considered, and give the wrong sign in the correlation of this ratio with the ^{14}N/^{15}N ratio. Lin et al. (2010) noticed that the 25 $M_\odot$ SN model by Rauscher et al. (2002) shows an ^{15}N spike in the He/N zone, and Meyer and coworkers (Meyer and Bojazi, 2011; Meyer et al., 2011) investigated how different SN models could result in high shock temperatures and produce enough ^{15}N. Nitrogen-15 production in the He/N zone would help to explain the correlation between the nitrogen and aluminum isotopic ratios. However, the finding of correlated ^{15}N and ^{18}O hotspots inside of LD grains (Groopman et al., 2012) seems to invalidate this possibility. Additional information about the formation environment of presolar graphite is, in principle, provided by the presence of indigenous polycyclic aromatic hydrocarbons (PAHs) (Messenger et al., 1998). PAHs with anomalous carbon ratios show different mass envelopes that indicate different formation conditions.

There exists ample evidence that most HD graphite grains have an origin in low-metallicity AGB stars. In contrast to LD

grains, many HD grains have large ^{30}Si excesses (**Figure 13**) and these excesses are correlated with high ^{12}C/^{13}C ratios (Amari et al., 2003, 2004, 2005b; Jadhav et al., 2006, 2013). These signatures point to parent stars of low metallicity. Nucleosynthesis models of AGB stars predict ^{30}Si/^{28}Si and ^{12}C/^{13}C ratios in such stars to be much higher than in stars of solar metallicity (Zinner et al., 2006d). These models also predict high C/O ratios. Under these conditions, graphite is expected to condense before SiC (Lodders and Fegley, 1997) and this is the likely reason that SiC grains with the carbon and silicon isotopic compositions of HD graphite grains are not found. High concentrations of the *s*-process elements zirconium, molybdenum, and ruthenium found in TiC subgrains (Bernatowicz et al., 1996; Croat et al., 2005a,b, 2008) agree with the expected and observed large overabundance of these elements in the envelope of AGB stars.

A few HD grains from the Orgueil fraction OR1f have extremely large isotopic anomalies in calcium and titanium (Jadhav et al., 2008, 2013). Such large anomalies are achieved in oxygen-rich regions of Type II supernovae, but these zones have high ^{12}C/^{13}C ratios, whereas the grains have ^{12}C/^{13}C < 20. Jadhav et al. (2008) have proposed that these grains formed in so-called born-again AGB stars, of which Sakurai's object is an example (e.g., Asplund et al., 1999). Such stars, which have lost most of their envelope, experience a late thermal pulse that mixes remaining hydrogen into the helium shell, producing low ^{12}C/^{13}C ratios by hydrogen burning on ^{12}C (Herwig, 2001a; Herwig et al., 2011). Helium-shell material with large calcium and titanium anomalies produced by neutron capture is exposed at the star's surface and is included into forming graphite grains.

Nicolussi et al. (1998c) have reported RIMS measurements of zirconium and molybdenum isotopic ratios in individual graphite grains from the highest Murchison density fraction KFC1 in which no other isotopic ratios had been measured. Several grains show *s*-process patterns for zirconium and molybdenum, similar to those exhibited by mainstream SiC grains, although two grains with a distinct *s*-process pattern for zirconium have normal molybdenum. Two grains have extreme ^{96}Zr excesses, indicating an SN origin, but the molybdenum isotopes in one are almost normal. Molybdenum, such as nitrogen, might have suffered isotopic equilibration or contamination in graphite. HD graphite grains apparently come from AGB stars as previously indicated by the krypton data (Amari et al., 1995b), from born-again AGB stars, and from supernovae. It remains to be seen whether also LD grains have multiple stellar sources.

A few graphite grains appear to come from novae. Laser extraction gas-source mass spectrometry of single grains shows that, like SiC grains, only a small fraction contains evidence for Ne–E. Two of these grains have ^{20}Ne/^{22}Ne ratios that are lower than ratios predicted to result from helium burning in any known stellar sources, implying decay of ^{22}Na (Nichols et al., 1995). Furthermore, their ^{22}Ne is not accompanied by ^{4}He, expected if neon was implanted. The ^{12}C/^{13}C ratios of these two grains are 4 and 10, in the range of SiC grains with a putative nova origin. Another graphite grain with ^{12}C/^{13}C = 8.5 has a large ^{30}Si excess of 760‰ (Amari et al., 2001a).

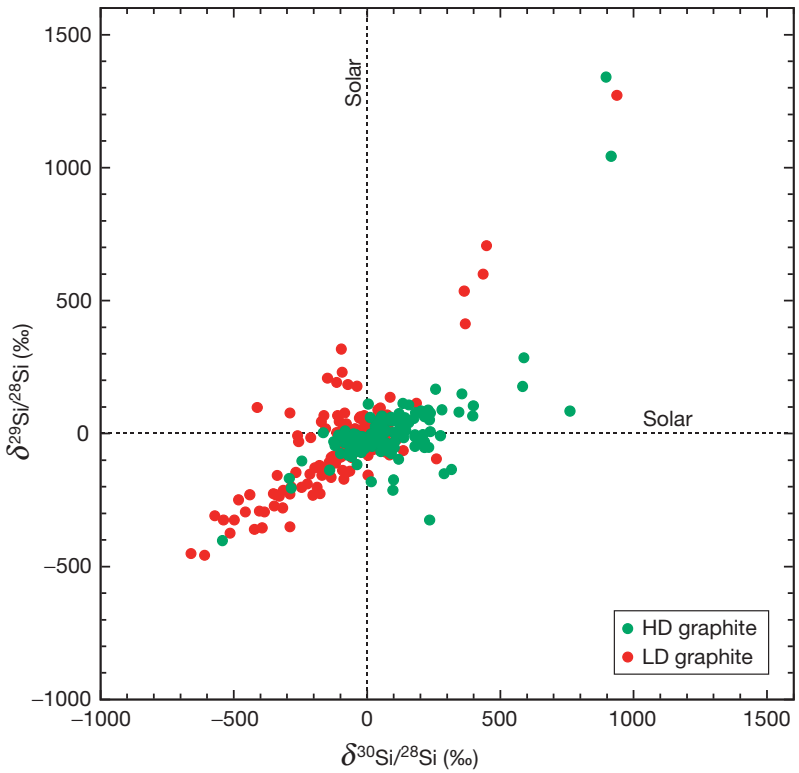

Figure 13 Silicon isotopic ratios in HD and LD graphite grains. As in **Figure 4**, isotopic ratios are plotted as δ-values. Source: Presolar database (Hynes and Gyngard, 2009).

In summary, LD graphite grains seems to have an SN origin and most HD graphite an origin in low-metallicity AGB stars. However, the apparent isotopic equilibration of elements, such as nitrogen and oxygen, and the generally low abundance of trace elements in many cases make it difficult to obtain enough diagnostic isotopic signatures to unambiguously identify the parent stars of presolar graphite grains.

1.4.9 Oxygen-Rich Grains

1.4.9.1 Oxide Grains

In contrast to the carbonaceous presolar phases, presolar oxide grains apparently do not carry any 'exotic' noble gas component. They have been identified by ion microprobe oxygen isotopic measurements of single grains from acid residues free of silicates. In contrast to SiC, essentially all of which is of presolar origin, most oxide grains found in meteorites formed in the solar system and only a small fraction is presolar. The oxygen isotopic compositions of the most abundant presolar oxide minerals are plotted in **Figure 14(a)**. Most of them are corundum, followed by spinel and hibonite (see presolar database, Hynes and Gyngard, 2009). In addition, five presolar chromite grains (Nittler et al., 2005b), five titanium oxide grains (Bose et al., 2010a; Nittler and Alexander, 1999; Nittler et al., 2008), and four iron oxide grains (Bose et al., 2010b; Floss et al., 2008) have been identified. The chromite grains listed here do not include the small (<150 nm) grains found in the search for ^{54}Cr carriers (Dauphas et al., 2010; Nittler et al., 2012; Qin et al., 2011).

These numbers, however, cannot be used to infer relative abundances of these mineral phases. Analyses were made on grains of different size with instruments having different spatial resolution and sensitivity. Furthermore, searches for presolar oxide grains have been made in different types of residues, some containing spinel, others not. Another complication is that more than half of all presolar corundum grains have been found by automatic direct $^{18}O/^{16}O$ imaging searches in the ion microprobe (Nittler et al., 1997), a method that does not detect grains with anomalies in the $^{17}O/^{16}O$ ratio but with close-to-normal $^{18}O/^{16}O$. The oxygen isotopic distribution of corundum in **Figure 14(a)** therefore does not reflect the true distribution. **Figure 14(a)** does not include submicrometer oxide grains that were found by NanoSIMS oxygen isotopic raster imaging of tightly packed grain separates or polished sections (Nguyen and Zinner, 2004; Nguyen et al., 2003; Mostefaoui and Hoppe, 2004; and many subsequent efforts; see section on silicates). Because of beam overlap onto adjacent, isotopically normal grains, the oxygen isotopic ratios of small grains analyzed in this way are diluted. Abundances for oxide grains obtained by raster imaging should be considered lower limits. Raster imaging of small grains from the Murray CM2 chondrite led to the identification of 252 presolar spinel and 32 presolar corundum grains (Nguyen et al., 2003). Additional small oxide grains have been detected during imaging searches for presolar silicates (Bose et al., 2010a,b, 2012; Floss and Stadermann, 2009a, 2012; Leitner et al., 2012b; Mostefaoui and Hoppe, 2004; Nagashima et al., 2004; Nguyen and Zinner, 2004; Nguyen et al., 2007, 2010c; Nittler et al., 2011; Stadermann et al., 2006; Vollmer et al., 2008, 2009b; Yada et al., 2008). The abundance of presolar oxide grains varies greatly from meteorite to meteorite. The highest abundances have been found in the most primitive meteorites, in the ungrouped carbonaceous chondrite Acfer 094 (~55 ppm; Nguyen et al., 2007), in the CR3 chondrite NWA852 (~39 ppm; Leitner et al., 2010), and in the CO3 chondrite ALH 77037 (~20 ppm; Bose et al., 2012; Nguyen et al., 2010c). This contrasts with an abundance of only 1.2 ppm for spinel and ~0.15 ppm for corundum in the CM2 meteorite Murray (Zinner et al., 2003b) and upper limits of a few ppm in ordinary chondrites (Mostefaoui et al., 2003, 2004; Tonotani et al., 2006).

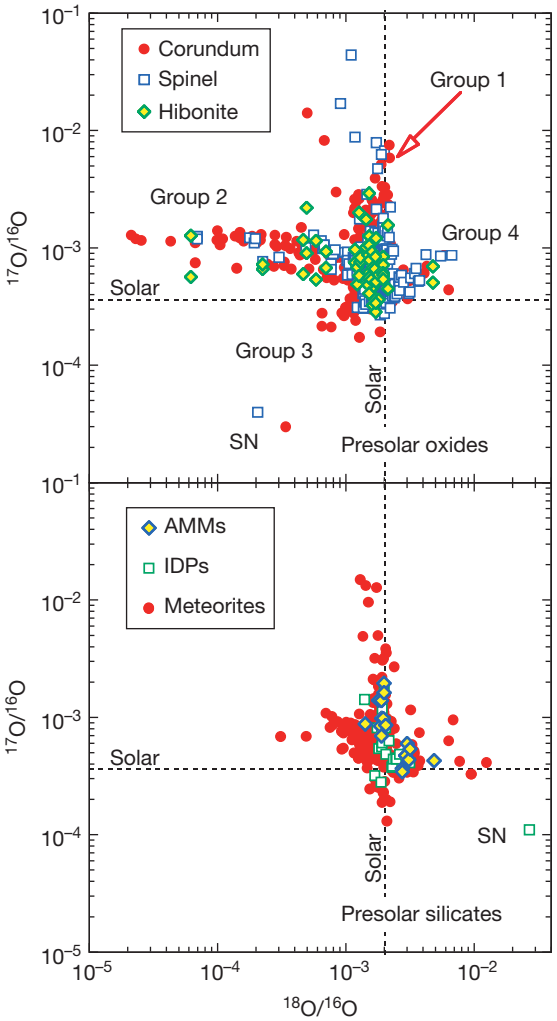

Figure 14 Oxygen isotopic ratios in individual presolar oxide grains (top) and in individual presolar silicate grains (bottom). Also indicated in the top figure are the four groups defined by Nittler et al. (1997). Source: Presolar database (Hynes and Gyngard, 2009).

Nittler et al. (1997) have classified presolar oxide grains into four different groups according to their oxygen isotopic ratios. Grains with $^{17}O/^{16}O >$ solar (3.82×10^{-4}) and $0.001 < {}^{18}O/^{16}O <$ solar (2.01×10^{-3}), comprising group 1, have oxygen isotopic ratios similar to those observed in RG and AGB stars (Harris and Lambert, 1984; Harris et al., 1987; Smith and Lambert, 1990), indicating such an origin also for

the grains. These compositions can be explained by hydrogen burning in the core of low- to intermediate-mass stars followed by mixing of core material into the envelope during the first dredge-up (also second dredge-up in low-metallicity stars with $M > 3\ M_{\odot}$) (Boothroyd and Sackmann, 1999; Boothroyd et al., 1994). Variations in $^{17}O/^{16}O$ ratios mainly correspond to differences in stellar mass, while those in $^{18}O/^{16}O$ can be explained by assuming that stars with different metallicities contributed oxide grains to the solar system. According to galactic chemical evolution models, $^{17}O/^{16}O$ and $^{18}O/^{16}O$ ratios are expected to increase as a function of stellar metallicity (Timmes et al., 1995). Grains with depletions in both ^{17}O and ^{18}O (group 3) could thus come from low-mass stars (producing only small ^{17}O enrichments) with lower than solar metallicity (originally having lower than solar $^{17}O/^{16}O$ and $^{18}O/^{16}O$ ratios). The oxygen isotopic ratios of group 3 grains have been used to obtain an estimate of the age of the galaxy (Nittler and Cowsik, 1997). Nittler (2009) used the isotopic compositions of group 1 and 3 grains to derive the masses and metallicities of their parent stars by comparing them with first dredge-up predictions. Group 2 grains have ^{17}O excesses and large ^{18}O depletions ($^{18}O/^{16}O < 0.001$). Such depletions cannot be produced by the first and second dredge-up but have been successfully explained by an extra mixing mechanism (cool-bottom processing) of low-mass ($M < 1.65\ M_{\odot}$) stars during the AGB phase that circulates material from the envelope through hot regions close to the hydrogen-burning shell (Denissenkov and Weiss, 1996; Nollett et al., 2003; Wasserburg et al., 1995). Recently, Palmerini et al. (2011) used new cross sections, especially for $^{14}N(p,\gamma)^{15}O$, for nucleosynthesis calculations in RGB and AGB stars and could explain the oxygen isotopic compositions of all group 2 grains, also those with low $^{17}O/^{16}O$ ratios (<0.0005), by considering stars with very low ($<1.5\ M_{\odot}$) masses. Group 4 grains have both ^{17}O and ^{18}O excesses. If they originated from AGB stars, they could either come from low-mass stars in which ^{18}O produced by helium burning of ^{14}N during early pulses was mixed into the envelope by third dredge-up (Boothroyd and Sackmann, 1988) or from stars with high metallicity. More likely for the grains with the largest ^{18}O excesses is an SN origin as suggested by Choi et al. (1998) if ^{18}O-rich material from the He/C zone can be admixed to material from oxygen-rich zones.

To date, only two grains with the typical isotopic signature expected for SN condensates, namely, a large ^{16}O excess (labeled SN in **Figure 14(a)**), have been identified: One is a corundum (Nittler et al., 1998), the other one a spinel grain (Gyngard et al., 2010c). Evidence for the initial presence of ^{44}Ti has been found in the latter grain, confirming an SN origin. All oxygen-rich zones (O/C, O/Ne, O/Si – see **Figure 9**) are dominated by ^{16}O (Rauscher et al., 2002; Thielemann et al., 1996; Woosley and Weaver, 1995). The paucity of such grains, whose abundance is expected to dominate that of carbonaceous phases with an SN origin, remains an unsolved mystery. It has been suggested that oxide grains from supernovae are smaller than those from RG stars but all automatic imaging searches of submicron grains have not uncovered any additional oxides with large ^{16}O excesses. Two corundum grains with high $^{17}O/^{16}O$ and low $^{18}O/^{16}O$ ratios do not fit into the four groups. These grains could come from stars with $\geq 5\ M_{\odot}$ that experienced hot-bottom burning, a condition during which the convective envelope extends into the hydrogen-burning shell (Boothroyd et al., 1995; Lattanzio et al., 1997). Recently, several oxide grains with very high $^{17}O/^{16}O$ ratios have been identified (Gyngard et al., 2010b,c, 2011; Nittler et al., 2011). Although RGB and AGB models with new $^{14}N(p,\gamma)^{15}O$ and $^{15}N(p,\gamma)^{16}O$ reaction rates increase the limit of the $^{17}O/^{16}O$ ratio that can be reached in these stars to ~ 0.006, several grains have higher ratios and likely have a nova origin (Gyngard et al., 2010b, 2011). To obtain a match between measured and predicted oxygen and magnesium isotopic ratios, mixing of nova material with material of solar isotopic composition is required (Gyngard et al., 2011).

Some but not all grains in the four groups show evidence for initial ^{26}Al (**Figure 15**; Choi et al., 1998, 1999; Gyngard et al., 2010c; Krestina et al., 2002; Nittler et al., 1997, 2005a, 2008; Zinner et al., 2005, 2006b). Aluminum-26 is produced in the hydrogen-burning shell (Forestini et al., 1991), and dredge-up of material during the TP-AGB phase is required. Thus grains without ^{26}Al must have formed before their parent stars reached this evolutionary stage. However, shell hydrogen burning can account only for $^{26}Al/^{27}Al$ ratios of up to $\sim 3 \times 10^{-3}$ (Forestini et al., 1991; Karakas and Lattanzio, 2003; Mowlavi and Meynet, 2000) and cool-bottom processing has to be invoked for grains with higher ratios (Nollett et al., 2003; Palmerini et al., 2011). Although group 2 grains generally have higher $^{26}Al/^{27}Al$ ratios, there is no simple correlation between $^{26}Al/^{27}Al$ and $^{18}O/^{16}O$ ratios. This is not surprising because in the theory of cool-bottom processing by Nollett et al. (2003), the two parameters (maximum temperature and circulation rate) affecting these ratios are almost completely decoupled. It should be noted that most SiC grains from AGB stars (mainstream, Y, and Z grains) have $^{26}Al/^{27}Al$ ratios that agree with models of shell hydrogen burning in AGB stars (see **Figure 5**). Carbon stars, the parent stars of SiC, follow oxygen-rich stars, the parents of oxide grains, in their evolutionary sequence. It could be that cool-bottom processing, which is responsible for the high $^{26}Al/^{27}Al$ ratios in oxide grains prevents oxygen-rich stars from

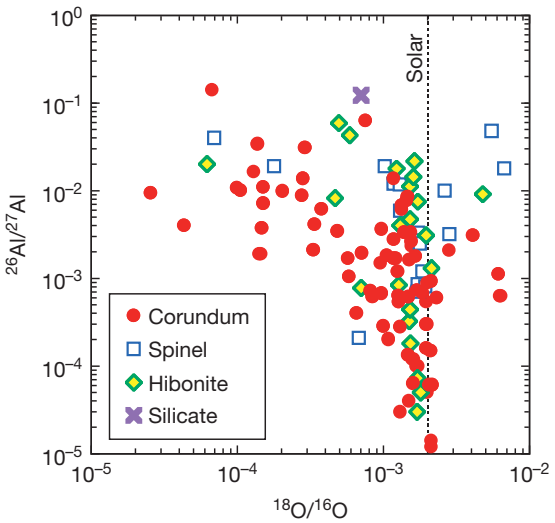

Figure 15 Inferred aluminum isotopic ratios in presolar oxide grains are plotted against their oxygen isotopic ratios. Source: Presolar database (Hynes and Gyngard, 2009).

becoming carbon stars. New models predict this for low-mass (<1.5–1.7 $M_{\odot}$) stars (Palmerini et al., 2011). Whereas corundum and hibonite have large Al/Mg ratios and the identification of radiogenic ^{26}Mg is simple, it is difficult to impossible to distinguish between radiogenic ^{26}Mg and ^{26}Mg of nucleosynthetic origin in spinel with its Al/Mg of only two. **Figure 16** shows magnesium isotopic ratios in spinel and some hibonite grains of the four groups, an SN spinel and nova candidates. Also included are a few silicate grains (Nguyen et al., 2010b, 2011b). The SN grain and grains of all four groups show ^{25}Mg deficits. In Type II SN models, the outer part of the He/C zone and the He/N zone have substantial ^{25}Mg depletions. In AGB stars, ^{25}Mg is predicted to be depleted because of ^{26}Al production via ^{25}Mg(p,γ)^{26}Al, and ^{25}Mg deficits are expected to be accompanied by ^{26}Mg excesses, but other reactions, such as α-capture on ^{22}Ne, are also important and predicted effects are smaller than those seen (Zinner et al., 2005). Galactic evolution of the magnesium isotopes is also likely to play a role in the composition of the grains (Nittler et al., 2008). However, one cannot explain consistently the isotopic ratios of all grains in this way. For example, several grains whose oxygen isotopic ratios indicate low-metallicity parent stars have large ^{25}Mg excesses, which is not expected from galactic evolution models (Nittler et al., 2008).

Titanium isotopic ratios have been determined in presolar corundum, hibonite, spinel, and titanium oxide grains (Choi et al., 1998; Gyngard et al., 2010c; Nittler et al., 2005a, 2008). Isotopic patterns vary from a V-shaped pattern with excesses in all titanium isotopes relative to ^{48}Ti to the inverse of it. The observed ^{50}Ti excesses agree with those predicted to result from neutron capture in AGB stars. The range of patterns indicates that, just as for SiC grains, galactic evolution affects the isotopic compositions of the parent stars of oxide grains. The identification of presolar hibonite grains (Choi et al., 1999; Krestina et al., 2002; Nittler et al., 2005a, 2008) provides the opportunity to measure calcium isotopic ratios and to look for ^{41}K excesses from ^{41}Ca decay. Inferred ^{41}Ca/^{40}Ca ratios range up to 4×10^{-4} (Choi et al., 1999; Nittler et al., 2005a, 2008; Zinner et al., 2006b), within the range of values predicted for the envelope of AGB stars (Wasserburg et al., 1994; Zinner et al., 2006b) if suppression of ^{41}Ca decay is taken into account (Nittler et al., 2008). One grain has a ratio of 4.3×10^{-4}, but other isotopic signatures indicate that it has an SN origin.

Two NanoSIMS studies have addressed the observation of ^{54}Cr excesses in leachates from carbonaceous chondrites (e.g., Rotaru et al., 1992; Trinquier et al., 2007). NanoSIMS imaging measurements of fine-grained Orgueil residues found that large ^{54}Cr excesses are carried by small (<200 nm) chromite grains (Dauphas et al., 2010; Qin et al., 2011). The ^{54}Cr/^{52}Cr ratios in these grains ranged up to 2.5× and 3.6× solar, but because of beam overlap of the O^- beam, it was estimated that ratios should be at least 11× and up to 50× solar (Qin et al., 2011). This was confirmed by Nittler et al. (2012) who, by analyzing CrO^- ions with a smaller Cs^+ beam, obtained ^{54}Cr/^{52}Cr ratios of up to 36× solar. What is puzzling is the normal oxygen isotopic composition of these grains.

While presolar aluminum oxide grains are here called corundum, it has to be pointed out that a TEM study shows the existence of polymorphs and of nonstoichiometric grains (Stroud et al., 2004a). Similarly, a TEM study of five hibonite grains (Zega et al., 2011) found only one of them to be pure

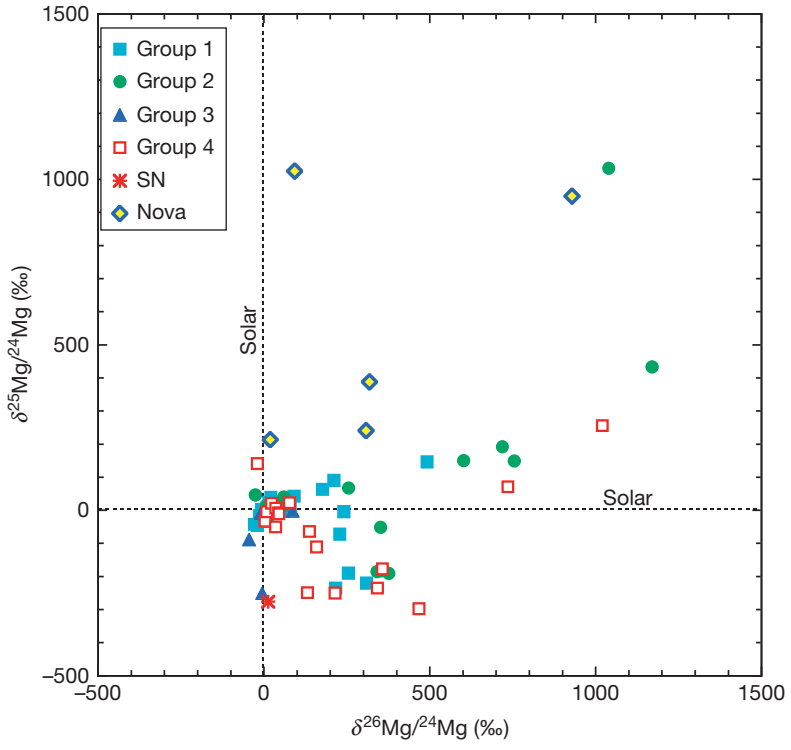

Figure 16 Magnesium isotopic ratios of spinel, hibonite, and silicate grains. Source: Presolar database (Gyngard, unpublished data; Hynes and Gyngard, 2009; Nguyen et al., 2010b, 2011b).

hibonite. The similarity in the crystalline structure between four hibonite grains with an RGB/AGB origin and a group 4 grain with a likely SN origin indicates similar formation conditions. This is in contrast to SiC grains where X grains differ from mainstream grains in their internal crystal structure (see **Section 1.4.6.4**).

1.4.9.2 Silicate Grains

Several attempts to identify presolar silicates in primitive meteorites were unsuccessful (Messenger and Bernatowicz, 2000; Nittler et al., 1997). This situation changed with the advent of the NanoSIMS and its capability of analyzing a large number (tens of thousands) of submicron grains for their oxygen isotopic compositions by raster imaging (Nguyen et al., 2003). This capability has also been achieved with the Cameca IMS 1270 equipped with an SCAPS device (Yurimoto et al., 2003), which allows direct imaging of the sample surface in a given isotope with high sensitivity. The first method has better spatial resolution and thus a higher detection efficiency of anomalous grains as fraction of all analyzed grains. The second method makes it possible to analyze a larger area in a given time but has lower spatial resolution, which leads to a lower detection efficiency and greater dilution of the isotopic ratios by contributions from adjacent grains than is the case for NanoSIMS analysis.

The first presolar silicates were discovered in IDPs (Messenger et al., 2003), followed by the discovery of presolar silicates in meteorites (Mostefaoui and Hoppe, 2004; Nagashima et al., 2004; Nguyen and Zinner, 2004) and Antarctic micrometeorites (AMMs) (Yada et al., 2008). With a few exceptions (ranging up to 1 μm), these grains are smaller than 0.5 μm size. As of early 2012, more than 500 presolar silicates have been identified in IDPs, meteorites, and AMMs. **Figure 14b** shows the oxygen isotopic ratios of presolar silicates analyzed in the NanoSIMS. A comparison with the oxygen isotopic ratios of presolar oxide grains (**Figure 14(a)**) shows that, on average, the isotopic compositions of the silicate grains are closer to normal. The reason for this difference is most probably the fact that the silicate grains are small and were analyzed by raster imaging in polished section or tightly packed grain separates where the overlap of the primary Cs^+ onto adjacent grains diluted the isotopic compositions. This effect has been demonstrated during the separated-grain and raster imaging analysis of small presolar spinel grains (Nguyen et al., 2003) and discussed by Nguyen et al. (2007). As a consequence, the anomalies in the grains plotted in **Figure 14(b)** should be considered lower limits. Isotopic dilution effects are even larger for silicate grains identified by SCAPS analysis. In spite of this limitation, the isotopic analysis of presolar silicates yielded interesting results. On average, silicate grains have more group 4 grains with large ^{18}O excesses than oxide grains (see **Figure 14**). The grain with an extreme ^{18}O excess and a large depletion in ^{17}O is classified as an SN grain. Its oxygen isotopic composition can be interpreted as a large ^{16}O and an even larger ^{18}O excess, both the signature of an SN origin (Messenger et al., 2005). The other grains with large ^{18}O excesses probably have an SN origin as well.

Most raster imaging searches have concentrated on primitive meteorites that have high abundances of presolar silicates. This includes Acfer 094, the first meteorite in which presolar silicates have been discovered. It has been studied in most detail (Bose et al., 2010a; Mostefaoui and Hoppe, 2004; Nagashima et al., 2004; Nguyen and Zinner, 2004; Nguyen et al., 2007; Vollmer et al., 2008; 2009a,b). Others in which presolar silicates have been found include the ungrouped carbonaceous chondrites Adelaide (Floss and Stadermann, 2012) and Ningqiang (Zhao et al., 2010, 2011a); CR chondrites QUE99177 (Floss and Stadermann, 2009b; Nguyen et al., 2010c), MET00426 (Floss and Stadermann, 2009b), and NWA852 (Leitner et al., 2012b); and CO chondrite ALH77307 (Bose et al., 2012; Nguyen et al., 2007, 2010c).

Figure 17 shows estimates of presolar silicate abundances in meteorites and IDPs. Uncertainties in the detection efficiency of small anomalous grains in thin section or tightly packed aggregates affect estimates of the abundances. From raster imaging analysis of Murray tightly packed spinel grains whose average diameter is 0.45 μm, Nguyen et al. (2003) determined a detection efficiency of 50%. However, most presolar silicates are smaller, implying even lower detection efficiencies. The abundances plotted in **Figure 17** do not include any corrections for detection efficiency and it has to be understood that they are lower limits and true abundances are probably higher by more than a factor of two. Because of limited statistics and because the detection efficiency of SCAPS analysis is essentially unknown,

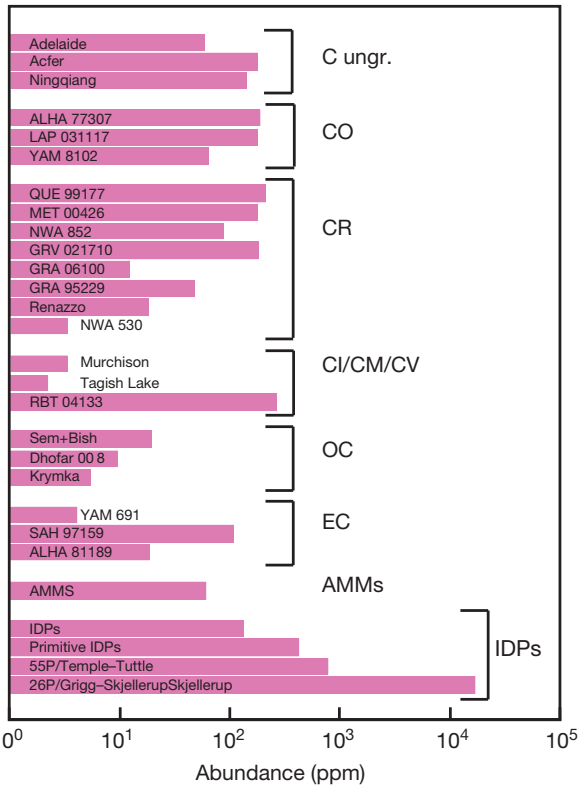

Figure 17 Abundances of presolar silicates in different types of meteorites. If several studies existed, averages are plotted. Sources: Bose et al. (2010a,b, 2012), Busemann et al. (2009), Davidson et al. (2010), Ebata and Yurimoto (2008), Floss and Stadermann (2005, 2009a, 2012), Floss et al. (2006, 2011), Haenecour and Floss (2011, 2012), Leitner et al. (2009, 2010, 2011, 2012b), Marhas and Hoppe (2005), Marhas et al. (2006), Mostefaoui et al. (2003), Nagashima et al. (2004, 2005), Nguyen et al. (2007, 2010c), Tonotani et al. (2006), Vollmer et al. (2008, 2009b), Yada et al. (2008), Zhao et al. (2010, 2011a,b).

only few SCAPS analyses are included in Figure 17. They are analyses of NAW530 (Nagashima et al., 2004), Murchison (Nagashima et al., 2005), OCs Dhofar008 and Krymka (Tonotani et al., 2006), and ECs Y591 and ALH81189 (Ebata and Yurimoto, 2008). Excluded were analyses of Adelaide (Kobayashi et al., 2005a), CO3 chondrite Y-81025 (Kobayashi et al., 2005a, b), and Tagish Lake (CI2).

Variations between different abundance determinations for the same meteorite are usually within statistical errors and averages are plotted. However, there are large real differences between different IDPs. Floss et al. (2006) defined a class of 'primitive IDPs' that contain bulk ^{15}N excesses and ^{15}N hotspots and derived a presolar silicate abundance of ~375 ppm compared to ~120 ppm for 'normal IDPs.' Abundances are even higher in IDPs from targeted collections: they are ~700 ppm in IDPs from the 55P/Tempel–Tuttle dust stream collector (Floss et al., 2011) and range from 3000 to 15 000 ppm in IDPs from the 26P/Grigg–Skjellerup dust stream collector (Busemann et al., 2009). Variations of the presolar silicate/oxide abundance ratio among different meteorites have received considerable attention (Floss and Stadermann, 2009a; Leitner et al., 2012a). Presolar silicate/oxide ratios vary from 1.6 in NWA852 (Leitner et al., 2009, 2010) to 3.1 in Acfer094 (Nguyen et al., 2007; Vollmer et al., 2009b) and Adelaide (Floss and Stadermann, 2012), to 6.1 in ALH77307 (Bose et al., 2012; Leitner et al., 2009; Nguyen et al., 2007, 2010c), to 24 in QUE99177 (Floss and Stadermann, 2009c; Nguyen et al., 2010c), and to 30 in MET00425 (Floss and Stadermann, 2009b). It has been argued that presolar silicates are more easily destroyed or made isotopically unrecognizable, and low presolar silicate/oxide ratios could indicate a high degree of processing (Leitner et al., 2012b). However, if we assume a ratio of 30 to be that in the most primitive meteorites, this would mean that 95% of all presolar silicates were destroyed in NWA852, 90% in Acfer094, and 80% in ALH77307. However, total presolar silicate abundances are comparable to those in QUE99177 and MET00425, and there is no evidence that these two meteorites are that much more primitive than the other ones. An alternative explanation would be some sorting between presolar silicates and oxides, but grain sizes are comparable and it is not clear how this could be accomplished.

Attempts to determine the mineralogy of presolar silicates have been made difficult by the small size of these grains. x-Ray analysis in the SEM or electron microprobe suffers from the problem that the volume excited by the electron beam is usually larger than that of the grains, and x-rays are thus also emitted from adjacent or underlying grains within the excitation volume (Nguyen and Zinner, 2004). In Auger spectroscopy, the signal (Auger electrons) is obtained only from the first few atomic layers and this method appears to be better suited to the determination of the elemental composition of submicrometer grains (Stadermann et al., 2009). It has been successfully applied to the analysis of many silicate and oxide grains identified as presolar by NanoSIMS isotopic analysis (Bose et al., 2010a; Floss and Stadermann, 2009a, 2012; Nguyen et al., 2010c; Vollmer et al., 2009b). All these cited studies noticed high iron contents. They also found that many silicates have nonstoichiometric compositions, be it in the ratio of cations to silicon or in the ratio of all to oxygen. The Fe + Mg (+Ca) to Si ratio can be used to distinguish between olivine and pyroxene. Figure 18 shows this ratio for silicates from Acfer094, QUE 99177, MET 00426, ALHA 77307, and Adelaide. As can be seen, many grains can be considered 'pyroxene-like' and 'olivine-like' because, within errors, they have ratios of one or two, respectively. However, many grains have ratios below one, between one and two, and above two. Grains from Adelaide represent a special case; most of them have ratios larger than two. They have high iron abundances and iron-rich rims indicate invasion of iron by diffusion (Floss and Stadermann, 2012). But even silicates from other meteorites have much higher iron contents than what is expected from astronomical observations that indicate that circumstellar dust around evolved stars is magnesium-rich (e.g., Demyk et al., 2000; Molster and Waters, 2003; Waters et al., 1996). To determine whether high iron contents are the result of alteration or are intrinsic is not easy. Only few iron isotopic analyses have been made. Analysis with a primary O^- beam suffers from beam overlap. Of 13 presolar silicates analyzed by Vollmer and Hoppe (2010), one group 1 grain with a high $^{17}O/^{18}O$ ratios has a $\delta^{54}Fe/^{56}Fe$ value of $-140 \pm 52‰$, another one of $+128 \pm 22‰$, the others are isotopically normal. A previously measured group 4 grain has an ^{54}Fe deficit of 110‰ (Mostefaoui and Hoppe, 2004). In order to reduce beam overlap, Ong et al. (2012) used a Cs^+ beam and analyzed negative FeO ions. Among eight presolar silicate grains from Acfer094, they found four with ^{57}Fe deficits ranging to $\delta^{54}Fe/^{56}Fe = -210 \pm 35‰$ and one with ^{54}Fe and ^{54}Fe excesses of ~75‰.

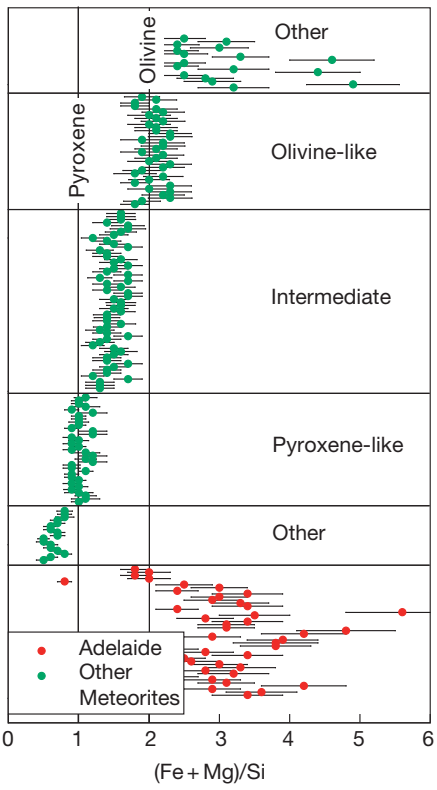

Figure 18 (Fe + Mg)/Si ratios determined from Auger nanoprobe measurements for silicates from the meteorites Acfer094, QUE 99177, MET 00426, ALHA 77307, and Adelaide. Sources: Floss and Stadermann (2009a, 2012), Bose et al. (2010a, 2012).

While the ^{57}Fe deficits are difficult to explain, these results show that, at least in some grains, iron must be intrinsic.

The method of choice for studying the grains' crystalline structure is analytical TEM, but the preparation of samples is very labor intensive, for silicate grains involving FIB removal of grains identified as presolar from NanoSIMS isotopic analysis (Messenger et al., 2003, 2005; Nguyen et al., 2005). While Auger analysis can distinguish between pyroxene-like and olivine-like compositions (**Figure 18**), only TEM analysis can provide unambiguous mineral identification (Keller and Messenger, 2011; Messenger et al., 2003, 2005; Nguyen et al., 2007, 2010a, 2011a; Vollmer et al., 2009a). Both crystalline and amorphous grains were found. When crystalline, grains tend to be olivine (Messenger et al., 2005; Vollmer et al., 2009a). TEM analysis led to the identification of a new mineral, $MgSiO_3$ perovskite, previously not found among presolar grains (Vollmer et al., 2007). This structure is not predicted to result from condensation and the authors propose shock transformation. Keller and Messenger (2011) identified four presolar GEMS (glass with embedded metal and sulfide) particles in IDPs and Vollmer et al. (2009a) one with crystalline iron minerals in Acfer094. Keller and Messenger (2011) argue that isotopically normal GEMS grains originated in the solar system, in contrast to Bradley's proposal that GEMS grains, even isotopically normal ones, are remnant IS amorphous silicates (Bradley, 1994; Bradley and Ishii, 2008).

Silicon isotopic ratios have been measured in presolar silicates from meteorites, IDPs, and AMMs (Bose et al., 2010a; Messenger et al., 2005; Mostefaoui and Hoppe, 2004; Nguyen et al., 2007; Vollmer et al., 2008; Yada et al., 2008). In a δ-value silicon three-isotope diagram, most measured ratios plot on a line parallel to the mainstream line of presolar SiC grains (see **Figure 4**) that goes approximately through the origin (normal isotopic composition). The silicate grains' compositions most likely reflect the initial compositions of the parent stars because during the oxygen-rich phase of RGB and AGB stars, not enough material that experienced neutron-capture nucleosynthesis is mixed into the envelope by the third dredge-up to change its silicon isotopic composition. An exception is the grain in the IDP that was identified to have an SN origin (Messenger et al., 2005). It has a large ^{29}Si depletion, in agreement with such an origin. Vollmer et al. (2008) found that group 4 grains tend to plot at the lower end of the mainstream line. Three group 1 grains with high $^{17}O/^{16}O$ ratios plot to the right of the mainstream line, similar to SiC Y grains.

Until recently, a group 2 silicate grain was the only one to have its magnesium isotopic composition measured (Nguyen and Zinner, 2004). It has a ^{26}Mg excess of 120‰ and an inferred $^{26}Al/^{27}Al$ ratio of 0.12. This ratio is second only to that of one corundum gain (**Figure 15**). Such a high ratio implies cool-bottom processing at a temperature of almost 6×10^7 K. In order to avoid beam overlap of the primary O^- beam onto adjacent grains, Nguyen et al. (2010b, 2011b) and Kodolányi and Hoppe (2010, 2011) used FIB to sputter an area around grains of interest clean of other grains. Grains with ^{25}Mg excesses and deficits were found (**Figure 16**). The two grains with excesses have high $^{17}O/^{18}O$ ratios, one possibly being a nova grain.

1.4.10 Diamond

Although diamond is the most abundant presolar grain species (~1400 ppm) and was the first to be isolated (Lewis et al., 1987), it remains the least understood. The only presolar isotopic signatures (indicating an SN origin) are those of Xe–HL and tellurium (Richter et al., 1998) and, to a marginal extent, also those of strontium and barium (Lewis et al., 1991). However, the carbon isotopic composition of bulk diamonds is essentially the same as that of the solar system (Russell et al., 1991, 1996), and diamonds are too small (the average size is ~2.6 nm – hence nanodiamonds) to have been analyzed as single grains. It remains to be seen whether this goal can be achieved with the atom probe (Heck et al., 2011; Stadermann et al., 2011). At present, it is not known whether or not this normal carbon isotopic composition is the result of averaging over grains that have large carbon isotopic anomalies and whether all nanodiamonds are of presolar origin. Nitrogen shows a ^{15}N depletion of 343‰, but isotopically light nitrogen is produced by the CN cycle in all stars and is therefore not very diagnostic. More recent measurements have shown that the nitrogen isotopic ratio of the sun (Marty et al., 2011) and of Jupiter (Owen et al., 2001) is very similar to that of the nanodiamonds, which therefore is not a presolar signature. Furthermore, the concentration of Xe–HL is such that only one diamond grain in a million contains a xenon atom. To date, all attempts to separate different, isotopically distinct, components among nanodiamonds have met with only limited success. Stepped pyrolysis indicates that nitrogen and the noble gas components Xe–HL and Ar–HL are decoupled, with nitrogen being released at lower temperature (Verchovsky et al., 1993a,b), and it is likely that nitrogen and the exotic gases are located in different carriers. A solar origin of a large fraction of the nanodiamonds remains a distinct possibility (Dai et al., 2002).

The light and heavy isotope enrichment in Xe–HL has been interpreted as being due to the *p*- and *r*-process and thus requires an SN origin (Clayton, 1989; Heymann and Dziczkaniec, 1979, 1980). In one model, Xe–H is made by a short neutron burst, with neutron densities intermediate between those characteristic for the *r*- and *s*-processes (Clayton, 1989; Howard et al., 1992). Ott (1996) kept the standard *r*-process but proposed that xenon is separated from iodine and tellurium precursors on a time scale of a few hours after their production. Measurements of tellurium isotopes in nanodiamonds show almost complete absence of the isotopes ^{120}Te, $^{122-126}$Te, and a slight excess of ^{128}Te relative to ^{130}Te (Richter et al., 1998). This pattern agrees much better with a standard *r*-process and early element separation than with the neutron-burst model. Clayton and coworkers (Clayton, 1989; Clayton et al., 1995) have tried to attribute also the diamonds and their carbon and nitrogen isotopic compositions to a Type II SN. This requires mixing of contributions from different SN zones. In contrast, Jørgensen (1988) proposed that diamond and Xe–HL were produced by different members of a binary system of low-mass (1–2 $M_\odot$) stars, diamond in the winds of one member, a carbon star, while Xe–HL by the other, which exploded as a Type Ia SN. However, at present, we do not have an unambiguous identification of the origin of the Xe–HL and tellurium and of the diamonds (in case they have a different origin).

Lyon (2005) applied matrix-assisted laser desorption and ionization (MALDI) analysis, a technique to determine the masses of very heavy organic molecules, to measure the mass and thus size distribution of nanodiamonds from Murchison and Allende. Average sizes determined in this way agree with TEM results (Daulton et al., 1996; Lewis et al., 1989). Verchovsky et al. (2006) have succeeded in isolating a fraction of slightly larger nanodiamonds by differential centrifugation. This fraction, at most 1% of all nanodiamonds, at a combustion temperature of diamonds releases heavy carbon, light nitrogen, *s*-process xenon, and ^{22}Ne, all isotopic signatures of an AGB star origin of this component. A NanoSIMS study of nanodiamonds did not provide any evidence for extinct ^{26}Al and ^{44}Ti other than what can be attributed to SiC impurities (Besmehn et al., 2011). Studies with aberration-corrected scanning TEM with single-atom sensitivity revealed that meteoritic nanodiamond residues contain two phases of carbon: crystalline nanodiamonds and glassy carbon, a disordered phase with sp^2 bonding (Stroud et al., 2011). It is unknown whether one or both of these phases are carriers of the anomalous isotopic signatures.

1.4.11 Conclusion and Future Prospects

The study of presolar grains has provided a wealth of information on galactic evolution, stellar nucleosynthesis, physical properties of stellar atmospheres, and conditions in the solar nebula and on meteoritic parent bodies. However, there are still many features that are not well understood with existing models of nucleosynthesis and stellar evolution and stellar structure. Examples are the carbon and nitrogen isotopic compositions of SiC AB grains, the ^{15}N and ^{29}Si excesses in SN grains, and the paucity of oxide grains from supernovae. The grain data, especially correlated isotopic ratios of many elements, thus provide a challenge to nuclear astrophysics in tightening constraints on theoretical models.

Continuing instrumental developments allow us to make new and more measurements on the grains and will likely lead to new discoveries. For example, the NanoSIMS features high spatial resolution and sensitivity, making isotopic analysis of small grains possible, and this capability has already resulted in the discovery of presolar silicate grains in IDPs, meteorites, and Antarctic micrometeorites (Messenger et al., 2003; Mostefaoui and Hoppe, 2004; Nagashima et al., 2004; Nguyen and Zinner, 2004; Yada et al., 2008); the identification of a large number of presolar spinel grains (Gyngard et al., 2010c; Nguyen et al., 2003; Zinner et al., 2003b); and the discovery of tiny grains with enormous ^{54}Cr excesses (Dauphas et al., 2010; Qin et al., 2011). The NanoSIMS also makes it possible to analyze internal grains that have been studied in detail in the TEM (Stadermann et al., 2005). Another example is the application of RIMS to grain studies. As the number of elements that can be analyzed is being expanded (e.g., to the rare-earth elements), unexpected discoveries, such as the molybdenum isotopic patterns in SiC X grains (Pellin et al., 1999), will probably result. RIMS measurements can also be made on grains, such as SiC and graphite, for which the isotopic ratios of many elements are measured with the ion microprobe. Recently, ICP-MS has been added to the arsenal of analytical instruments applied to the analysis of presolar grains (Yin et al., 2006). The atom probe offers the promise to determine the carbon isotopic ratios of individual nanodiamonds (Heck et al., 2012; Lewis et al., 2012).

It is clear that the discovery of presolar grains and their detailed study in the laboratory have opened a new and fruitful field of astrophysical research. In our effort to understand the distant stars, the microscope successfully complements the telescope.

Acknowledgments

I thank Sachiko Amari, Maitrayee Bose, Christine Floss, Frank Gyngard, Peter Hoppe, Natasha Krestina, Ann Nguyen, Larry Nittler, and Roger Strebel for providing unpublished data and Sachiko Amari, Tom Bernatowicz, and Scott Messenger for providing micrographs. I also thank Frank Gyngard, Mairin Hynes, and Wei Jia Ong for maintaining the presolar database. I am grateful to many of my colleagues for many years of discussion and interactions. Andy Davis provided useful comments on the manuscript.

References

Alexander CMO'D (1993) Presolar SiC in chondrites: How variable and how many sources? *Geochimica et Cosmochimica Acta* 57: 2869–2888.

Alexander CMO'D and Nittler LR (1999) The galactic evolution of Si, Ti, and O isotopic ratios. *The Astrophysical Journal* 519: 222–235.

Alexander CMO'D, Swan P, and Prombo CA (1994) Occurrence and implications of silicon nitride in enstatite chondrites. *Meteoritics* 29: 79–85.

Amari S (2003) Presolar graphite: Noble gases and their origins. *Publications of the Astronomical Society of Australia* 20: 378–381.

Amari S (2006) Presolar graphite from the Murchison meteorite: Neon revisited. *New Astronomy Reviews* 50: 578–581.

Amari S (2009) Sodium-22 from supernovae: A meteorite connection. *The Astrophysical Journal* 690: 1424–1431.

Amari S, Anders E, Virag A, and Zinner E (1990) Interstellar graphite in meteorites. *Nature* 345: 238–240.

Amari S, Gallino R, and Pignatari M (2006) Presolar graphite from the Murchison meteorite: Noble gases revisited. *Lunar and Planetary Science* 37: #2409.

Amari S, Gao X, Nittler LR, et al. (2001a) Presolar grains from novae. *The Astrophysical Journal* 551: 1065–1072.

Amari S, Hoppe P, Zinner E, and Lewis RS (1992) Interstellar SiC with unusual isotopic compositions: Grains from a supernova? *The Astrophysical Journal* 394: L43–L46.

Amari S, Hoppe P, Zinner E, and Lewis RS (1995a) Trace-element concentrations in single circumstellar silicon carbide grains from the Murchison meteorite. *Meteoritics* 30: 679–693.

Amari S, Jennings C, Nguyen A, Stadermann FJ, Zinner E, and Lewis RS (2002) NanoSIMS isotopic analysis of small presolar SiC grains from the Murchison and Indarch meteorites. *Lunar and Planetary Science* 33: #1205.

Amari S, Lewis RS, and Anders E (1994) Interstellar grains in meteorites: I. Isolation of SiC, graphite, and diamond; size distributions of SiC and graphite. *Geochimica et Cosmochimica Acta* 58: 459–470.

Amari S, Lewis RS, and Anders E (1995b) Interstellar grains in meteorites: III. Graphite and its noble gases. *Geochimica et Cosmochimica Acta* 59: 1411–1426.

Amari S, Nittler LR, Zinner E, Gallino R, Lugaro M, and Lewis RS (2001b) Presolar SiC grains of type Y: Origin from low-metallicity asymptotic giant branch stars. *The Astrophysical Journal* 546: 248–266.

Amari S, Nittler LR, Zinner E, Lodders K, and Lewis RS (2001c) Presolar SiC grains of type A and B: Their isotopic compositions and stellar origins. *The Astrophysical Journal* 559: 463–483.

Amari S, Stadermann FJ, Zinner E, and Lewis RS (2003) Continued study of presolar graphite from Murchison separate KFA1. *Lunar and Planetary Science* 34: #1864.

Amari S, Zinner E, Clayton DD, and Meyer BS (1998) Presolar grains from supernovae: The case for a type Ia SN source. *Meteoritics & Planetary Science* 33: A10.

Amari S, Zinner E, and Gallino R (2012) Presolar graphite from the Murchison meteorite; puzzles related to its origins. *Lunar and Planetary Science* 43: #1031.

Amari S, Zinner E, Gallino R, Lugaro M, Straniero O, and Domínguez I (2005a) Probing the Galactic chemical evolution of Si and Ti with presolar SiC grains. In: Terasawa M, Kubano S, Kishida T, Kajino T, Motobayashi T, and Nomato K (eds.) *Origin of Matter and Evolution of the Galaxies 2003*, vol. 59, p. 70. Riken, Japan: Publ. World Scientific.

Amari S, Zinner E, and Lewis RS (1996) ^{41}Ca in presolar graphite of supernova origin. *The Astrophysical Journal* 470: L101–L104.

Amari S, Zinner E, and Lewis RS (1999) A singular presolar SiC grain with extreme ^{29}Si and ^{30}Si excesses. *The Astrophysical Journal* 517: L59–L62.

Amari S, Zinner E, and Lewis RS (2000) Isotopic compositions of different presolar silicon carbide size fractions from the Murchison meteorite. *Meteoritics & Planetary Science* 35: 997–1014.

Amari S, Zinner E, and Lewis RS (2004) Comparison study of presolar graphite separates KE3 and KFA1 from the Murchison meteorite. *Lunar and Planetary Science* 35: #2103.

Amari S, Zinner E, and Lewis RS (2005b) Isotopic analysis of presolar graphite from the KFB1 Murchison separate. *Meteoritics & Planetary Science* 40: A15.

Anders E and Grevesse N (1989) Abundances of the elements: Meteoritic and solar. *Geochimica et Cosmochimica Acta* 53: 197–214.

Anders E and Zinner E (1993) Interstellar grains in primitive meteorites: Diamond, silicon carbide, and graphite. *Meteoritics* 28: 490–514.

Arlandini C, Käppeler F, Wisshak K, et al. (1999) Neutron capture in low-mass asymptotic giant branch stars: Cross sections and abundance signatures. *The Astrophysical Journal* 525: 886–900.

Arnett D (1996) *Supernovae and Nucleosynthesis*. Princeton: Princeton University Press 598 pp.

Arnould M, Meynet G, and Paulus G (1997) Wolf–Rayet stars and their nucleosynthetic signatures in meteorites. In: Bernatowicz TJ and Zinner E (eds.) *Astrophysical Implications of the Laboratory Study of Presolar Materials*, pp. 179–202. New York: AIP.

Asplund M, Grevesse N, and Sauval AJ (2005) The solar chemical composition. In: Barnes TG and Bash FN (eds.) *Cosmic Abundances as Records of Stellar Evolution and Nucleosynthesis*, *ASP Conference Series* p. 25.

Asplund M, Lambert DL, Kipper T, Pollacco D, and Shetrone MD (1999) The rapid evolution of the born-again giant Sakurai's object. *Astronomy and Astrophysics* 343: 507–518.

Avila JN, Ireland T, Gyngard F, et al. (in press) Ba isotopic compositions in stardust SiC grains from the Murchison meteorite: Insights into the stellar origins of large SiC grains. *Geochimica et Cosmochimica Acta*. http://dx.doi.org/10.1016/j.gca.2013.03.039.

Avila JN, Ireland TR, Lugaro M, et al. (2012a) U–Th–Pb isotopic compositions in stardust SiC grains from the Murchison meteorite. *Lunar and Planetary Science* 43: #2709.

Avila JN, Lugaro M, Ireland TR, et al. (2012b) Tungsten isotopic compositions in stardust SiC grains from the Murchison meteorite: Constraints on the s-process in the Hf–Ta–W–Re–Os region. *The Astrophysical Journal* 744: 49–62.

Barzyk JG, Savina MR, Davis AM, et al. (2007) Constraining the ^{13}C neutron source in AGB stars through isotopic analysis of trace elements in presolar SiC. *Meteoritics & Planetary Science* 42: 1103–1119.

Becker SA and Iben I Jr. (1979) The asymptotic giant branch evolution of intermediate-mass stars as a function of mass and composition. I. Through the second dredge-up phase. *The Astrophysical Journal* 232: 831–853.

Bernatowicz TJ, Akande OW, Croat TK, and Cowsik R (2005) Constraints on grain formation around carbon stars from laboratory studies of presolar graphite. *The Astrophysical Journal* 631: 988–1000.

Bernatowicz TJ, Amari S, and Lewis RS (1992) TEM studies of a circumstellar rock. *Lunar and Planetary Science* 23: 91–92.

Bernatowicz TJ, Amari S, Zinner EK, and Lewis RS (1991) Interstellar grains within interstellar grains. *The Astrophysical Journal* 373: L73–L76.

Bernatowicz TJ, Cowsik R, Gibbons PC, et al. (1996) Constraints on stellar grain formation from presolar graphite in the Murchison meteorite. *The Astrophysical Journal* 472: 760–782.

Bernatowicz TJ, Croat TK, and Daulton TL (2006) Origin and evolution of carbonaceous presolar grains in stellar environments. In: Lauretta DS and McSween HY Jr. (eds.) *Meteorites and the Early Solar System II*, pp. 109–126. Tucson: University of Arizona.

Bernatowicz T, Fraundorf G, Tang M, et al. (1987) Evidence for interstellar SiC in the Murray carbonaceous meteorite. *Nature* 330: 728–730.

Bernatowicz TJ, Messenger S, Pravdivtseva O, Swan P, and Walker RM (2003) Pristine presolar silicon carbide. *Geochimica et Cosmochimica Acta* 67: 4679–4691.

Bernatowicz TJ and Zinner E (eds.) (1997) *Astrophysical Implications of the Laboratory Study of Presolar Materials*. New York: AIP 750 pp.

Besmehn A and Hoppe P (2001) Silicon- and calcium-isotopic compositions of presolar silicon nitride grains from the Indarch enstatite chondrite. *Lunar and Planetary Science* 32: #1188.

Besmehn A and Hoppe P (2003) A NanoSIMS study of Si- and Ca–Ti-isotopic compositions of presolar silicon carbide grains from supernovae. *Geochimica et Cosmochimica Acta* 67: 4693–4703.

Besmehn A, Hoppe P, and Ott U (2011) Search for extinct aluminum-26 and titanium-44 in nanodiamonds from the Allende CV3 and Murchison CM2 meteorites. *Meteoritics & Planetary Science* 46: 1265–1275.

Black DC (1972) On the origins of trapped helium, neon and argon isotopic variations in meteorites II. Carbonaceous meteorites. *Geochimica et Cosmochimica Acta* 36: 377–394.

Black DC and Pepin RO (1969) Trapped neon in meteorites. II. *Earth and Planetary Science Letters* 6: 395–405.

Boato G (1954) The isotopic composition of hydrogen and carbon in the carbonaceous chondrites. *Geochimica et Cosmochimica Acta* 6: 209–220.

Boothroyd AI and Sackmann I-J (1988) Low-mass stars. III. Low-mass stars with steady mass loss: Up to the asymptotic giant branch and through the final thermal pulses. *The Astrophysical Journal* 328: 653–670.

Boothroyd AI and Sackmann I-J (1999) The CNO isotopes: Deep circulation in red giants and first and second dredge-up. *The Astrophysical Journal* 510: 232–250.

Boothroyd AI, Sackmann I-J, and Wasserburg GJ (1994) Predictions of oxygen isotope ratios in stars and of oxygen-rich interstellar grains in meteorites. *The Astrophysical Journal* 430: L77–L80.

Boothroyd AI, Sackmann I-J, and Wasserburg GJ (1995) Hot bottom burning in asymptotic giant branch stars and its effect on oxygen isotopic abundances. *The Astrophysical Journal* 442: L21–L24.

Bose M, Floss C, and Stadermann FJ (2010a) An investigation into the origin of Fe-rich presolar silicates in Acfer 094. *The Astrophysical Journal* 714: 1624–1636.

Bose M, Floss C, Stadermann FJ, and Speck AK (2012) Stellar and interstellar material in the CO3 chondrite ALHA 77307: An isotopic and elemental investigation. *Geochimica et Cosmochimica Acta* 93: 77–101.

Bose M, Zhao X, Floss C, Stadermann FJ, and Lin Y (2010b) Stardust material in the paired enstatite chondrites: SAH 97096 and SAH 97159. *Proceedings of Science (NIC-XI)* 138.

Bradley JP (1994) Chemically anomalous, preaccretionally irradiated grains in interplanetary dust from comets. *Science* 265: 925–929.

Bradley JP and Ishii HA (2008) Comment on "The shape and composition of interstellar silicate grains" *Astronomy and Astrophysics* 486: 781–784.

Brown LE and Clayton DD (1992) SiC particles from asymptotic giant branch stars: Mg burning and the *s*-process. *The Astrophysical Journal* 392: L79–L82.

Brownlee DE, Joswiak D, Matrajt G, Messenger S, and Ito M (2009) Silicon carbide in Comet WILD 2 & the abundance of pre-solar grains in the Kuiper belt. *Lunar and Planetary Science* 40: 2195.

Burbidge EM, Burbidge GR, Fowler WA, and Hoyle F (1957) Synthesis of the elements in stars. *Reviews of Modern Physics* 29: 547–650.

Busemann H, Nguyen AN, Cody GD, et al. (2009) Ultra-primitive interplanetary dust particles from the comet 26P/Grigg–Skjellerup dust stream collection. *Earth and Planetary Science Letters* 288: 44–57.

Busso M, Gallino R, Lambert DL, Travaglio C, and Smith VV (2001) Nucleosynthesis and mixing on the asymptotic giant branch. III. Predicted and observed s-process abundances. *The Astrophysical Journal* 557: 802–821.

Busso M, Gallino R, and Wasserburg GJ (1999) Nucleosynthesis in asymptotic giant branch stars: Relevance for Galactic enrichment and solar system formation. *Annual Review of Astronomy and Astrophysics* 37: 239–309.

Cameron AGW (1957) Stellar evolution, nuclear astrophysics and nucleogenesis. *Publications of the Astronomical Society of the Pacific* 69: 201–222.

Cameron AGW (1962) The formation of the sun and planets. *Icarus* 1: 13–69.

Caughlan GR and Fowler WA (1988) Thermonuclear reaction rates V. *Atomic Data and Nuclear Data Tables* 40: 283–334.

Charbonnel C (1995) A consistent explanation for ^{12}C/^{13}C, ^{7}Li, and ^{3}He anomalies in red giant stars. *The Astrophysical Journal* 453: L41–L44.

Choi B-G, Huss GR, Wasserburg GJ, and Gallino R (1998) Presolar corundum and spinel in ordinary chondrites: Origins from AGB stars and a supernova. *Science* 282: 1284–1289.

Choi B-G, Wasserburg GJ, and Huss GR (1999) Circumstellar hibonite and corundum and nucleosynthesis in asymptotic giant branch stars. *The Astrophysical Journal* 522: L133–L136.

Clayton DD (1975) Na-22, Ne–E, extinct radioactive anomalies and unsupported Ar-40. *Nature* 257: 36–37.

Clayton DD (1983a) Discovery of s-process Nd in Allende residue. *The Astrophysical Journal* 271: L107–L109.

Clayton DD (1983b) *Principles of Stellar Evolution and Nucleosynthesis*. Chicago: University of Chicago Press 612 pp.
Clayton DD (1989) Origin of heavy xenon in meteoritic diamonds. *The Astrophysical Journal* 340: 613–619.
Clayton DD (1997) Placing the sun and mainstream SiC particles in galactic chemodynamic evolution. *The Astrophysical Journal* 484: L67–L70.
Clayton DD (2003) Presolar galactic merger spawned the SiC grain mainstream. *The Astrophysical Journal* 598: 313–324.
Clayton DD (2011) A new astronomy with radioactivity: Radiogenic carbon chemistry. *New Astronomy Reviews* 55: 155–165.
Clayton DD, Arnett WD, Kane J, and Meyer BS (1997) Type X silicon carbide presolar grains: Type Ia supernova condensates? *The Astrophysical Journal* 486: 824–834.
Clayton RN, Grossman L, and Mayeda TK (1973) A component of primitive nuclear composition in carbonaceous meteorites. *Science* 182: 485–488.
Clayton RN, Hinton RW, and Davis AM (1988) Isotopic variations in the rock-forming elements in meteorites. *Philosophical Transactions of the Royal Society of London A* 325: 483–501.
Clayton DD, Liu W, and Dalgarno A (1999) Condensation of carbon in radioactive supernova gas. *Science* 283: 1290–1292.
Clayton DD, Meyer BS, Sanderson CI, Russell SS, and Pillinger CT (1995) Carbon and nitrogen isotopes in type II supernova diamonds. *The Astrophysical Journal* 447: 894–905.
Clayton DD and Nittler LR (2004) Astrophysics with presolar stardust. *Annual Review of Astronomy and Astrophysics* 42: 39–78.
Clayton DD, Obradovic M, Guha S, and Brown LE (1991) Silicon and titanium isotopes in SiC from AGB stars. *Lunar and Planetary Science* 22: 221–222.
Clayton DD and Timmes FX (1997a) Implications of presolar grains for Galactic chemical evolution. In: Bernatowicz TJ and Zinner E (eds.) *Astrophysical Implications of the Laboratory Study of Presolar Materials*, pp. 237–264. New York: AIP.
Clayton DD and Timmes FX (1997b) Placing the Sun in galactic chemical evolution: Mainstream SiC particles. *The Astrophysical Journal* 483: 220–227.
Clayton DD and Ward RA (1978) *s*-Process studies: Xenon and krypton isotopic abundances. *The Astrophysical Journal* 224: 1000–1006.
Cristallo S, Straniero O, Gallino R, Piersanti L, Domínguez I, and Lederer MT (2009) Evolution, nucleosynthesis, and yields of low-mass asymptotic giant branch stars at different metallicities. *The Astrophysical Journal* 696: 797–820.
Croat TK, Berg T, Bernatowicz TJ, and Jadhav M (2013) Refractory metal nuggets within presolar graphite: First condensates from a circumstellar environment. *Meteoritics & Planetary Science* 48: 686–699.
Croat TK, Berg T, Jadhav M, and Bernatowicz TJ (2012) Presolar refractory metal nuggets. *Lunar and Planetary Science* 43: #1503.
Croat TK, Bernatowicz T, Amari S, Messenger S, and Stadermann FJ (2003) Structural, chemical, and isotopic microanalytical investigations of graphite from supernovae. *Geochimica et Cosmochimica Acta* 67: 4705–4725.
Croat TK, Jadhav M, Lebsack E, and Bernatowicz T (2011a) A unique supernova graphite: Contemporaneous condensation of all things carbonaceous. *Lunar and Planetary Science* 42: #1533.
Croat TK, Jadhav M, Lebsack E, and Bernatowicz T (2011b) TiC and rutile within a supernova graphite. *Meteoritics & Planetary Science* 46: A51.
Croat TK, Stadermann FJ, and Bernatowicz TJ (2005a) Internal grains within KFC graphites: Implications for their stellar source. *Lunar and Planetary Science* 36: #1507.
Croat TK, Stadermann FJ, and Bernatowicz TJ (2005b) Presolar graphite from AGB stars: Microstructure and s-process enrichment. *The Astrophysical Journal* 631: 976–987.
Croat TK, Stadermann F, and Bernatowicz T (2008) Correlated isotopic and microstructural studies of turbostratic presolar graphites from the Murchison meteorite. *Meteoritics & Planetary Science* 43: 1497–1516.
Croat TK, Stadermann FJ, and Bernatowicz TJ (2010) Unusual ^{29,30}Si-rich SiCs of massive star origin found within graphite from the Murchison meteorite. *The Astronomical Journal* 139: 2159–2169.
Dai ZR, Bradley JP, Joswiak DJ, Brownlee DE, Hill HGM, and Genge MJ (2002) Possible *in situ* formation of meteoritic nanodiamonds in the early Solar System. *Nature* 418: 157–159.
Daulton TL, Bernatowicz TJ, Lewis RS, Messenger S, Stadermann FJ, and Amari S (2002) Polytype distribution in circumstellar silicon carbide. *Science* 296: 1852–1855.
Daulton TL, Bernatowicz TJ, Lewis RS, Messenger S, Stadermann FJ, and Amari S (2003) Polytype distribution of circumstellar silicon carbide: Microstructural characterization by transmission electron microscopy. *Geochimica et Cosmochimica Acta* 67: 4743–4767.
Daulton TL, Eisenhour DD, Bernatowicz TJ, Lewis RS, and Buseck PR (1996) Genesis of presolar diamonds: Comparative high-resolution transmission electron microscopy study of meteoritic and terrestrial nano-diamonds. *Geochimica et Cosmochimica Acta* 60: 4853–4872.
Dauphas N, Remusat L, Chen JH, et al. (2010) Neutron-rich chromium isotope anomalies in supernova nanoparticles. *The Astrophysical Journal* 720: 1577–1591.
Davidson J, Busemann H, Alexander CMO'D, et al. (2009) Presolar SiC abundances in primitive meteorites by NanoSIMS raster ion imaging of insoluble organic matter. *Lunar and Planetary Science* 40: #1853.
Davidson J, Busemann H, Franchi IA, and Grady MM (2010) Presolar grain inventories of the ungrouped C3 Adelaide and the CV3 RBT 04133. *Lunar and Planetary Science* 41: #2230.
Davis AM (2011) Stardust in meteorites. *Proceedings of the National Academy of Sciences* 108: 19142–19146.
Davis AM, Pellin MJ, Tripa CE, et al. (2002) Multielement analyses of single presolar SiC grains from supernovae. *Geochimica et Cosmochimica Acta* 66: A171.
Demyk K, Dartois E, Wiesemeyer H, Jones AP, and d'Hendecourt L (2000) Structure and chemical composition of the silicate dust around OH/IR stars. *Astronomy and Astrophysics* 364: 170–178.
Deneault EA-N, Clayton DD, and Heger A (2003) Supernova reverse shocks and SiC growth. *The Astrophysical Journal* 594: 312–325.
Deneault EA-N, Clayton DD, and Meyer BS (2006) Growth of carbon grains in supernova ejecta. *The Astrophysical Journal* 638: 234–240.
Denissenkov PA and Weiss A (1996) Deep diffusive mixing in globular-cluster red giants. *Astronomy and Astrophysics* 308: 773–784.
Ebata S and Yurimoto H (2008) Identification of silicate and carbonaceous presolar grains in the type 3 enstatite chondrites. *Origin of Matter and Evolution of Galaxies*, vol. 1016, pp. 412–414. New York: AIP.
Ebel DS and Grossman L (2001) Condensation from supernova gas made of free atoms. *Geochimica et Cosmochimica Acta* 65: 469–477.
Ebisuzaki T and Shibazaki N (1988) The effects of mixing of the ejecta on the hard x-ray emissions from SN 1987A. *The Astrophysical Journal* 327: L5–L8.
El Eid M (1994) CNO isotopes in red giants: Theory versus observations. *Astronomy and Astrophysics* 285: 915–928.
Fazio C, Gallino R, Pignatari M, et al. (2003) Isotopic composition of Kr in presolar mainstream SiC grains. *Geochimica et Cosmochimica Acta* 67: A91.
Ferrarotti AS and Gail H-P (2006) Composition and quantities of dust produced by AGB-stars and returned to the interstellar medium. *Astronomy and Astrophysics* 447: 553–576.
Floss C and Stadermann FJ (2005) Presolar (circumstellar and interstellar) phases in Renazzo: The effects of parent body processing. *Lunar and Planetary Science* 36: #1390.
Floss C and Stadermann F (2009a) Auger Nanoprobe analysis of presolar ferromagnesian silicate grains from primitive CR chondrites QUE 99177 and MET 00426. *Geochimica et Cosmochimica Acta* 73: 2415–2440.
Floss C and Stadermann F (2009b) High abundances of circumstellar and interstellar C-anomalous phases in the primitive CR3 chondrites QUE 99177 and MET 00426. *The Astrophysical Journal* 697: 1242–1255.
Floss C and Stadermann FJ (2009c) Interstellar components in the primitive CR3 chondrites QUE 99177 and MET 00426. *Lunar and Planetary Science* 40: #1083.
Floss C and Stadermann FJ (2012) Presolar silicate and oxide abundances and compositions in the ungrouped carbonaceous chondrite Adelaide and the K chondrite Kakangari: The effects of secondary processing. *Meteoritics & Planetary Science* 47: 992–1009.
Floss C, Stadermann FJ, and Bose M (2008) Circumstellar Fe oxide from the Acfer 094 carbonaceous chondrite. *The Astrophysical Journal* 672: 1266–1271.
Floss C, Stadermann FJ, Bradley JP, et al. (2006) Identification of isotopically primitive interplanetary dust particles: A NanoSIMS isotopic imaging study. *Geochimica et Cosmochimica Acta* 70: 2371–2399.
Floss C, Stadermann FJ, Mertz AF, and Bernatowicz TJ (2011) A NanoSIMS and Auger Nanoprobe investigation of an isotopically primitive interplanetary dust particle from the 55P/Tempel–Tuttle targeted stratospheric dust collector. *Meteoritics & Planetary Science* 45: 1889–1905.
Forestini M, Paulus G, and Arnould M (1991) On the production of ^{26}Al in AGB stars. *Astronomy and Astrophysics* 252: 597–604.
Frost CA and Lattanzio JC (1996) AGB stars: What should be done? In: Noel A, Fraipont-Caro D, Gabriel M, Grevesse N, and Demarque P (eds.) *Stellar Evolution: What Should Be Done*. 32nd Liège Int. Astroph. Coll, pp. 307–325. Liège, Belgium: Université de Liège.
Gail H-P, Zhukovska SV, Hoppe P, and Trieloff M (2009) Stardust from asymptotic giant branch stars. *The Astrophysical Journal* 698: 1136–1154.
Gallino R, Busso M, and Lugaro M (1997) Neutron capture nucleosynthesis in AGB stars. In: Bernatowicz TJ and Zinner E (eds.) *Astrophysical Implications of the Laboratory Study of Presolar Materials*, pp. 115–153. New York: AIP.

Gallino R, Busso M, Picchio G, and Raiteri CM (1990) On the astrophysical interpretation of isotope anomalies in meteoritic SiC grains. *Nature* 348: 298–302.

Gallino R, Raiteri CM, and Busso M (1993) Carbon stars and isotopic Ba anomalies in meteoritic SiC grains. *The Astrophysical Journal* 410: 400–411.

Gallino R, Raiteri CM, Busso M, and Matteucci F (1994) The puzzle of silicon, titanium and magnesium anomalies in meteoritic silicon carbide grains. *The Astrophysical Journal* 430: 858–869.

Grevesse N, Noels A, and Sauval AJ (1996) Standard abundances. In: Holt SS and Sonneborn G (eds.) *Cosmic Abundances*, pp. 117–126. San Francisco: BookCrafters, Inc.

Gröner E and Hoppe P (2006) Automated ion imaging with the NanoSIMS ion microprobe. *Applied Surface Science* 252: 7148–7151.

Groopman E, Bernatowicz T, and Zinner E (2012) C, N, and O isotopic heterogeneities in low-density supernova graphite grains from Orgueil. *The Astrophysical Journal* 754: L8(6pp).

Guber KH, Koehler PE, Derrien H, et al. (2003) Neutron capture reaction rates for silicon and their impact on the origin of presolar mainstream SiC grains. *Physical Review C: Nuclear Physics* 67: 062802-1–062802-5.

Guber KH, Spencer RR, Koehler PE, and Winters RR (1997) New ^{142,144}Nd (n, g) cross sections and the s-process origin of the Nd anomalies in presolar meteoritic silicon carbide grains. *Physical Review Letters* 78: 2704–2707.

Gyngard F, Amari S, Zinner E, and Ott U (2009a) Cosmic-ray exposure ages of large presolar SiC grains. *Publications of the Astronomical Society of Australia* 26: 278–283.

Gyngard F, Amari S, Zinner E, and Ott U (2009b) Erratum: "Interstellar exposure ages of large presolar SiC grains from the Murchison meteorite" (2009, ApJ 694, 359). *The Astrophysical Journal* 700: 1995.

Gyngard F, Amari S, Zinner E, and Ott U (2009c) Interstellar exposure ages of large presolar SiC grains from the Murchison meteorite. *The Astrophysical Journal* 694: 359–366.

Gyngard F, Nittler LR, and Zinner E (2010a) Presolar SiC grains of Type C. *Meteoritics & Planetary Science* 45: A72.

Gyngard F, Nittler LR, Zinner E, and Jose J (2010b) Oxygen-rich stardust grains from novae. *Proceedings of Science (NIC-XI)* 141.

Gyngard F, Nittler LR, Zinner E, Jose J, and Cristallo S (2011) New reaction rates and implications for nova nucleosynthesis and presolar grains. *Lunar and Planetary Science* 42: #2675.

Gyngard F, Zinner E, Nittler LR, Morgand A, Stadermann FJ, and Hynes KM (2010c) Automated NanoSIMS measurements of spinel stardust from the Murray meteorite. *The Astrophysical Journal* 717: 107–120.

Haenecour P and Floss C (2011) High abundance of stardust in the CO3.0 chondrite LaPaz 031117. *Meteoritics & Planetary Science* 46: A85.

Haenecour P and Floss C (2012) Stardust in fine-grained chondrule rims and matrix in Lapaz 031117: Insights into the conditions of the dust accretion in the solar nebula. *Lunar and Planetary Science* 43: #1107.

Halbout J, Mayeda TK, and Clayton RN (1986) Carbon isotopes and light element abundances in carbonaceous chondrites. *Earth and Planetary Science Letters* 80: 1–18.

Hammer NJ, Janka H-T, and Müller E (2010) Three-dimensional simulations of mixing instabilities in supernova explosions. *The Astrophysical Journal* 714: 1371–1385.

Harris MJ and Lambert DL (1984) Oxygen isotopic abundances in the atmospheres of seven red giant stars. *The Astrophysical Journal* 285: 674–682.

Harris MJ, Lambert DL, Hinkle KH, Gustafsson B, and Eriksson K (1987) Oxygen isotopic abundances in evolved stars. III. 26 carbon stars. *The Astrophysical Journal* 316: 294–304.

Heck PR, Amari S, Hoppe P, Baur H, Lewis RS, and Wieler R (2009a) Erratum: "Ne isotopes in individual presolar graphite grains from the Murchison meteorite together with He, C, O, Mg–Al isotopic analyses as tracers of their origins" (2009, ApJ, 701, 1415). *The Astrophysical Journal* 705: 1095–1097.

Heck PR, Amari S, Hoppe P, Baur H, Lewis RS, and Wieler R (2009b) Ne isotopes in individual presolar graphite grains from the Murchison meteorite together with He, C, O, Mg–Al isotopic analyses as tracers of their origins. *The Astrophysical Journal* 701: 1415–1425.

Heck PR, Gyngard F, Ott U, et al. (2009c) Interstellar residence times of presolar SiC dust grains from the Murchison carbonaceous meteorite. *The Astrophysical Journal* 698: 1155–1164.

Heck PR, Marhas KK, Baur H, Hoppe P, and Wieler R (2005) Presolar He and Ne in single circumstellar SiC grains extracted from the Murchison and Murray meteorites. *Lunar and Planetary Science* 36: 1938.

Heck PR, Marhas KK, Gallino R, Hoppe P, Baur H, and Wieler R (2006) Helium and neon in single presolar grains from the meteorites Murchison and Murray. *Memorie della Societa Astronomica Italiana* 77: 903–906.

Heck PR, Marhas KK, Hoppe P, Gallino R, Baur H, and Wieler R (2007) Presolar He and Ne isotopes in single circumstellar SiC grains. *The Astrophysical Journal* 656: 1208–1222.

Heck PR, Pellin MJ, Davis AM, et al. (2011) Atom-probe tomographic analyses of meteoritic nanodiamond residue from Allende. *Lunar and Planetary Science* 42: #2070.

Heck PR, Pellin MJ, Davis AM, et al. (2012) Atom-probe tomographic analysis: Towards carbon isotope ratios in individual nanodiamonds. *Lunar and Planetary Science* 43: #1790.

Herant M, Benz W, Hix WR, Fryer CL, and Colgate SA (1994) Inside the supernova: A powerful convective engine. *The Astrophysical Journal* 435: 339–361.

Herwig F (2001a) Stellar evolution and nucleosynthesis of Post-AGB stars. In: Szczerba R and Górny SK (eds.) *Post-AGB Objects as a Phase of Stellar Evolution*. *Astrophys. and Space Sci. Lib.*, vol. 265, p. 9. Dordrecht: Kluwer Academic Publishers.

Herwig F (2001b) The evolutionary timescale of Sakurai's object: A test of convection theory? *The Astrophysical Journal* 554: L71–L74.

Herwig F (2005) Evolution of asymptotic giant branch stars. *Annual Review of Astronomy and Astrophysics* 43: 435–479.

Herwig F, Amari S, Lugaro M, and Zinner E (2004) Could SiC A + B grains have originated in a post-AGB thermal pulse? In: Kwok S, Dopita M, and Sutherland R (eds.) *Planetary Nebulae: Their Evolution and Role in the Universe*, PASP Conf. Ser., IAU Symp. 209, Publ. Vol. Canberra, Australia, pp. 311–312

Herwig F, Pignatari M, Woodward PR, et al. (2011) Convective-reactive proton-^{12}C combustion in Sakurai's object (V4334 Sagittarii) and implications for the evolution and yields from the first generations of stars. *The Astrophysical Journal* 727: 89 15 pp.

Heymann D and Dziczkaniec M (1979) Xenon from intermediate zones of supernovae. In: *Proc. Lunar Planet. Sci. Conf.* 10: 1943–1959.

Heymann D and Dziczkaniec M (1980) A first roadmap for kryptology. In: *Proc. Lunar Planet. Sci. Conf.* 11: 1179–1213.

Holzapfel C, Soldera F, Vollmer C, Hoppe P, and Mücklich F (2009) TEM foil preparation of sub-micrometre sized individual grains by focused ion beam technique. *Journal of Microscopy* 235: 59–66.

Hoppe P (2004) Stardust in meteorites. In: Witt A, Clayton GC, and Draine BT (eds.) *Astrophysics of Dust*, *Publ. ASP Conference Series*, vol. 309, 265–283.

Hoppe P (2010) Measurements of presolar grains. *Proceedings of Science (NIC-XI)* 021.

Hoppe P, Amari S, Zinner E, Ireland T, and Lewis RS (1994) Carbon, nitrogen, magnesium, silicon and titanium isotopic compositions of single interstellar silicon carbide grains from the Murchison carbonaceous chondrite. *The Astrophysical Journal* 430: 870–890.

Hoppe P, Amari S, Zinner E, and Lewis RS (1995) Isotopic compositions of C, N, O, Mg, and Si, trace element abundances, and morphologies of single circumstellar graphite grains in four density fractions from the Murchison meteorite. *Geochimica et Cosmochimica Acta* 59: 4029–4056.

Hoppe P, Annen P, Strebel R, et al. (1997) Meteoritic silicon carbide grains with unusual Si-isotopic compositions: Evidence for an origin in low-mass low-metallicity asymptotic giant branch stars. *The Astrophysical Journal* 487: L101–L104.

Hoppe P and Besmehn A (2002) Evidence for extinct vanadium-49 in presolar silicon carbide grains from supernovae. *The Astrophysical Journal* 576: L69–L72.

Hoppe P, Fujiya W, and Zinner E (2012) Sulfur molecule chemistry in supernova ejecta recorded by silicon carbide stardust. *The Astrophysical Journal* 745: L26–L30.

Hoppe P, Leitner J, Gröner E, Marhas KK, Meyer BS, and Amari S (2010) NanoSIMS studies of small presolar SiC grains: New insights into supernova nucleosynthesis, chemistry, and dust formation. *The Astrophysical Journal* 719: 1370–1384.

Hoppe P, Leitner J, Meyer BS, The L-S, Lugaro M, and Amari S (2009a) An unusual presolar silicon carbide grain from a supernova: Implications for the production of silicon-29 in Type II supernovae. *The Astrophysical Journal* 691: L20–L23.

Hoppe P, Leitner J, Vollmer C, et al. (2009b) Heavy element abundances in presolar silicon carbide grains from low-metallicity AGB stars. *Publications of the Astronomical Society of Australia* 26: 284–288.

Hoppe P, Marhas KK, Gallino R, Straniero O, Amari S, and Lewis RS (2004) Aluminum-26 in submicrometer-sized presolar SiC grains. *Lunar and Planetary Science* 35: #1302.

Hoppe P and Ott U (1997) Mainstream silicon carbide grains from meteorites. In: Bernatowicz TJ and Zinner E (eds.) *Astrophysical Implications of the Laboratory Study of Presolar Materials*, pp. 27–58. New York: AIP.

Hoppe P, Strebel R, Eberhardt P, Amari S, and Lewis RS (1996a) Small SiC grains and a nitride grain of circumstellar origin from the Murchison meteorite: Implications for stellar evolution and nucleosynthesis. *Geochimica et Cosmochimica Acta* 60: 883–907.

Hoppe P, Strebel R, Eberhardt P, Amari S, and Lewis RS (1996b) Type II supernova matter in a silicon carbide grain from the Murchison meteorite. *Science* 272: 1314–1316.

Hoppe P, Strebel R, Eberhardt P, Amari S, and Lewis RS (2000) Isotopic properties of silicon carbide X grains from the Murchison meteorite in the size range 0.5–1.5 mm. *Meteoritics & Planetary Science* 35: 1157–1176.

Hoppe P and Zinner E (2000) Presolar dust grains from meteorites and their stellar sources. *Journal of Geophysical Research* 105: 10371–10385.

Hoppe P and Zinner E (2012) Sulfur-isotopic signature of presolar SiC grains of type X. *Lunar and Planetary Science* 43: #1414.

Howard WM, Meyer BS, and Clayton DD (1992) Heavy-element abundances from a neutron burst that produces Xe–H. *Meteoritics* 27: 404–412.

Hughes JP, Rakowski CE, Burrows DN, and Slane PO (2000) Nucleosynthesis and mixing in Cassiopeia A. *The Astrophysical Journal* 528: L109–L113.

Huss GR, Hutcheon ID, and Wasserburg GJ (1997) Isotopic systematics of presolar silicon carbide from the Orgueil (CI) carbonaceous chondrite: Implications for solar system formation and stellar nucleosynthesis. *Geochimica et Cosmochimica Acta* 61: 5117–5148.

Huss GR and Lewis RS (1995) Presolar diamond, SiC, and graphite in primitive chondrites: Abundances as a function of meteorite class and petrologic type. *Geochimica et Cosmochimica Acta* 59: 115–160.

Huss GR, Meshik AP, Smith JB, and Hohenberg CM (2003) Presolar diamond, silicon carbide, and graphite in carbonaceous chondrites: Implications for thermal processing in the solar nebula. *Geochimica et Cosmochimica Acta* 67: 4823–4848.

Huss GR and Smith JB (2007) Titanium isotopic compositions of well-characterized silicon carbide grains from Orgueil (CI): Implications for *s*-process nucleosynthesis. *Meteoritics & Planetary Science* 42: 1055–1075.

Hutcheon ID, Huss GR, Fahey AJ, and Wasserburg GJ (1994) Extreme ^{26}Mg and ^{17}O enrichments in an Orgueil corundum: Identification of a presolar oxide grain. *The Astrophysical Journal* 425: L97–L100.

Hynes KM, Amari S, Bernatowicz TJ, Lebsack E, Gyngard F, and Nittler LR (2011) Combined TEM and NanoSIMS analysis of subgrains in a SiC AB grain. *Lunar and Planetary Science* 42: #2332.

Hynes KM, Croat TK, Amari S, Mertz AF, and Bernatowicz TJ (2006) A transmission electron microscopy study of ultramicrotomed SiC-X grains. *Lunar and Planetary Science* 37: #2202.

Hynes KM, Croat TK, Amari S, Mertz AF, and Bernatowicz TJ (2010) Structural and isotopic microanalysis of presolar SiC from supernovae. *Meteoritics & Planetary Science* 45: 596–614.

Hynes KM and Gyngard F (2009) The presolar grain database: http://presolar.wustl.edu/~pgd. *Lunar and Planetary Science* 40: #1198.

Iben I Jr. and Renzini A (1983) Asymptotic giant branch evolution and beyond. *Annual Review of Astronomy and Astrophysics* 21: 271–342.

Ireland TR, Zinner EK, and Amari S (1991) Isotopically anomalous Ti in presolar SiC from the Murchison meteorite. *The Astrophysical Journal* 376: L53–L56.

Jadhav M, Amari S, Marhas KK, Zinner E, Maruoka T, and Gallino R (2008) New stellar sources for high-density, presolar graphite grains. *The Astrophysical Journal* 682: 1479–1485.

Jadhav M, Amari S, Zinner E, and Maruoka T (2006) Isotopic analysis of presolar graphite grains from Orgueil. *New Astronomy Reviews* 50: 591–595.

Jadhav M, Zinner E, Amari S, Maruoka T, Marhas KK, and Gallino R (2013) Multi-element isotopic analyses of presolar graphite grains from Orgueil. *Geochimica et Cosmochimica Acta* 113: 193–224.

Jones A, Tielens A, Hollenbach D, and McKee C (1997) The propagation and survival of interstellar grains. In: Bernatowicz TJ and Zinner E (eds.) *Astrophysical Implications of the Laboratory Study of Presolar Materials*, pp. 595–613. New York: AIP.

Jørgensen UG (1988) Formation of Xe–HL-enriched diamond grains in stellar environments. *Nature* 332: 702–705.

José J, Coc A, and Hernanz M (1999) Nuclear uncertainties in the NeNa–MgAl cycles and production of ^{22}Na and ^{26}Al during nova outbursts. *The Astrophysical Journal* 520: 347–360.

José J and Hernanz M (2007) The origin of presolar nova grains. *Meteoritics & Planetary Science* 42: 1135–1143.

José J, Hernanz M, Amari S, Lodders K, and Zinner E (2004) The imprint of nova nucleosynthesis in presolar grains. *The Astrophysical Journal* 612: 414–428.

José J, Hernanz M, Amari S, and Zinner E (2003) Constraining models of classical nova outbursts with the Murchison meteorite. *Publications of the Astronomical Society of Australia* 20: 351–355.

Käppeler F, Beer H, and Wisshak K (1989) *s*-Process nucleosynthesis–nuclear physics and the classic model. *Reports on Progress in Physics* 52: 945–1013.

Karakas AI (2010) Updated stellar yields from AGB models. *Monthly Notices of the Royal Astronomical Society* 403: 1413–1425.

Karakas AI, Campbell SW, and Stancliffe RJ (2010) Is extra mixing really needed in asymptotic giant branch stars? *The Astrophysical Journal* 713: 374–382.

Karakas AI and Lattanzio JC (2003) Production of aluminium and the heavy magnesium isotopes in asymptotic giant branch stars. *Publications of the Astronomical Society of Australia* 20: 279–293.

Kashiv Y (2004) *Trace Element Abundances in Single Presolar Silicon Carbide Grains by Synchrotron X-ray Fluorescence*. PhD Thesis, The University of Chicago

Kashiv Y, Cai Z, Lai B, et al. (2001) Synchroton x-ray fluorescence: A new approach for determining trace element concentrations in individual presolar grains. *Lunar and Planetary Science* 32: #2192.

Kashiv Y, Cai Z, Lai B, et al. (2002) Condensation of trace elements into presolar SiC stardust grains. *Lunar and Planetary Science* 33: #2056.

Kashiv Y, Davis AM, Gallino R, et al. (2010) Extinct ^{93}Zr in single presolar SiC grains from low mass asymptotic giant branch stars and condensation from Zr-depleted gas. *The Astrophysical Journal* 713: 212–219.

Keller LP and Messenger S (2011) On the origin of GEMS grains. *Geochimica et Cosmochimica Acta* 75: 5336–5365.

Kifonidis K, Plewa T, Janka H-T, and Müller E (2003) Non-spherical core collapse supernovae I. Neutrino-driven convection, Rayleigh–Taylor instabilities, and the formation and propagation of metal clumps. *Astronomy and Astrophysics* 408: 621–649.

Kobayashi S, Tonotani A, Sakamoto N, Nagashima K, Krot AN, and Yurimoto H (2005a) Presolar silicate grains from primitive carbonaceous chondrites Y-81025, ALHA 77307, Adelaide and Acfer 094. *Lunar and Planetary Science* 36: #1931.

Kobayashi S, Tonotani A, Sakamoto N, Nagashima K, Krot AN, and Yurimoto H (2005b) Abundances of presolar silicates in primitive carbonaceous chondrites Yamato-81025, ALHA 77307, Adelaide and Acfer 094. *Antarctic Meteorites* 29: 30–31.

Kodolányi J and Hoppe P (2010) A promising method to obtain more accurate Mg isotope compositional data on presolar silicate particles. *Proceedings of Science (NIC-XI)* 142.

Kodolányi J and Hoppe P (2011) The Mg isotope composition of presolar silicate grains from AGB stars: Constraints on the Mg isotope inventory of the local interstellar medium at solar birth. *Meteoritics & Planetary Science* 46: A127.

Koehler PE, Spencer RR, Guber KH, et al. (1998) High resolution neutron capture and transmission measurement on ^{137}Ba and their impact on the interpretation of meteoritic barium anomalies. *Physical Review C: Nuclear Physics* 57: R1558–R1561.

Kovetz A and Prialnik D (1997) The composition of nova ejecta from multicycle evolution models. *The Astrophysical Journal* 477: 356–367.

Krestina N, Hsu W, and Wasserburg GJ (2002) Circumstellar oxide grains in ordinary chondrites and their origin. *Lunar and Planetary Science* 33: #1425.

La Cognata M, Spitaleri C, Mukhamedzhanov AM, et al. (2008) Measurement of the 20 and 90 keV resonances in the ^{18}O(p, a)^{15}N reaction via the Trojan Horse method. *Physical Review Letters* 101: 152501.

La Cognata M, Spitaleri C, Mukhamedzhanov A, et al. (2010) A novel approach to measure the cross section of the ^{18}O(p, a)^{15}N resonant reaction in the 0–200 keV energy range. *The Astrophysical Journal* 708: 796–811.

Lambert DL (1991) The abundance connection - the view from the trenches. In: Michaud G and Tutukov A (eds.) *Evolution of Stars: The Photospheric Abundance Connection*, pp. 451–460. Dordrecht: Kluwer Academic Publishers.

Lambert DL, Gustafsson B, Eriksson K, and Hinkle KH (1986) The chemical composition of carbon stars. I. Carbon, nitrogen, and oxygen in 30 cool carbon stars in the galactic disk. *The Astrophysical Journal Supplement Series* 62: 373–425.

Langer N, Heger A, Wellstein S, and Herwig F (1999) Mixing and nucleosynthesis in rotating TP-AGB stars. *Astronomy and Astrophysics* 346: L37–L40.

Larimer JW and Bartholomay M (1979) The role of carbon and oxygen in cosmic gases: Some applications to the chemistry and mineralogy of enstatite chondrites. *Geochimica et Cosmochimica Acta* 43: 1455–1466.

Lattanzio JC, Frost CA, Cannon RC, and Wood PR (1997) Hot bottom burning nucleosynthesis in 6M_O stellar models. *Nuclear Physics A* 621: 435c–438c.

Lee T (1988) Implications of isotopic anomalies for nucleosynthesis. In: Kerridge JF and Matthews MS (eds.) *Meteorites and the Early Solar System*, pp. 1063–1089. Tucson: University of Arizona Press.

Leitner J, Hoppe P, Vollmer C, and Zipfel J (2010) The inventory of presolar grains in primitive meteorites: A NanoSIMS study of C-, N-, and O-isotopes in NWA 852. *Proceedings of Science (NIC-XI)* 144.

Leitner J, Hoppe P, and Zipfel J (2009) NanoSIMS investigation of presolar silicates and oxides in primitive solar system materials. *Lunar and Planetary Science* 40: #1512.

Leitner J, Hoppe P, and Zipfel J (2011) The stardust inventory of the CR chondrites Graves Nunataks 95229 and 06100 assessed by NanoSIMS. *Lunar and Planetary Science* 42: #1713.

Leitner J, Hoppe P, and Zipfel J (2012a) The stardust inventories of graves Nunataks 95229 and Renazzo: Implications for the distribution of presolar grains in CR chondrites. *Lunar and Planetary Science* 43: #1835.

Leitner J, Vollmer C, Hoppe P, and Zipfel J (2012b) Characterization of presolar material in the CR chondrite Northwest Africa 852. *The Astrophysical Journal* 745: 38–52.

Levine J, Savina MR, Stephan T, et al. (2009) Resonance ionization mass spectrometry for precise measurements of isotope ratios. *International Journal of Mass Spectrometry* 288: 36–43.

Lewis RS, Amari S, and Anders E (1990) Meteoritic silicon carbide: Pristine material from carbon stars. *Nature* 348: 293–298.

Lewis RS, Amari S, and Anders E (1994) Interstellar grains in meteorites: II. SiC and its noble gases. *Geochimica et Cosmochimica Acta* 58: 471–494.

Lewis RS, Anders E, and Draine BT (1989) Properties, detectability and origin of interstellar diamonds in meteorites. *Nature* 339: 117–121.

Lewis RS, Anders E, Wright IP, Norris SJ, and Pillinger CT (1983) Isotopically anomalous nitrogen in primitive meteorites. *Nature* 305: 767–771.

Lewis RS, Huss GR, and Lugmair G (1991) Finally, Ba & Sr accompanying Xe–HI in diamonds from Allende. *Lunar and Planetary Science* 22: 807–808.

Lewis JB, Isheim D, Floss C, et al. (2012) Meteoritic nanodiamond analysis by atom-probe tomography. *Lunar and Planetary Science* 43: #2192.

Lewis RS, Tang M, Wacker JF, Anders E, and Steel E (1987) Interstellar diamonds in meteorites. *Nature* 326: 160–162.

Lin Y, Amari S, and Pravdivtseva O (2002) Presolar grains from the Qingzhen (EH3) meteorite. *The Astrophysical Journal* 575: 257–263.

Lin Y, Gyngard F, and Zinner E (2010) Isotopic analysis of supernova SiC and Si_3N_4 grains from the Qingzhen (EH3) chondrite. *The Astrophysical Journal* 709: 1157–1173.

Little-Marenin IR (1986) Carbon stars with silicate dust in their circumstellar shells. *The Astrophysical Journal* 307: L15–L19.

Lodders K (2003) Solar system abundances and condensation temperatures of the elements. *The Astrophysical Journal* 591: 1220–1247.

Lodders K and Amari S (2005) Presolar grains from meteorites: Remnants from the early times of the solar system. *Chemie der Erde* 65: 93–166.

Lodders K and Fegley B Jr. (1995) The origin of circumstellar silicon carbide grains found in meteorites. *Meteoritics & Planetary Science* 30: 661–678.

Lodders K and Fegley B Jr. (1997) Condensation chemistry of carbon stars. In: Bernatowicz TJ and Zinner E (eds.) *Astrophysical Implications of the Laboratory Study of Presolar Materials*, pp. 391–423. New York: AIP.

Lodders K and Fegley B Jr. (1998) Presolar silicon carbide grains and their parent stars. *Meteoritics & Planetary Science* 33: 871–880.

Lodders K and Fegley B Jr. (1999) Condensation chemistry of circumstellar grains. In: Le Bertre T, Lèbre A, and Waelkens C (eds.) *Asymptotic Giant Branch Stars*, pp. 279–289. Utah, USA: Astron. Soc. of the Pacific.

Lodders K, Palme H, and Gail H-P (2009) Abundances of the elements in the solar system. In: Trümper JE (ed.) *Landolt-Börnstein – Group VI Astronomy and Astrophysics Numerical Data and Functional Relationships in Science and Technology 4B: Solar System*, pp. 560–598. Heidelberg: Springer.

Lugaro M (2005) *Stardust from Meteorites*. Singapore: World Scientific Publishing 209 pp.

Lugaro M, Davis AM, Gallino R, Pellin MJ, Straniero O, and Käppeler F (2003) Isotopic compositions of strontium, zirconium, molybdenum, and barium in single presolar SiC grains and asymptotic giant branch stars. *The Astrophysical Journal* 593: 486–508.

Lugaro M, Davis AM, Gallino R, Savina MR, and Pellin MJ (2004) Constraints on AGB models from the heavy-element composition of presolar SiC grains. *Memorie della Societa Astronomica Italiana* 75: 723–728.

Lugaro M, Zinner E, Gallino R, and Amari S (1999) Si isotopic ratios in mainstream presolar SiC grains revisited. *The Astrophysical Journal* 527: 369–394.

Lyon IC (2005) MALDI analysis of presolar nanodiamonds: Mass spectrometric determination of the mass distribution of nanodiamonds from meteorites and a technique to manipulate individual nanodiamonds. *Meteoritics & Planetary Science* 40: 981–987.

Marhas KK, Amari S, Gyngard F, Zinner E, and Gallino R (2008) Iron and nickel isotopic ratios in presolar SiC grains. *The Astrophysical Journal* 689: 622–645.

Marhas KK and Hoppe P (2005) Presolar grains in the Tagish Lake meteorite. *Meteoritics & Planetary Science* 40: A95.

Marhas KK, Hoppe P, and Ott U (2007) NanoSIMS studies of Ba isotopic compositions in single presolar silicon carbide grains from AGB stars and supernovae. *Meteoritics & Planetary Science* 42: 1077–1101.

Marhas KK, Hoppe P, Stadermann FJ, Floss C, and Lea AS (2006) The distribution of presolar grains in CI and CO meteorites. *Lunar and Planetary Science* 37: #1959.

Marty B, Chaussidon M, Wiens RC, Jurewicz AJG, and Burnett DS (2011) A ^{15}N-poor isotopic composition for the Solar System as shown by Genesis solar wind samples. *Science* 332: 1533–1536.

Mathis JS (1990) Interstellar dust and extinction. *Annual Review of Astronomy and Astrophysics* 28: 37–70.

Meier MMM, Heck PR, Amari S, Baur H, and Wieler R (2012) Graphite grains in supernova ejecta – Insights from a noble gas study of 91 individual KFC1 presolar graphite grains from the Murchison meteorite. *Geochimica et Cosmochimica Acta* 76: 147–160.

Mendybaev RA, Beckett JR, Grossman L, Stolper E, Cooper RF, and Bradley JP (2002) Volatilization kinetics of silicon carbide in reducing gases: An experimental study with applications to the survival of presolar grains in the solar nebula. *Geochimica et Cosmochimica Acta* 66: 661–682.

Messenger S, Amari S, Gao X, et al. (1998) Indigenous polycyclic aromatic hydrocarbons in circumstellar graphite grains from primitive meteorites. *The Astrophysical Journal* 502: 284–295.

Messenger S and Bernatowicz TJ (2000) Search for presolar silicates in Acfer 094. *Meteoritics & Planetary Science* 35: A109.

Messenger S, Joswiak D, Ito M, Matrajt G, and Brownlee DE (2009) Discovery of presolar SiC from Comet WILD-2. *Lunar and Planetary Science* 40: #1790.

Messenger S, Keller LP, and Lauretta DS (2005) Supernova olivine from cometary dust. *Science* 309: 737–741.

Messenger S, Keller LP, Stadermann FJ, Walker RM, and Zinner E (2003) Samples of stars beyond the solar system: Silicate grains in interplanetary dust. *Science* 300: 105–108.

Meyer BS (1994) The r-, s-, and p-processes in nucleosynthesis. *Annual Review of Astronomy and Astrophysics* 32: 153–190.

Meyer BS and Bojazi MJ (2011) Production of nitrogen-15 in explosive helium burning and supernova presolar grains. *Lunar and Planetary Science* 42: #2376.

Meyer BS, Bojazi MJ, The L-S, and Eid FE (2011) Presolar silicon carbide x grains, explosive hydrogen burning, and the evolution of massive stars. *Meteoritics & Planetary Science* 46: A160.

Meyer BS, Clayton DD, and The L-S (2000) Molybdenum and zirconium isotopes from a supernova neutron burst. *The Astrophysical Journal* 540: L49–L52.

Meyer BS, Nittler LR, Nguyen AN, and Messenger S (2008) Nucleosynthesis and chemical evolution of oxygen. *Reviews in Mineralogy and Geochemistry* 68: 31–53.

Meyer BS and Zinner E (2006) Nucleosynthesis. In: Lauretta DS and McSween HY Jr. (eds.) *Meteorites and the Early Solar System II*, pp. 69–108. Tucson: University of Arizona.

Molster FJ and Waters LBFM (2003) The mineralogy of interstellar and circumstellar dust. In: Henning T (ed.) *Astromineralogy*, pp. 121–170. New York: Springer.

Mostefaoui S and Hoppe P (2004) Discovery of abundant in situ silicate and spinel grains from red giant stars in a primitive meteorite. *The Astrophysical Journal* 613: L149–L152.

Mostefaoui S, Hoppe P, Marhas KK, and Gröner E (2003) Search for in situ presolar oxygen-rich dust in meteorites. *Meteoritics & Planetary Science* 38: A99.

Mostefaoui S, Marhas KK, and Hoppe P (2004) Discovery of an in-situ presolar silicate grain with GEMS-like composition in the Bishunpur matrix. *Lunar and Planetary Science* 35: #1593.

Mowlavi N and Meynet G (2000) Aluminum 26 production in asymptotic giant branch stars. *Astronomy and Astrophysics* 361: 959–976.

Nagashima K, Krot AN, and Yurimoto H (2004) Stardust silicates from primitive meteorites. *Nature* 428: 921–924.

Nagashima K, Sakamoto N, and Yurimoto H (2005) Destruction of presolar silicates by aqueous alteration observed in Murchison CM2 chondrite. *Lunar and Planetary Science* 36: #1671.

Nguyen AN, Keller LP, and Messenger S (2011a) Microstructures of rare silicate stardust from nova and supernovae. *Meteoritics & Planetary Science* 46: A177.

Nguyen AN, Keller LP, Rahman Z, and Messenger S (2010a) Microstructure of a supernova silicate grain. *Meteoritics & Planetary Science* 45: A151.

Nguyen AN, Messenger S, Ito M, and Rahman Z (2010b) Mg isotopic measurement of FIB-isolated presolar silicate grains. *Lunar and Planetary Science* 41: #2413.

Nguyen AN, Messenger S, Ito M, and Rahman Z (2011b) Fe and Mg isotopic analyses of isotopically unusual presolar silicate grains. *Lunar and Planetary Science* 42: #2711.

Nguyen AN, Nittler LR, Stadermann FJ, Stroud RM, and Alexander CMO'D (2010c) Coordinated analyses of presolar grains in the Allan Hills 77307 and Queen Elizabeth Range 99177 meteorites. *The Astrophysical Journal* 719: 166–189.

Nguyen AN, Stadermann FJ, Zinner E, Stroud RM, Alexander CMO'D, and Nittler LR (2007) Characterization of presolar silicate and oxide grains in primitive carbonaceous chondrites. *The Astrophysical Journal* 656: 1223–1240.

Nguyen AN and Zinner E (2004) Discovery of ancient silicate stardust in a meteorite. *Science* 303: 1496–1499.

Nguyen A, Zinner E, and Lewis RS (2003) Identification of small presolar spinel and corundum grains by isotopic raster imaging. *Publications of the Astronomical Society of Australia* 20: 382–388.

Nguyen AN, Zinner E, and Stroud RM (2005) Continued characterization of presolar silicate grains from the Acfer 094 carbonaceous chondrite. *Lunar and Planetary Science* 36: #2196.

Nichols RH Jr., Kehm K, and Hohenberg CM (1995) Microanalytical laser extraction of noble gases: Techniques and applications. In: Hyman M and Rowe M (eds.) *Advances in Analytical Geochemistry*, vol. 2, pp. 119–140. Hampton Hill, England: JAI Press Inc.

Nicolussi GK, Davis AM, Pellin MJ, Lewis RS, Clayton RN, and Amari S (1997) *s*-Process zirconium in presolar silicon carbide grains. *Science* 277: 1281–1284.

Nicolussi GK, Pellin MJ, Lewis RS, Davis AM, Amari S, and Clayton RN (1998a) Molybdenum isotopic composition of individual presolar silicon carbide grains from the Murchison meteorite. *Geochimica et Cosmochimica Acta* 62: 1093–1104.

Nicolussi GK, Pellin MJ, Lewis RS, Davis AM, Clayton RN, and Amari S (1998b) Strontium isotopic composition in individual circumstellar silicon carbide grains: A record of *s*-process nucleosynthesis. *Physical Review Letters* 81: 3583–3586.

Nicolussi GK, Pellin MJ, Lewis RS, Davis AM, Clayton RN, and Amari S (1998c) Zirconium and molybdenum in individual circumstellar graphite grains: New isotopic data on the nucleosynthesis of heavy elements. *The Astrophysical Journal* 504: 492–499.

Nittler LR (2003) Presolar stardust in meteorites: Recent advances and scientific frontiers. *Earth and Planetary Science Letters* 209: 259–273.

Nittler LR (2005) Constraints on heterogeneous galactic chemical evolution from meteoritic stardust. *The Astrophysical Journal* 618: 281–296.

Nittler LR (2008) Presolar stardust in the solar system: Recent advances for nuclear astrophysics. *Proceedings of Science (NIC-X)* 013.

Nittler LR (2009) On the mass and metallicity distributions of the parent AGB stars of O-rich presolar stardust grains. *Publications of the Astronomical Society of Australia* 26: 271–277.

Nittler LR and Alexander CMO'D (1999) Automatic identification of presolar Al- and Ti-rich oxide grains from ordinary chondrites. *Lunar and Planetary Science* 30: #2041.

Nittler LR and Alexander CMO'D (2003) Automated isotopic measurements of micron-sized dust: Application to meteoritic presolar silicon carbide. *Geochimica et Cosmochimica Acta* 67: 4961–4980.

Nittler LR, Alexander CMO'D, Gallino R, et al. (2008) Aluminum-, calcium- and titanium-rich oxide stardust in ordinary chondrite meteorites. *The Astrophysical Journal* 682: 1450–1478.

Nittler LR, Alexander CMO'D, Gao X, Walker RM, and Zinner EK (1994) Interstellar oxide grains from the Tieschitz ordinary chondrite. *Nature* 370: 443–446.

Nittler LR, Alexander CMO'D, Gao X, Walker RM, and Zinner E (1997) Stellar sapphires: The properties and origins of presolar Al_2O_3 in meteorites. *The Astrophysical Journal* 483: 475–495.

Nittler LR, Alexander CMO'D, and Nguyen AN (2006) Extreme ^{13}C and ^{15}N enrichments in a Murchison presolar SiC grain. *Meteoritics & Planetary Science* 41: A134.

Nittler LR, Alexander CMO'D, Stadermann FJ, and Zinner EK (2005a) Presolar Al-, Ca-, and Ti-rich oxide grains in the Krymka meteorite. *Lunar and Planetary Science* 36: #2200.

Nittler LR, Alexander CMO'D, Stadermann FJ, and Zinner EK (2005b) Presolar chromite in Orgueil. *Meteoritics & Planetary Science* 40: A114.

Nittler LR, Alexander CMO'D, Wang J, and Gao X (1998) Meteoritic oxide grain from supernova found. *Nature* 393: 222.

Nittler LR, Amari S, Zinner E, Woosley SE, and Lewis RS (1996) Extinct ^{44}Ti in presolar graphite and SiC: Proof of a supernova origin. *The Astrophysical Journal* 462: L31–L34.

Nittler LR and Cowsik R (1997) Galactic age estimates from O-rich stardust in meteorites. *Physical Review Letters* 78: 175–178.

Nittler LR and Dauphas N (2006) Meteorites and the chemical evolution of the Milky Way. In: Lauretta DS and McSween HY Jr. (eds.) *Meteorites and the Early Solar System II*, pp. 127–146. Tucson: University of Arizona.

Nittler LR, Gallino R, Lugaro M, Straniero O, Domínguez I, and Zinner E (2005c) Si and C isotopes in presolar silicon carbide grains from AGB stars. *Nuclear Physics A* 758: 348c–351c.

Nittler LR, Gyngard F, Zinner E, and Stroud RM (2011) Mg and Ca isotopic anomalies in presolar oxides: Large anomalies in a group 3 hibonite grain. *Lunar and Planetary Science* 42: #1872.

Nittler LR and Hoppe P (2005) Are presolar silicon carbide grains from novae actually from supernovae? *The Astrophysical Journal* 631: L89–L92.

Nittler LR, Hoppe P, Alexander CMO'D, et al. (1995) Silicon nitride from supernovae. *The Astrophysical Journal* 453: L25–L28.

Nittler LR, Wang J, and Alexander CMO'D (2012) Confirmation of extreme ^{54}CR enrichments in Orgueil nano-oxides and correlated O-isotope measurements. *Lunar and Planetary Science* 43: #2442.

Nollett KM, Busso M, and Wasserburg GJ (2003) Cool bottom processes on the thermally pulsing asymptotic giant branch and the isotopic composition of circumstellar dust grains. *The Astrophysical Journal* 582: 1036–1058.

Ong WJ, Floss C, and Gyngard F (2012) Negative secondary ion measurements of $^{54}Fe/^{56}Fe$ and $^{57}Fe/^{56}Fe$ in presolar silicate grains from Acfer 094. *Lunar and Planetary Science* 43: #1225.

Ott U (1993) Interstellar grains in meteorites. *Nature* 364: 25–33.

Ott U (1996) Interstellar diamond xenon and timescales of supernova ejecta. *The Astrophysical Journal* 463: 344–348.

Ott U, Altmaier M, Herpers U, et al. (2005) Spallation recoil II: Xenon evidence for young SiC grains. *Meteoritics & Planetary Science* 40: 1635–1652.

Ott U and Begemann F (1990) Discovery of s-process barium in the Murchison meteorite. *The Astrophysical Journal* 353: L57–L60.

Ott U and Begemann F (2000) Spallation recoil and age of presolar grains in meteorites. *Meteoritics & Planetary Science* 35: 53–63.

Ott U, Heck PR, Gyngard F, et al. (2009) He and Ne ages of large presolar silicon carbide grains: Solving the recoil problem. *Publications of the Astronomical Society of Australia* 26: 297–302.

Ott U, Yin Q-Z, and Lee C-T (2006) S-process signatures in bulk presolar silicon carbide: A multi-element study. *Memorie della Societa Astronomica Italiana* 75: 891–896.

Owen T, Mahaffy PR, Niemann HB, Atreya S, and Wong M (2001) Protosolar nitrogen. *The Astrophysical Journal* 553: L77–L79.

Palme H and Jones A (2004) Solar system abundances of the elements. Davis AM (ed.) *Meteorites, Planets, and Comets*. 1st edn., In: Holland HD and Turekian KK (eds.) *Treatise on Geochemistry*, 1st edn., vol. 1, pp. 41–61. Oxford: Elsevier-Pergamon.

Palmerini S, La Cognata M, Cristallo S, and Busso M (2011) Deep mixing in evolved stars. I. The effect of reaction rate revisions from C to A1. *The Astrophysical Journal* 729: 3 21 pp.

Pellin MJ, Calaway WF, Davis AM, Lewis RS, Amari S, and Clayton RN (2000a) Toward complete isotopic analysis of individual presolar silicon carbide grains: C, N, Si, Sr, Zr, Mo, and Ba in single grains of type X. *Lunar and Planetary Science* 31: #1917.

Pellin MJ, Davis AM, Calaway WF, Lewis RS, Clayton RN, and Amari S (2000b) Zr and Mo isotopic constraints on the origin of unusual types of presolar SiC grains. *Lunar and Planetary Science* 31: #1934.

Pellin MJ, Davis AM, Lewis RS, Amari S, and Clayton RN (1999) Molybdenum isotopic composition of single silicon carbide grains from supernovae. *Lunar and Planetary Science* 30: #1969.

Pellin MJ, Savina MR, Calaway WF, et al. (2006) Heavy metal isotopic anomalies in supernovae presolar grains. *Lunar and Planetary Science* 37: #2041.

Pignatari M, Gallino R, Reifarth R, et al. (2003) S-process xenon in presolar silicon carbide grains and AGB models with new cross sections. *Meteoritics & Planetary Science* 38: A152.

Pignatari M, Gallino R, Straniero O, and Davis AM (2004a) The origin of xenon trapped in presolar mainstream SiC grains. *Memorie della Societa Astronomica Italiana* 75: 729–734.

Pignatari M, Gallino R, Straniero O, Reifarth R, Käppeler F, and Davis AM (2004b) Stellar origin of the meteoritic Xe–S anomalous component. *Memorie della Societa Astronomica Italiana* 75: 182–185.

Podosek FA, Prombo CA, Amari S, and Lewis RS (2004) *s*-Process Sr isotopic compositions in presolar SiC from the Murchison meteorite. *The Astrophysical Journal* 605: 960–965.

Prombo CA, Podosek FA, Amari S, and Lewis RS (1993) *s*-Process Ba isotopic compositions in presolar SiC from the Murchison meteorite. *The Astrophysical Journal* 410: 393–399.

Qin L, Nittler LR, Alexander CMO'D, Wang J, Stadermann FJ, and Carlson RW (2011) Extreme ^{54}Cr-rich nano-oxides in the CI chondrite Orgueil – Implication for a late supernova injection into the solar system. *Geochimica et Cosmochimica Acta* 75: 629–644.

Rauscher T, Heger A, Hoffman RD, and Woosley SE (2002) Nucleosynthesis in massive stars with improved nuclear and stellar physics. *The Astrophysical Journal* 576: 323–348.

Reynolds JH and Turner G (1964) Rare gases in the chondrite Renazzo. *Journal of Geophysical Research* 69: 3263–3281.

Richter S, Ott U, and Begemann F (1993) *s*-Process isotope abundance anomalies in meteoritic silicon carbide: New data. In: Käppeler F and Wisshak K (eds.) *Nuclei in the Cosmos II*, pp. 127–132. Bristol/Philadelphia: Institute of Physics Publishing.

Richter S, Ott U, and Begemann F (1994) s-Process isotope abundance anomalies in meteoritic silicon carbide: Data for Dy. In: Somorjai E and Fülöp Z (eds.) Proceedings of the European Workshop on Heavy Element Nucleosynthesis, pp. 44–46. Debrecen: Inst. Nucl. Res. Hungarian Acad. of Sci.

Richter S, Ott U, and Begemann F (1998) Tellurium in pre-solar diamonds as an indicator for rapid separation of supernova ejecta. *Nature* 391: 261–263.

Rotaru M, Birck JL, and Allègre CJ (1992) Clues to early solar system history from chromium isotopes in carbonaceous chondrites. *Nature* 358: 465–470.

Russell SS, Arden JW, and Pillinger CT (1991) Evidence for multiple sources of diamond from primitive chondrites. *Science* 254: 1188–1191.

Russell SS, Arden JW, and Pillinger CT (1996) A carbon and nitrogen isotope study of diamond from primitive chondrites. *Meteoritics & Planetary Science* 31: 343–355.

Russell SS, Ott U, Alexander CMO'D, Zinner EK, Arden JW, and Pillinger CT (1997) Presolar silicon carbide from the Indarch (EH4) meteorite: Comparison with silicon carbide populations from other meteorite classes. *Meteoritics & Planetary Science* 32: 719–732.

Savina MR, Davis AM, Tripa CE, et al. (2003a) Barium isotopes in individual presolar silicon carbide grains from the Murchison meteorite. *Geochimica et Cosmochimica Acta* 67: 3201–3214.

Savina MR, Davis AM, Tripa CE, et al. (2004) Extinct technetium in presolar silicon carbide grains: Implications for stellar nucleosynthesis. *Science* 303: 649–652.

Savina MR, Levine J, Stephan T, et al. (2010) Chromium isotopes in presolar SiC grains. *Lunar and Planetary Science* 41: #2568.

Savina MR, Pellin MJ, Davis AM, Lewis RS, and Amari S (2007) p-Process signature in a unique presolar silicon carbide grain. *Lunar and Planetary Science* 38: #1338.

Savina MR, Pellin MJ, Tripa CE, Veryovkin IV, Calaway WF, and Davis AM (2003b) Analyzing individual presolar grains with CHARISMA. *Geochimica et Cosmochimica Acta* 67: 3215–3225.

Savina MR, Tripa CE, Pellin MJ, et al. (2003c) Isotopic composition of molybdenum and barium in single presolar silicon carbide grains of type A + B. *Lunar and Planetary Science* 34: #2079.

Smith VV and Lambert DL (1990) The chemical composition of red giants. III. Further CNO isotopic and s-process abundances in thermally pulsing asymptotic giant branch stars. *The Astrophysical Journal Supplement Series* 72: 387–416.

Speck AK, Barlow MJ, and Skinner CJ (1997) The nature of silicon carbide in carbon star outflows. *Monthly Notices of the Royal Astronomical Society* 234: 79–84.

Speck AK, Hofmeister AM, and Barlow MJ (1999) The SiC problem: Astronomical and meteoritic evidence. *The Astrophysical Journal* 513: L87–L90.

Srinivasan B and Anders E (1978) Noble gases in the Murchison meteorite: Possible relics of *s*-process nucleosynthesis. *Science* 201: 51–56.

Stadermann FJ, Croat TK, Bernatowicz TJ, et al. (2005) Supernova graphite in the NanoSIMS: Carbon, oxygen and titanium isotopic compositions of a spherule and its TiC sub-components. *Geochimica et Cosmochimica Acta* 69: 177–188.

Stadermann FJ, Floss C, Bose M, and Lea AS (2009) The use of Auger spectroscopy for the in situ elemental characterization of sub-micrometer presolar grains. *Meteoritics & Planetary Science* 44: 1033–1049.

Stadermann FJ, Floss C, and Wopenka B (2006) Circumstellar aluminum oxide and silicon carbide in interplanetary dust particles. *Geochimica et Cosmochimica Acta* 70: 6168–6179.

Stadermann FJ, Isheim D, Zhao X, et al. (2011) Atom-probe tomographic characterization of meteoritic nanodiamonds and presolar SiC. *Lunar and Planetary Science* 42: #1595.

Starrfield S, Truran JW, Wiescher MC, and Sparks WM (1998) Evolutionary sequences for Nova V1974 Cygni using new nuclear reaction rates and opacities. *Monthly Notices of the Royal Astronomical Society* 296: 502–522.

Stephan T, Davis AM, Pellin MJ, Savina MR, and Veryovkin IV (2010) CHILI – the Chicago Instrument of Laser Ionization – a progress report. *Lunar and Planetary Science* 41: #2321.

Stephan T, Davis AM, Pellin MJ, et al. (2011) Making CHILI (Chicago Instrument for Laser Ionization) – A tool for the analysis of stardust. *Lunar and Planetary Science* 42: #1995.

Stroud RM and Bernatowicz TJ (2005) Surface and internal structure of pristine presolar silicon carbide. *Lunar and Planetary Science* 36: #2010.

Stroud RM, Chisholm MF, Heck PR, Alexander CMO'D, and Nittler LR (2011) Supernova shockwave-induced co-formation of glassy carbon and nanodiamond. *The Astrophysical Journal* 738: L27 5 pp.

Stroud RM, Nittler LR, and Alexander CMO'D (2004a) Polymorphism in presolar Al_2O_3 grains from asymptotic giant branch stars. *Science* 305: 1455–1457.

Stroud RM, Nittler LR, Alexander CMO'D, Bernatowicz TJ, and Messenger SR (2003) Transmission electron microscopy of non-etched presolar silicon carbide. *Lunar and Planetary Science* 34: #1755.

Stroud RM, Nittler LR, and Hoppe P (2004b) Microstructures and isotopic compositions of two SiC X grains. *Meteoritics & Planetary Science* 39: A101.

Suess HE and Urey HC (1956) Abundances of the elements. *Reviews of Modern Physics* 28: 53–74.

Tang M and Anders E (1988a) Interstellar silicon carbide: How much older than the solar system? *The Astrophysical Journal* 335: L31–L34.

Tang M and Anders E (1988b) Isotopic anomalies of Ne, Xe, and C in meteorites. II. Interstellar diamond and SiC: Carriers of exotic noble gases. *Geochimica et Cosmochimica Acta* 52: 1235–1244.

Thielemann F-K, Nomoto K, and Hashimoto M-A (1996) Core-collapse supernovae and their ejecta. *The Astrophysical Journal* 460: 408–436.

Tielens AGGM (1990) Carbon stardust: From soot to diamonds. In: Tarter JC, Chang S, and deFrees DJ (eds.) *Carbon in the Galaxy: Studies from Earth and Space*, NASA Conf. Publ. 3061, pp. 59–111.

Timmes FX and Clayton DD (1996) Galactic evolution of silicon isotopes: Application to presolar SiC grains from meteorites. *The Astrophysical Journal* 472: 723–741.

Timmes FX, Woosley SE, Hartmann DH, and Hoffman RD (1996) The production of ^{44}Ti and ^{60}Co in supernovae. *The Astrophysical Journal* 464: 332–341.

Timmes FX, Woosley SE, and Weaver TA (1995) Galactic chemical evolution: Hydrogen through zinc. *The Astrophysical Journal Supplement Series* 98: 617–658.

Tizard JM, Lyon IC, and Henkel T (2005) The gentle separation of interstellar SiC grains from meteorites. *Meteoritics & Planetary Science* 40: 335–342.

Tonotani A, Kobayashi S, Nagashima K, et al. (2006) Presolar grains from primitive ordinary chondrites. *Lunar and Planetary Science* 37: #1539.

Travaglio C, Gallino R, Amari S, Zinner E, Woosley S, and Lewis RS (1999) Low-density graphite grains and mixing in type II supernovae. *The Astrophysical Journal* 510: 325–354.

Treffers R and Cohen M (1974) High-resolution spectra of cold stars in the 10- and 20-micron regions. *The Astrophysical Journal* 188: 545–552.

Trinquier A, Birck J-L, and Allègre CJ (2007) Widespread ^{54}Cr heterogeneity in the inner solar system. *The Astrophysical Journal* 655: 1179–1185.

Verchovsky AB, Fisenko AV, Semjonova LF, Bridges J, Lee MR, and Wright IP (2006) Nanodiamonds from AGB stars: A new type of presolar grain in meteorites. *The Astrophysical Journal* 651: 481–490.

Verchovsky AB, Franchi IA, Arden JW, Fisenko AV, Semionova LF, and Pillinger CT (1993a) Conjoint release of N, C, He, and Ar from C_d by stepped pyrolysis: Implications for the identification of their carriers. *Meteoritics* 28: 452–453.

Verchovsky AB, Russell SS, Pillinger CT, Fisenko AV, and Shukolyukov YA (1993b) Are the Cs light nitrogen and noble gases are located in the same carrier? *Lunar and Planetary Science* 24: 1461–1462.

Verchovsky AB and Wright IP (2004) Physical parameters of AGB winds derived from the implanted species in meteoritic SiC grains. *Memorie della Societa Astronomica Italiana* 75: 623–626.

Verchovsky AB, Wright IP, and Pillinger CT (2004) Astrophysical significance of asymptotic giant branch stellar wind energies recorded in meteoritic SiC grains. *The Astrophysical Journal* 607: 611–619.

Vollmer C, Brenker FE, Hoppe P, and Stroud R (2009a) Direct laboratory analysis of silicate stardust from red giant stars. *The Astrophysical Journal* 700: 774–782.

Vollmer C and Hoppe P (2010) First Fe isotopic measurement of highly ^{17}O-enriched stardust silicate. *Lunar and Planetary Science* 41: #1200.

Vollmer C, Hoppe P, and Brenker FE (2008) Si isotopic compositions of presolar silicate grains from red giant stars and supernovae. *The Astrophysical Journal* 684: 611–617.

Vollmer C, Hoppe P, Brenker FE, and Holzapfel C (2007) Stellar $MgSiO_3$ perivskite: A shock-transformed stardust silicate found in a meteorite. *The Astrophysical Journal* 666: L49–L52.

Vollmer C, Hoppe P, Stadermann FJ, Floss C, and Brenker FE (2009b) NanoSIMS analysis and Auger electron spectroscopy of silicate and oxide stardust from the carbonaceous chondrite Acfer 094. *Geochimica et Cosmochimica Acta* 73: 7127–7149.

Wallerstein G, Iben I Jr., Parker P, et al. (1997) Synthesis of the elements in stars: Forty years of progress. *Reviews of Modern Physics* 69: 995–1084.

Wasserburg GJ (1987) Isotopic abundances: Inferences on solar system and planetary evolution. *Earth and Planetary Science Letters* 86: 129–173.

Wasserburg GJ, Boothroyd AI, and Sackmann I-J (1995) Deep circulation in red giant stars: A solution to the carbon and oxygen isotope puzzles? *The Astrophysical Journal* 447: L37–L40.

Wasserburg GJ, Busso M, Gallino R, and Raiteri CM (1994) Asymptotic giant branch stars as a source of short-lived radioactive nuclei in the solar nebula. *The Astrophysical Journal* 424: 412–428.

Waters LBFM, Molster FJ, de Jong T, et al. (1996) Mineralogy of oxygen-rich dust shells. *Astronomy and Astrophysics* 315: L361–L364.

Wisshak K, Voss F, Käppeler F, and Kazakov L (1997) Neutron capture in neodymium isotopes: Implications for the s-process. *Nuclear Physics A* 621: 270c–273c.

Woosley SE and Weaver TA (1995) The evolution and explosion of massive stars. II. Explosive hydrodynamics and nucleosynthesis. *The Astrophysical Journal Supplement Series* 101: 181–235.

Wopenka B, Groopman E, and Zinner E (2011a) Orgueil low-density presolar carbon ain't graphite but glassy carbon. *Meteoritics & Planetary Science* 46: A252.

Wopenka B, Jadhav M, Lebsack E, and Zinner E (2010) Raman and isotopic studies of large presolar SiC grains. *Lunar and Planetary Science* 41: #1390.

Wopenka B, Jadhav M, and Zinner E (2011b) Raman analysis of high-density presolar graphite grains from the Orgueil carbonaceous chondrite. *Lunar and Planetary Science* 42: #1162.

Yada T, Floss C, Stadermann FJ, et al. (2008) Stardust in Antarctic micrometeorites. *Meteoritics & Planetary Science* 43: 1287–1298.

Yin Q-A, Lee C-T, and Ott U (2006) Signatures of the s-process in presolar silicon carbide grains: Barium through hafnium. *The Astrophysical Journal* 647: 676–684.

Yoshida T (2007) Supernova mixtures reproducing isotopic ratios of presolar grains. *The Astrophysical Journal* 666: 1048–1068.

Yoshida T and Hashimoto M (2004) Numerical analyses of isotopic ratios of presolar grains from supernovae. *The Astrophysical Journal* 606: 592–604.

Yurimoto H, Nagashima K, and Kunihiro T (2003) High precision isotope micro-imaging of materials. *Applied Surface Science* 203–204: 793–797.

Zega TJ, Conel Alexander MO'D, Nittler LR, and Stroud RM (2011) A transmission electron microscopy study of presolar hibonite. *The Astrophysical Journal* 730: 83–92.

Zega TJ, Nittler L, Busemann H, Hoppe P, and Stroud RM (2007) Coordinated isotopic and mineralogic analyses of planetary materials enabled by in situ lift-out with a focused ion beam scanning electron microscope. *Meteoritics & Planetary Science* 42: 1373–1386.

Zhao X, Floss C, Stadermann FJ, Bose M, and Lin Y (2011a) Continued investigation of presolar silicate grains in the carbonaceous chondrite Ningqiang. *Lunar and Planetary Science* 42: #1982.

Zhao X, Floss C, Stadermann FJ, Lin Y, and Bose M (2011b) The stardust investigation into the CR2 chondrite GRV 021710. *Meteoritics & Planetary Science* 46: A261.

Zhao X, Stadermann FJ, Floss C, Bose M, and Lin Y (2010) Characterization of presolar grains from the carbonaceous chrondrite Ningqiang. *Lunar and Planetary Science* 41: #1431.

Zinner E (1997) Presolar material in meteorites: An overview. In: Bernatowicz TJ and Zinner E (eds.) *Astrophysical Implications of the Laboratory Study of Presolar Materials*, pp. 3–26. New York: AIP.

Zinner E (1998a) Stellar nucleosynthesis and the isotopic composition of presolar grains from primitive meteorites. *Annual Review of Earth and Planetary Sciences* 26: 147–188.

Zinner E (1998b) Trends in the study of presolar dust grains from primitive meteorites. *Meteoritics & Planetary Science* 33: 549–564.

Zinner EK (2008) Stardust in the laboratory. *Publications of the Astronomical Society of Australia* 25: 7–17.

Zinner E, Amari S, Gallino R, and Lugaro M (2001) Evidence for a range of metallicities in the parent stars of presolar SiC grains. *Nuclear Physics A* 688: 102–105.

Zinner E, Amari S, Guinness R, and Jennings C (2003a) Si isotopic measurements of small SiC and Si_3N_4 grains from the Indarch (EH4) meteorite. *Meteoritics & Planetary Science* 38: A60.

Zinner E, Amari S, Guinness R, et al. (2003b) Presolar spinel grains from the Murray and Murchison carbonaceous chondrites. *Geochimica et Cosmochimica Acta* 67: 5083–5095.

Zinner E, Amari S, Guinness R, et al. (2007) NanoSIMS isotopic analysis of small presolar grains: Search for Si_3N_4 grains from AGB stars, and Al and Ti isotopic compositions of rare presolar SiC grains. *Geochimica et Cosmochimica Acta* 71: 4786–4813.

Zinner E, Amari S, and Jadhav M (2006a) On the stellar sources of presolar graphite. *Proceedings of Science (NIC-IX)* 019.

Zinner E, Amari S, and Lewis RS (1991) s-Process Ba, Nd, and Sm in presolar SiC from the Murchison meteorite. *The Astrophysical Journal* 382: L47–L50.

Zinner E, Amari S, Wopenka B, and Lewis RS (1995) Interstellar graphite in meteorites: Isotopic compositions and structural properties of single graphite grains from Murchison. *Meteoritics* 30: 209–226.

Zinner E, Gyngard F, and Nittler LR (2010) Automated C and Si isotopic analysis of presolar SiC grains from the Indarch enstatite chondrite. *Lunar and Planetary Science* 41: #1359.

Zinner E, Moynier F, and Stroud R (2011) Laboratory technology and cosmochemistry. *Proceedings of the National Academy of Sciences* 108: 19135–19141.

Zinner E, Nittler LR, Alexander CMO'D, and Gallino R (2006b) The study of radioisotopes in presolar dust grains. *New Astronomy Reviews* 50: 574–577.

Zinner E, Nittler LR, Gallino R, et al. (2006c) Si and C isotopic ratios in AGB stars: SiC grain data, models, and the galactic evolution of the Si isotopes. *Meteoritics & Planetary Science* 41: A198.

Zinner E, Nittler LR, Gallino R, et al. (2006d) Silicon and carbon isotopic ratios in AGB stars: SiC grain data, models, and the Galactic evolution of the Si isotopes. *The Astrophysical Journal* 650: 350–373.

Zinner E, Nittler LR, Hoppe P, Gallino R, Straniero O, and Alexander CMO'D (2005) Oxygen, magnesium and chromium isotopic ratios of presolar spinel grains. *Geochimica et Cosmochimica Acta* 69: 4149–4165.